ABSTRACT

Title of dissertation: ALLOSTERY IN GROEL: ITS ROLE IN THE REFOLDING OF PROTEIN SUBSTRATES

John Peter Grason, Doctor of Philosophy, 2003

Dissertation directed by: Professor George H. Lorimer
Department of Chemistry and Biochemistry

The *Escherichia coli* chaperonin GroEL assists in the re-folding of misfolded substrate proteins (SPs). In response to the binding of ATP, GroEL undergoes large, allosteric structural transitions, resulting in an expansion of its central cavity and a capping of the cavity by the co-chaperonin GroES. Bound SP is released into the central cavity following the structural transitions. The exact mechanism by which GroEL assists in the re-folding of SPs is unknown, though there is evidence that GroEL has the ability to forcefully unfold bound SPs, giving them another chance to fold to the native state.

The studies in this dissertation concentrate on relating the allosteric domain movements of GroEL to the unfolding of SPs: 1) As a means of controlling the domain movements, an intersubunit salt bridge was replaced with a pair of cysteine residues, allowing for the controlled introduction of cross-links that could tether the GroEL rings in their closed conformation. 2) The possible allosteric basis of SP's ability to stimulate the ATPase activity of GroEL was explored using standard kinetic assays. 3) The

kinetics of GroES release from the GroEL/GroES complex in response to ATP binding were studied using stopped-flow fluorescence measurements, with an emphasis on determining why SP binding accelerates the rate of release. From these studies, it was concluded that the subunits within a GroEL ring move in a single concerted motion, maximizing the potential unfolding force exerted by GroEL against bound SP. It was also found that SP stimulates ATPase activity by binding to and holding a ring in the more active, closed conformation. To do this, SP must exert a force on the ring, and in order to undergo its structural changes, GroEL must in turn perform work on the SP. GroES release is stimulated for a similar reason. Since unfolded SP increases the number of reaction cycles and decreases the amount of time SP spends encapsulated in the central cavity, it is proposed that a GroEL-assisted refolding mechanism that includes an active unfolding event makes the most sense in physiological terms.

ALLOSTERY IN GROEL: ITS ROLE IN THE REFOLDING OF PROTEIN SUBSTRATES

by

John Peter Grason

Dissertation submitted to the Faculty of the Graduate School of the
University of Maryland, College Park in partial fulfillment
of the requirements for the degree of
Doctor of Philosophy
2003

Advisory Committee:

Professor George H. Lorimer, Chair
Professor Dorothy Beckett
Professor Victor Muñoz
Professor Richard Stewart
Professor Devarajan Thirumalai

DEDICATION

This dissertation is dedicated to my wife,
Jennifer,
for absolutely everything,
and who deserves this degree far more than I ever will…

…To my grandfather, Martin Sheska…

…and to Cody.

ACKNOWLEDGEMENTS

It is impossible to complete a project such as this without the help of many people. All of the good things presented in this dissertation are due to them. The mistakes are entirely my own.

Many thanks to…

…my advisor, Dr. George Lorimer, for constant guidance, for countless stimulating discussions, for always being accessible, for providing me with a great project, for convincing me (several times) to finish this degree, …and for never requiring me to teach (and that last one's a big one).

…Gilles Curien, for teaching me the skills and techniques used in all aspects of this project. I was very fortunate to have Gilles as my first mentor when I arrived in the lab. He's an outstanding scientist, and a great friend as well.

…my colleague of the past two years, Jen Gresham. Thank you for all the conversations, all the lunches, all the help, for convincing me (more than several times) to finish this degree, for reading the first draft of this dissertation, for putting up with me, and most importantly, for being a fantastic friend.

…all my lab mates over the years. Thanks to Edward Hammond, Mark Uebel, Lusiana Widjaja, and Jen Grason for all their help and all the good times.

…my Lehigh colleagues. Thanks to Linda Lowe-Krentz, Al Gilotti, Marianne Hamel, and Cheryl Isleib-Blaukovitch for providing me with a wonderful introduction to working in a lab.

…the members of my dissertation committee, for giving up their time to carefully read this document and help me fulfill this final requirement.

…my family, for all their encouragement and support.

…Jen's family, for always being there for me.

…and finally, my wife Jennifer, of course, for all her love and unwavering support, and for being my most important motivation in finishing this degree.

TABLE OF CONTENTS

TABLE OF CONTENTS (CONT.)

TABLE OF CONTENTS (CONT.)

LIST OF FIGURES

LIST OF ABBREVIATIONS

°C	degrees Celsius
[X]	concentration of X
Å	Angstroms
ADP	adenosine diphosphate
α-LA	α-lactalbumin (bovine)
Amp	ampicillin
AMP-PNP	5'-adenylylimidodiphosphate
ATP	adenosine triphosphate
BME	β-mercaptoethanol
cryo-EM	cryo-electron microscopy
Cys	cysteine
DEAE	diethylaminoethyl (weak anionic exchanger)
DMF	N,N-dimethylformamide
DMSO	dimethylsulfoxide
DNA	deoxyribonucleic acid
DTT	dithiothreitol
E. coli	*Escherichia coli*
EDTA	ethylenediaminetetraacetic acid
F5M	fluorescein-5-maleimide
FRET	fluorescence resonance energy transfer
$GroEL_D$	GroEL E315C labeled with IAEDANS
$GroEL_{IAX}$	GroEL D83C/K327C (intrasubunit double cys pair)
$GroEL_{IRX}$	GroEL R197C/E386C (intersubunit double cys pair)

$GroEL_{WT}$	wild-type GroEL
$GroES_{A}$	GroES 98C labeled with F5M
$GroES_{His}$	GroES with His_6 tag
$GroES_{WT}$	wild-type GroES
His	histidine
IAEDANS	5-((((2-iodoacetyl)amino)ethyl)amino) naphthalene-1-sulfonic acid
IPTG	isopropyl-β-D-thiogalactopyranoside
K^+	potassium ion
KAc	potassium acetate
kDa	kilodaltons
KNF	Koshland-Nemethy-Filmer model of allostery
LB	Luria-Bertani broth
LDH	lactate dehydrogenase (bovine)
MDH	malate dehydrogenase (pig heart mitochondrial)
Mg	magnesium
MgAc	magnesium Acetate
mPDM	*meta*-phenylenedimaleimide
mS	milliSiemens/centimeter
ms	milliseconds
MW	molecular weight
MWC	Monod-Wyman-Changeux model of allostery
NaAc	sodium acetate
NADH	nicotinamide adenine dinucleotide
NaOH	sodium hydroxide

NEM	N-ethylmaleimide
Ni-NTA	nickel-nitrilotriacetic acid
nm	nanometers
NMR	nuclear magnetic resonance
oPDM	*ortho*-phenylenedimaleimide
PAGE	polyacrylamide gel electrophoresis
PBP	phosphate binding protein
PCR	polymerase chain reaction
PEP	phosphoenolpyruvate
PK	pyruvate kinase (bovine)
pPDM	*para*-phenylenedimaleimide
Q	quaternary ammonium (strong anionic exchanger)
R	**R**elaxed state in MWC terminology
Rubisco	Ribulose bisphosphate carboxylase
SDS	sodium dodecyl sulfate
SP	substrate protein
SP	sulfopropyl (strong cationic exchanger)
SR1	single-ring mutant of GroEL
T	**T**ight state in MWC terminology
TEMED	N,N,N',N'-tetramethylethylenediamine
Tet	tetracycline
Tris	Tris (hydroxymethyl) aminomethane
Trp	tryptophan
u	units of enzyme activity

Chapter 1

Introduction and Specific Aims

Proteins are the essential molecular machines that sustain the chemical reactions of life. The unique, three-dimensional structure of a protein determines its specificity and its function, and the structure of a protein is determined entirely by its primary amino acid sequence (1). A protein is synthesized as a linear strand of these amino acids by the ribosome, and must then fold correctly into higher order structures. The folding of proteins is a remarkable event in nature, requiring the proper rotation of molecular bonds, the forming of salt bridges and hydrogen bonds, and the collapse of a core of hydrophobic amino acids. A correctly folded protein is only marginally more stable than many other possible structures. It is therefore not surprising that proteins occasionally do not reach their correct, final structure; it is more surprising that most do. Incorrectly folded proteins are not functional; most will form insoluble aggregates, eventually subject to proteolysis. However, for some incorrectly folded proteins, all is not lost. They still have a chance to fold to their correct structure thanks to a group of proteins known as chaperonins, members of a broader group of proteins known as chaperones. Molecular chaperones are proteins which affect the fold or conformation of other proteins (2). An example is Hsp70, which unfolds proteins and assists in importing them into mitochondria (3). Another is Hsp90, which assists in the folding of signal transduction proteins (4). A third example, chaperonins, rescue misfolded proteins and allow them to refold.

GroEL/Hsp60 is the best understood of all the chaperonins (for reviews see (2, 5)), and exemplifies a protein that operates as a molecular machine. Georgopoulos and coworkers originally discovered it as a protein that was essential for the growth of *Escherichia coli* (*E. coli*), along with its co-chaperonin GroES/Hsp10 (6). Since that

time, there have been hundreds of publications dealing with various aspects of GroEL: its structure, its ATP-driven structural changes, its effect on substrate proteins (SPs), and even its possible role in disease. However, the mechanism by which it accomplishes its primary function, using ATP to rescue misfolded proteins, remains controversial. One school of thought says that GroEL is a passive participant in protein refolding. It simply binds misfolded proteins, sequesters them to prevent them from aggregating, and provides them with an environment favorable to folding (7). Others believe that GroEL plays a more active role in refolding, in that it binds misfolded substrates, forcibly unfolds them, and gives them another chance to fold correctly (8). The answer remains elusive, but the work presented in this dissertation provides support for the active mechanism.

1.1 The Structure of GroEL

GroEL is a tetradecamer and a double toroid, arranged as two rings stacked back to back. Each ring is composed of seven identical subunits, with a molecular weight of approximately 57 kD per subunit (9). The crystal structure of the GroEL monomer (10) shows the protein arranged into three distinct domains (Figure 1-1). The equatorial domain is responsible for most of the inter-subunit contacts between monomers of the same ring and all of the inter-ring contacts. This domain also contains the binding site for ATP, one binding site per subunit, for a total of 14 ATP binding sites per GroEL tetradecamer. The residues responsible for the binding and hydrolysis of ATP are the most conserved residues among the GroEL homologues from several organisms (11). The second large domain is the apical domain, which is known to contain the binding sites for the substrate polypeptide as well as the co-chaperonin GroES (12). These two

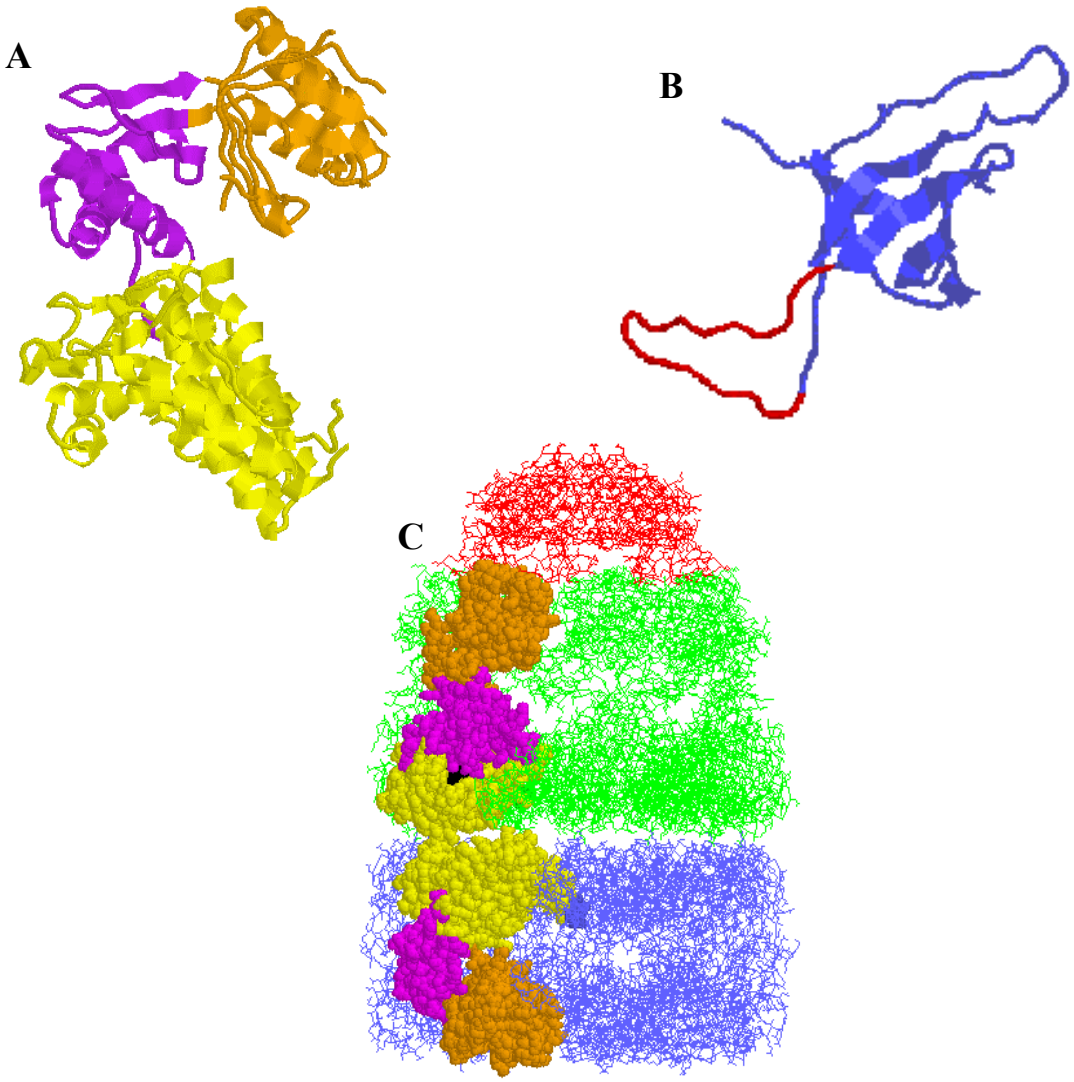

Figure 1-1: The Structure of GroEL, GroES and the GroEL/GroES "Bullet" Complex. **A**) The structure of a single GroEL subunit (from PDB file 1grl (10)). The apical domain is highlighted in orange, the equatorial domain in yellow, and the intermediate domain in purple. **B**) The structure of a single GroES subunit (from PDB file 1aon (14)). The mobile loop (the GroEL binding site) is highlighted in red. **C**) The GroEL/GroES bullet (from PDB file 1aon (14)). The *trans* ring is colored blue, the *cis* ring is colored green, and the GroES ring is colored red. A single subunit in each GroEL ring is highlighted using the same domain color scheme as in **A** to show the change in conformation a subunit undergoes in response to ATP and GroES. (See section 2.11).

domains are connected by a smaller domain known as the intermediate domain, with hinge regions formed at the inter-domain connecting points. Arranged as a 14-mer, the GroEL subunits form two large, non-connecting central cavities in which the SP binds and is later sequestered (13). During the cycle of GroEL assisted protein folding, GroES binds to one end of the GroEL double ring, forming a cap over one of the central cavities (14). GroES is a ring comprised of seven identical 10 kD subunits (15), each containing an unstructured mobile loop which can bind to the GroEL apical domain. It should be noted that $GroES_7$-$GroEL_{14}$-$GroES_7$ particles, or "footballs", have been seen in cryo-electron microscopy studies (16), though it is not at all clear whether these species are obligate parts of the reaction cycle (17). Over the course of its reaction cycle, GroEL undergoes several large structural changes, first visualized using cryo-EM (18), which are described in detail below.

1.2 Why Does Nature Need GroEL?

Why is a chaperone such as GroEL necessary? The answer has to do with the pathways by which proteins are believed to fold. The folding mechanism of most proteins can be best described by an energy landscape, which is strewn with many local energy minima, the most pronounced of which represents the native (properly folded) state (19). It is certainly true that some proteins can achieve their native state with no assistance, under normal cellular conditions. However, the other minima represent intermediate folding conformations in which the protein may become trapped on its way to achieving the native state. What happens to a protein once it enters one of these traps depends on the protein. Some proteins are able to escape the traps through fluctuations in thermal energy. However, other proteins cannot rescue themselves and under normal

conditions would remain misfolded and inactive, or would aggregate. GroEL is believed to facilitate refolding by binding these trapped intermediates, possibly unfolding them, and releasing them into a sequestered environment in which folding can begin anew. Rescuing proteins from these energy wells necessarily requires energy input, and this energy is supplied by the binding and hydrolysis of ATP. ATP not only provides the energy for protein refolding, but also acts as the timer that controls the process (20). ATP is the driving force for the important allosteric structural changes that are the critical elements of the GroEL reaction cycle.

1.3 The Workings of GroEL

It was first realized in the late 1980's that the GroE complex was important in post-translational protein processing when it was shown that GroEL and GroES together were required for the assembly of ribulose bisphosphate carboxylase (Rubisco) oligomers. This was first demonstrated with native Rubisco particles within a transformed *E. coli* cell (21) and later with unfolded Rubisco protomers and purified GroEL/ES *in vitro* in an Mg-ATP dependent reaction (22). It was soon shown that not only Rubisco but many different proteins were able to bind to GroEL in their unfolded, but not native, states (23). More recent experiments using artificial peptides suggest that GroEL does not prefer to recognize any particular secondary structure (24). This implies that GroEL is not only promiscuous in its selection of SPs, but it is able to discriminate between folded and unfolded proteins. GroEL's ability to bind a large variety of proteins explains the observation that the folding rate of proteins that fold spontaneously under certain conditions is usually decreased in the presence of GroEL. This is due to GroEL binding the folding intermediates of proteins that do not require it for folding, thus

slowing their progress to the native state. The crystal structure of GroEL (10), along with mutagenesis studies that identified the substrate binding sites (12), shed light on GroEL's preference for unfolded substrates. The surfaces of the apical domains that face the inside of the central cavity contain several highly conserved hydrophobic residues (11) that correspond well to the identified SP binding site. These residues on each subunit form a contiguous ring of hydrophobicity that lines the central cavity (Figure 1-2) (10).

Figure 1-2: Movement of the SP Binding Sites in Response to ATP/GroES. As GroEL undergoes its allosteric transitions upon binding ATP (the R state) and GroES (the R' state), the hydrophobic SP binding sites which line the entrance to the inner cavity are dispersed from their T state positions. This is the motion that would provide the power stroke to active unfolding. (See section 2.11).

These binding sites are specific for non-native peptides (25, 26), because unfolded proteins tend to contain exposed hydrophobic surfaces, surfaces that become buried upon the peptide achieving the correct fold (27, 28). Upon the movement of the apical domains following ATP binding, these hydrophobic residues become buried, releasing the SP into the central cavity. Because the interaction between the SP and GroEL is strong, it is possible that the SP might remain bound as the apical domains undergo their large conformational change. In that case, the protein would stretch with them, and actively unfold (29).

1.4 The GroE Reaction Cycle

The controlling force behind the GroE cycling mechanism is ATP. It was realized early on that the actions of GroEL were ATP dependent and indeed Mg and ATP are absolutely required for the reconstitution of active Rubisco *in vitro* (22). Later it was determined that K^+ was required for the binding of ATP and that the ATPase activity of GroEL increased with increasing K^+ concentrations (30, 31). Since then, a large number of experiments have attempted to elucidate in great detail how ATP controls the GroE cycle (Figure 1-3). In the absence of GroES, the cycle time of a single ring of GroEL

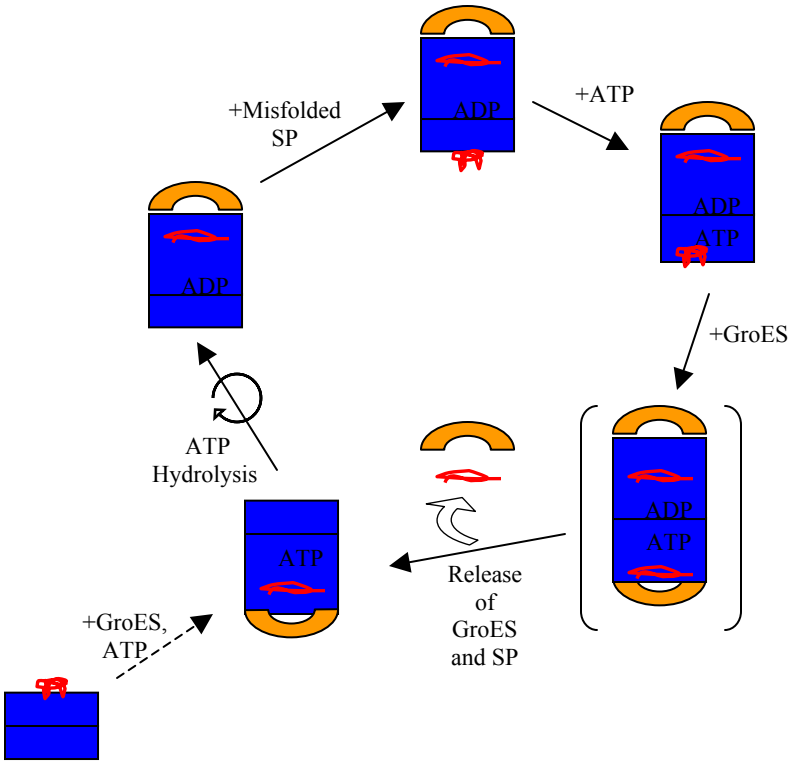

Figure 1-3: The GroE Reaction Cycle. GroEL is shown in blue, GroES in orange, and SP in red. The events depicted are described in the text. The GroES/GroEL/GroES complex is shown in brackets due to the uncertainty that this football complex is actually a requisite part of the cycle.

(the hemicycle time) varies from about 7-60 seconds at 37°C depending on a number of factors, including the $[K^+]$ and the presence or absence of unfolded substrate protein. Seven ATPs are able to bind to each ring of GroEL. ATP binding within a ring occurs with a high degree of positive cooperativity (32, 33). Prior to ATP binding, a GroEL ring is in its most compact conformation, the T state (Figure 1-4), in which the central cavity volume is at a minimum, and the SP binding sites are most accessible (Figure 1-2). Thus, it is this conformation to which unfolded SP binds most favorably (33, 34). ATP binding to a single ring results in large structural changes critical to the function of the system in which the domains can be treated as moving as rigid bodies around the inter-domain hinge regions (Figure 1-4). ATP binding results in the so-called T→R transition, (in which T and R refer to the tight and relaxed allosteric states of classic MWC theory) (33). In this transition, the intermediate domains move downward, toward the equatorial plate. The apical domains move slightly upward and twist about 25° in a anticlockwise direction relative to the equatorial domain (35, 36). This results in an expansion of the volume of the central cavity and also disperses the SP binding sites (Figure 1-2). Only ATP binding, not hydrolysis, is required for these structural changes, since a non-hydrolysable ATP analogue, AMP-PNP, is also able to induce these events (8, 37). In the presence of GroES, these structural transitions are accentuated, and GroEL undergoes the R→R' transition. The intermediate domain moves 20° toward the equatorial domain, an event which moves residues critical for subsequent ATP hydrolysis into closer proximity to the bound ATP, sequestering the ATP within its binding site (14) . The apical domains move upward 60° and twist 90° in a clockwise direction compared to their T state positions (35). Since the apical domains had already moved 25° anticlockwise during the

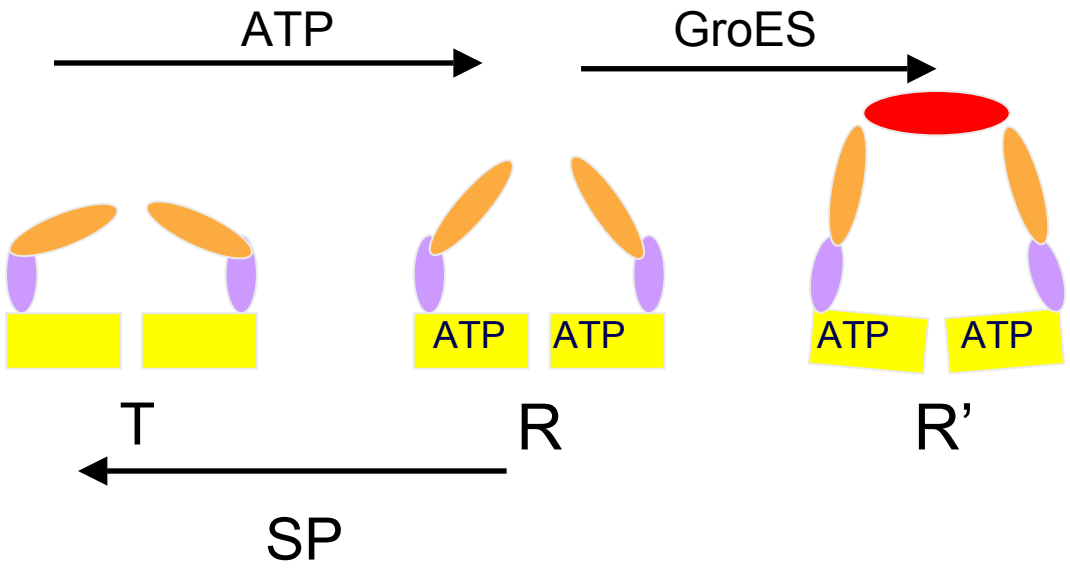

Figure 1-4: Allosteric Structural Transitions of GroEL. The domain movements within a single ring in response to ligands are drawn. The equatorial domains are shown in yellow, the intermediate domains in purple, the apical domains in orange, and GroES is shown in red. The binding of ATP favors transition to the R state, and, in the presence of GroES, the R' state. SP prefers to bind to the T state, when the SP binding sites are most exposed.

T→R transition, they therefore must move 115° in a clockwise direction during the R→R' transition (36).[1] This has a significant effect on the properties of the central cavity. The cavity increases drastically in volume from 85,000 $Å^3$ to 175,000 $Å^3$ (14). The hydrophobic SP binding sites become completely buried in the walls of the central cavity (Figure 1-2), and the cavity now becomes hydrophilic in nature (14). SP that may have been bound to the SP binding sites must be released into the expanded cavity, which is now capped by GroES. Because of the cavity's hydrophilicity, it now provides a favorable folding environment for the released SP. The domain movements of both the

[1] The allosteric pathway is typically represented in the literature as T→R→R'. However, this mechanism is based, at least in part, on the assumption that the T state cannot bind ATP, and that therefore GroES cannot bind to the T state. This assumption is now known to be incorrect (see Chapters 3 and 4), and therefore it is possible that the actual pathway is R→T→R', or even some other variant.

T→R transition and R→R' transition are concerted in nature; all seven subunits undergo the motion at the same time, as evidenced by structural analyses (14) and molecular dynamics simulations (38). Once in the R' state, the so-called $GroEL_{14}$-$GroES_7$ "bullet" structure, ATP hydrolysis occurs in a quantized manner, demonstrated by the release of 7 moles of inorganic phosphate per GroEL 14-mer in the presence of GroES (20). The resulting ADP bullet (the *cis*-complex) is highly stable (20). SP that may be sequestered beneath the GroES cap is unfolded, as has been shown using fluorescence anisotropy measurements (39) and hydrogen/tritium exchange measurements (8), among other methods. Thus, ATP binding serves as the driving force for releasing unfolded protein into the central cavity. The coupling of ATP binding and hydrolysis to large, cooperative structural changes is a general feature of molecular chaperones such as, for example, Hsp90 (4).

The GroEL/GroES/ADP/±SP complex remains intact until ATP binds to the distal ring (*trans* ring) (Figure 1-3) (20, 37). ATP binding causes the release of the ligands from the *cis* ring, with GroES necessarily leaving first, followed by the SP and ADP. The allosteric signal that *trans*-ATP binding initiates is currently unknown, although the signal may be communicated through a subtle structural change that occurs at the inter-ring interface (equatorial plate) upon the formation of the asymmetric complex. The center of the plate moves away from the *cis*-cavity by a few degrees during complex formation (Figure 1-4) (14, 29). *Trans*-ATP binding may somehow affect this "tilting" of the equatorial domains and cause *cis*-GroES release. Once GroES is released from the *cis* ring, the ring collapses back to a more compact state, although whether it is the T or R state is unclear, and it probably depends on whether or not SP is present (see Chapter 5).

A new *cis*-complex can now be constructed on the *trans* ring once ATP is bound, although the exact order of events is poorly defined. It is known that ATP hydrolysis must occur in the *cis*-ring prior to SP and GroES binding to the *trans* ring (17), although it is not known whether *trans*-GroES binding must occur in order for GroES to dissociate from the *cis* ring. Thus, it is not known whether GroES/GroEL/GroES football complexes are a requisite part of the reaction cycle (Figure 1-3). However, because one folding chamber is falling apart as the other is forming, the GroE system is inherently efficient. The clearing of ligands from one ring does not have to occur prior to the addition of ligands to the other ring, thus allowing the two rings to operate in an alternating fashion (17). GroEL operating in this manner has been called a "two-stroke motor" (29).

It is worth noting at this point that the reaction pathway of GroEL is not an entirely reversible process; that is, some elements of the pathway are "driven" in one direction by the presence of GroES (Figure 1-5). In the absence of GroES, the binding of SP to the T (or R) states is reversible, as is the T→R allosteric transition itself. ATP binding is also reversible. However, once GroES becomes involved, the events are forced to occur in a certain order. For example, the R'→T transition cannot occur within a ring when GroES is bound. GroES is not released prior to ATP hydrolysis in the *cis*-ring (17). SP cannot be released prior to GroES release. This is an important point, because in the presence of GroES, the system cannot reach an equilibrium, making

Figure 1-5: Certain Steps of the GroE Reaction Pathway are "Driven" Forward by GroES. The reversible and irreversible steps of the reaction pathway for one GroEL ring are depicted. The GroEL ring is noted in the scheme as its allosteric state, T or R. No assumptions are made as to the relative rates or favorability of the events. This scheme simply depicts whether or not they can occur. Forbidden transitions are noted with an X. Species which cannot exist are noted in red.

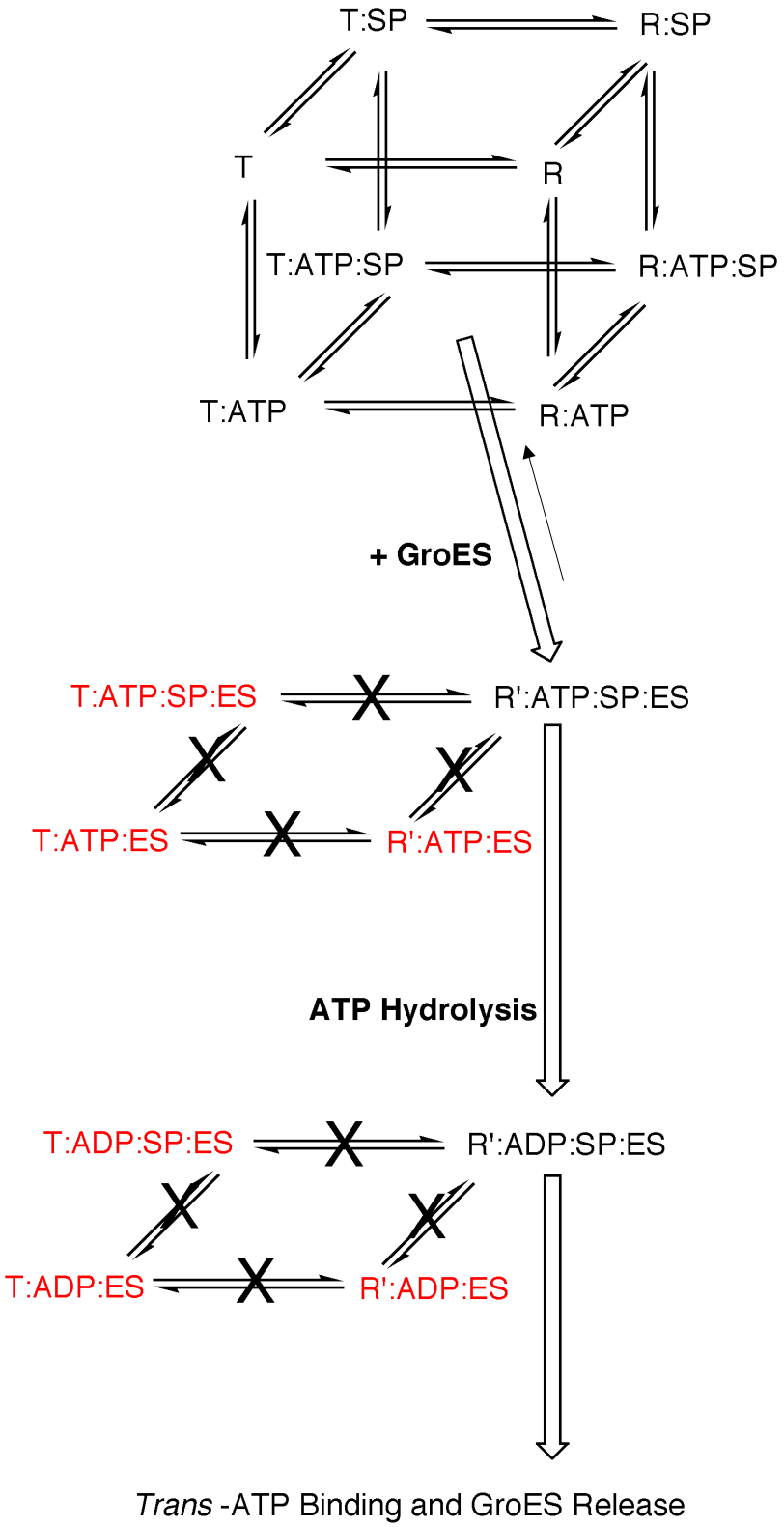

Trans -ATP Binding and GroES Release

steady-state kinetic measurements of the pathway only somewhat useful in defining the rates of reaction.

1.5 Active or Passive Refolding?

The previous section defined the events that occur during the reaction cycle, and they have been well characterized and well accepted, at least in a general sense. However, what actually is happening to the SP between the time it binds to the closed T ring and when it is ejected into the central cavity remains unclear. This is the major point of contention: whether GroEL plays a passive or an active role in the (un)folding of the SP (8).

The passive refolding hypothesis, also known as the Anfinsen's cage model, (7, 40) states that the inner cavity of GroEL simply serves as a sequestered, hydrophilic environment for the SP, allowing it to fold in isolation and avoid aggregation. For example, rhodanese has been shown to fold to the native state while trapped inside the central cavity, (39). In this experiment, a single-ringed mutant of GroEL (SR1) was used in order to prevent ATP binding to the *trans* ring from releasing GroES, thus trapping rhodanese in the central cavity for an extended period of time and preventing more than one turnover from occurring. Rhodanese refolded with a half-time of 7 minutes. Re-folding experiments using malate dehydrogenase (MDH) as a substrate protein were also said to be consistent with this mechanism, since little unfolding (as measured by deuterium exchange) was seen immediately following ATP/GroES addition to SR1/MDH (41). Significant de-protection was seen only at later time points following a period of isolation in the SR1 cavity. Such experiments, however, significantly perturb the GroEL reaction cycle by artificially extending the time SP spends in the central cavity (5). As

will be shown in this dissertation, SP is given only, at most, 12 seconds to fold in the central cavity before it is released. Therefore, substrates that refold in 7 minutes within the GroEL/GroES complex are clearly not doing so under physiological conditions. In other studies with rhodanese, in which GroES is allowed to release from GroEL on its normal time scale, multiple rounds of SP binding and release are necessary in order for rhodanese to reach the native state (42). Therefore, experiments which artificially extend the lifetime of the GroEL/GroES complex are ignoring what is happening to the SP during the multiple turnovers.

The active unfolding model views GroEL as a molecular machine, one that does actual work on the SP. In this view, ATP binding and hydrolysis is coupled to the forceful unfolding of the protein. This type of mechanism has been described by Todd *et al*. (19) as an "iterative annealing mechanism" in that misfolded proteins can bind repeatedly to GroEL, with each round of subsequent ATP binding and hydrolysis causing unfolding of the misfolded substrate. Repeated binding and unfolding, or annealing, cycles optimize the final yield of properly folded substrate (5, 19). When the apical domains move upon ATP binding, the bound substrate is pulled apart and unfolded as the substrate binding sites move and twist away from each other (8, 29). By doing so, the protein now has another chance to fold to the native state. Once unfolded the protein is given a chance to refold within the cavity, but is ejected from the cavity upon the release of GroES whether it has folded correctly or not (20, 29). Since the cycle time of a GroEL ring is about 7-13 seconds in the presence of SP at 37°C at 100 mM K^+, the protein would have to be unfolded within that time span. This was demonstrated using hydrogen/tritium exchange experiments with labeled Rubisco (8). In fact, an unfolding

event occurred within five seconds, consistent with unfolding occurring during the domain movements and before the protein is suspended in the central cavity. Hydrogen/deuterium exchange experiments have also demonstrated the viability of iterative annealing in GroEL, in that GroEL is able to repeatedly cause de-protection of core amide protons during rounds of ATP binding and hydrolysis (43-45). Finally, a theoretical study (46) has been done which has modeled SPs as beads on a string, folding in a cubic box representing the central cavity. The interior environment of the box was alternately switched between being hydrophobic and hydrophilic. The studies concluded that the yield of native protein was maximized when the cavity environment changed relatively rapidly, consistent with the iterative annealing mechanism (46). The passive mechanism would prefer that the central cavity remain hydrophilic indefinitely.

Recent experiments have shown that GroEL is required for the refolding of aconitase, a substrate that is too large to fit within the central cavity (47). Therefore, at least in this case, encapsulation and the sequestration of the SP cannot lead to its refolding. Since the GroEL is binding the aconitase, however, it is tempting to suggest that its refolding is caused by active unfolding, where encapsulation is not necessarily required. Examples such as these, along with the work presented in this thesis, show that active unfolding of SP by GroEL is an attractive and plausible mechanism to explain the actions of GroEL on at least some of its known substrates.

1.6 Allosteric Domain Movements Drive Unfolding

If active unfolding does take place, then it must be driven by the large, allosteric domain movements that occur in response to ATP similar to what has been hypothesized to occur in Hsp70 (3). Therefore, in order to definitively show that active unfolding

occurs, a detailed understanding of GroEL's complex ATP binding properties must be obtained. Horovitz and colleagues have developed a model of nested cooperativity to explain why GroEL's ATPase activity rises at increasing, relatively low ATP concentrations but then decreases as [ATP] is increased even further (Figure 1-6) (33).

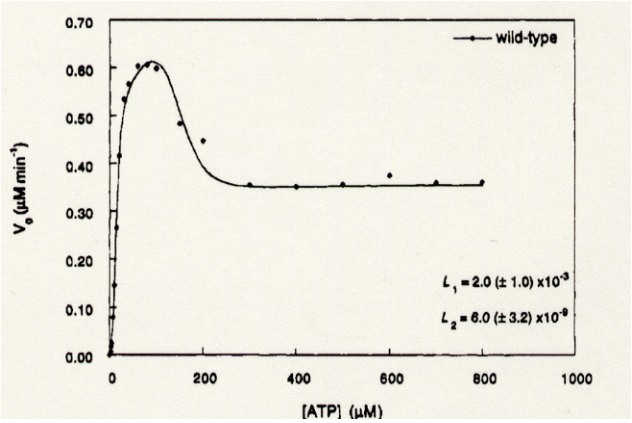

Figure 1-6: ATPase Rate Dependence on [ATP]. These data, taken from Yifrach and Horovitz (33), show the unusual [ATP] dependence of GroEL ATPase activity which prompted the formulation of the nested cooperativity model.

Ligand-free GroEL has both rings in their most compact form and with their hydrophobic binding sites both facing the central cavity. This is known as the TT state. The T state has a high affinity for substrate protein (due to the exposed binding sites) and low affinity for ATP. Actually, as originally defined, it was assumed that the T state could not bind or hydrolyze ATP, an exclusive binding assumption. Upon the binding of ATP, the T → R transition occurs where the apical domains begin to move upward and the binding sites move apart (Figures 1-2 and 1-4). The R state has a low affinity for substrate and a high affinity for ATP. According to the model of nested cooperativity, ATP binds with positive cooperativity within the same ring which undergoes the T → R transition in a concerted all or none motion: an MWC allosteric transition (48). Between rings, ATP binds with negative cooperativity and thus GroEL undergoes a stepwise TT → TR → RR

transition with increasing concentrations of ATP: a KNF transition (49). In this model, the ATPase rate rises with increasing, relatively low ATP concentrations due to the population of the TR state, in which the T ring is inactive and the R ring is highly active. (The use of the word "highly" here is relative; GroEL actually has a very weak ATPase rate, about 2-3 turnovers/minute under normal conditions). The ATPase rate decreases at high [ATP] due to the shifting of the equilibrium to the RR state, in which the two R rings combined have a lower activity than the R ring alone in the TR state. Two allosteric constants can be defined for these transitions: L_1=[TR]/[TT] and L_2=[RR]/[TR], with $L_2 << L_1$ due to the inter-ring negative cooperativity (33, 50). Because protein unfolding is coupled to these structural transitions, these constants define what is happening to a substrate when bound to GroEL. These constants, especially L_1 in the presence of GroES, dictate how long a substrate is exposed to a hydrophobic (T state) versus hydrophilic (R state) environment and consequently how long a substrate remains bound to GroEL versus how long it is encapsulated within the cavity. ATP binding increases L_1 since the R state has a higher affinity for ATP, and SP binding decreases L_1 since the T state has a higher affinity for the substrate (33, 34). However, it is difficult to relate these equilibrium constants to the actual GroEL mechanism, since, in the presence of GroES, the system is never at equilibrium. Because GroES and ATP are always present, GroEL is constantly in motion. A more useful quantitative description would involve the rate constants of each transition. However, this is also difficult to accomplish since it is hard to isolate one structural transition from another in real time.

1.7 Specific Aims

The goal of this work was to gain a better understanding of the allosteric transitions which accompany the potential unfolding of substrates by GroEL, and the transitions which accompany other steps in the GroEL reaction cycle. This topic was approached in three general ways, which are described here briefly, and expounded on later in the introductions to the individual dissertation chapters:

1) In order to better understand the T $\rightarrow$ R and subsequent R $\rightarrow$ R' transitions, which are the important events in SP unfolding, it was critical to be able to control these transitions. Previous work in the lab made use of a GroEL mutant in which an intrasubunit salt bridge, D83/K327, that is present in the T state but broken in the R state, was replaced with cysteine residues (51). This allowed for the controlled introduction of disulfide bonds or chemical cross-links that served to lock rings into the T conformation. For this dissertation, a detailed study was done on a mutant in which an *inter*subunit salt bridge was replaced with a double cysteine pair. This salt bridge, R197/E386, was chosen because introduction of disulfide bonds or chemical cross-links could potentially prevent the large, twisting motion which the apical domains must undergo during the T $\rightarrow$ R and the subsequent R $\rightarrow$ R' transition and which would serve as a driving force in SP unfolding. The effect of cross-linking this mutant on the various aspects of GroEL behavior was examined using a wide variety of techniques.
2) The effect of substrate protein on GroEL's ATPase activity and the T/R equilibrium was examined. This work expanded on data obtained by Yifrach and Horovitz (34) in which the addition of unfolded SP increased ATPase activity

approximately 4-fold. They attributed this increase in rate to a shift in the equilibrium from the RR state to what they considered to be the more active TR state. The studies presented here attempt to discover whether or not this is the actual reason for substrate stimulation. They expand on this result by using a wider range of SPs, and by looking at the effect of SP on ATPase activity in real time. The double cysteine mutants were used in these experiments in order to determine the effect of SP on GroEL that has been locked in the T state. The ultimate goal of these studies was to design a general mechanism that could explain the effects of SP, cross-linking, and the T $\rightarrow$ R transition on ATPase activity.

3) The release of GroES from the $GroES_7$-$GroEL_{14}$ bullet complex in response to ATP binding to the *trans* ring was examined in great detail. This event has been implicated as being the rate-limiting step in the GroEL reaction cycle (17). This work expands on a result obtained by Rye *et al*. (17) in which they found that SP increases the rate of GroES release from the bullet complex. The work presented here addresses the underlying reasons for this result, and specifically concentrates on whether the allosteric state of the *trans* ring affects the rate of release. This work makes use of GroEL and GroES mutants labeled with fluorescent probes that can act as a fluorescence resonance energy transfer (FRET) pair (52). Release kinetics were studied in a stopped-flow fluorescence instrument using these labeled mutants under a wide range of conditions.

Chapter 2

General Methods and Experimental Procedures

This chapter details the experimental procedures and laboratory techniques used in all studies presented in this dissertation. Techniques that are more specific to the studies in an individual chapter are discussed in the methods section of that chapter.

2.1 A Note on Protein Concentration

All GroEL and GroES concentrations noted in this dissertation, unless otherwise indicated, are the *monomer* concentrations. In situations where the oligomer concentrations are informative, they will be distinguished by the presence of subscripts, ie. $GroEL_{14}$ and $GroES_7$.

2.2 Site Directed Mutagenesis of GroEL and GroES

All GroEL and GroES mutants were prepared using plasmids pGEL1 and pGES1 respectively (a kind gift of Dr. Ed Eisenstein). These plasmids have the *E. coli* GroEL or GroES gene cloned in a pkk233-2 expression vector (Amersham) (53), a vector that confers ampicillin (Amp) resistance. Site-directed mutagenesis was accomplished using either the U.S.E. Mutagenesis Kit (Amersham) or the Quick-Change kit (Stratagene), using the protocols detailed in the kits. The mutagenic primers used for each mutant are given in the individual chapters. The primers were designed in all cases possible to add or delete a convenient restriction site in order to provide an easy way of detecting potentially successful mutagenesis even before sequencing. In the cases where the Stratagene kit was used for mutagenesis, ordering primers that were gel-purified was found to be a critical factor in successful mutagenesis due to this kit's reliance on PCR as its method of introducing mutations. All restriction enzymes were purchased from Roche. Small-scale plasmid preps of 3 ml of culture or less (minipreps) were done using standard SDS/NaOH lysis and phenol/chloroform extraction protocols (54) or were done

using the Qiagen Qiaprep Spin Miniprep Kit. Plasmid extractions of 100 ml of culture were done with the Qiagen Hi-Speed Plasmid Midi Kit. For all mutants, the final mutated plasmid was transformed into *E. coli* strain JM105 (Amersham) by electroporation using a BTX electroporator. Once transformed, glycerol stocks and purified plasmid were prepared from the same single colony from an overnight plate. All plasmids were sequenced at the University of Maryland DNA sequencing facility. For GroEL mutants, three sequencing primers were required to obtain full coverage of the sequence with some overlap. These primers were EL5' (5'CATCCGGCTCGTATAATGTG3'), EL3' (5'ATCAGACCGCTTCTGCG TTC3'), and EL570 (5'GAAGGTATGCAGTTCGAC3'). For GroES mutants, only EL5' and EL3' were used, and these provided a full read from both the 5' and 3' directions. All mutants discussed in this dissertation had confirmed correct sequences.

2.3 Polyacrylamide Gel Electrophoresis (PAGE)

Gel solutions were prepared according to standard recipes (54, 55) using a pre-mixed 30% acrylamide/bis-acrylamide (29:1) solution from Bio-Rad. Unless otherwise noted, gels were poured using 0.75 mm spacers 10 x 8 cm glass plates. The apparatus used was the Hoefer SE250 Mini-Vertical unit. Gels were typically run at 15 mAmps per gel, using Tris/glycine/SDS running buffer. Gels were visualized by staining with PhastBlue (a Coomassie Blue variant by Amersham), and de-staining with 30% methanol/10% acetic acid followed by 10% ethanol/10% acetic acid. Typically, gels contained SDS and loading buffer contained DTT. Occasionally, native PAGE was performed instead, and this was done by leaving the SDS out of the gel solutions, loading buffer, and running buffer. More often, non-reducing SDS-PAGE was needed, and this

was done simply by leaving DTT out of the loading buffer. When quantitative results were desired, special care was taken to ensure that all gel plates were clean and dust-free. The first and last lanes were usually not used for quantitation due to band curvature. 40 pmols of protein was found to be an ideal amount of protein for quantitation, and GroEL was usually quantitated on a 12% gel. Gels were quantitated by densitometry using the PDSI hardware and ImageQuant software from Molecular Dynamics.

2.4 Purification of GroEL

The importance of using GroEL which was as pure as possible in these experiments cannot be overstated. It is a point that is insufficiently appreciated in much of the published work on GroEL. Contaminating protein can have significant effects on measurements of ATPase rates, to name just one example. In a few cases, results here differ with the published results of other groups. In most of these cases, these differences can be attributed to the impurity of the GroEL used to obtain the published results.

GroEL was purified according to established protocols with several modifications. 4.5 to 6 liters of JM105 *E. coli* containing the pGEL1 plasmid, with or without mutations, were grown at 37°C in LB media containing 100 ug/ml Amp to an optical density of about 0.3 at 600 nm. Protein overexpression was initiated with the addition of IPTG to a final concentration of 0.5 mM, at which point the temperature was decreased to 30°C. Induction was allowed to proceed for 12-16 hours. Cells were harvested by centrifugation and resuspended in lysis buffer containing 50 mM Tris pH 8, 1 mM EDTA, 5 mM $MgCl_2$, 1 mM DTT, 5 mM ε-amino-n-caproic acid, and 1 mM benzamidine. The cells were lysed by sonication using a Branson sonicator at power level 5 with a 50% duty cycle for 75 seconds for each 50 ml portion of cell suspension.

Following removal of cell debris by centrifugation at 32,500 x g, 4°C for 30 minutes, nucleic acid was removed by precipitation with streptomycin sulfate at a final concentration of 6 mg/ml. Precipitate was removed by centrifugation at 32,500 x g, 4°C for 60 minutes, and the supernatant was collected as the crude lysate. The lysate, typically 150 ml, was loaded onto a 500 ml DEAE Sepharose Fast Flow column (Amersham) which had been equilibrated with 500 ml of 200 mM Tris pH 8 and 1800 ml of Buffer A (50 mM Tris pH 8, 1 mM EDTA, 5 mM $MgCl_2$, and 1 mm DTT). Following elution of the flow-through, the remaining protein was eluted with a 2L gradient from 0 mM to 500 mM NaCl on a Pharmacia FPLC System. The fractions containing GroEL (as determined by SDS-PAGE) typically eluted at a conductivity of about 28 mS, with a total volume of 170 ml. To concentrate this large volume, saturated ammonium sulfate was added to a final concentration of 65% and the solution was left stirring at 4°C overnight. The following day, the precipitate was recovered by centrifugation at 10,000 x g, 4°C for 30 minutes, and resuspended in 15-20 ml of S300 buffer (50 mM Tris pH 7.5, 1 mM EDTA, 10 mM $MgCl_2$, and 1 mM DTT). The protein was then de-salted by loading it onto a 300 ml S300 Sephacryl gel filtration column (Amersham) that had been equilibrated with 300 ml of S300 buffer. The flow-through (about 60 ml) was collected and concentrated to about 10 mg/ml using Centriplus concentrators (Millipore) with a MW cutoff of 50,000 Da. This crude GroEL was then stored at -80°C until the subsequent steps could be performed.

The final part of the purification involved an acetone precipitation modified from Voziyan and Fisher (56), and was the critical step in obtaining high purity GroEL. The idea behind this step is that due to GroEL's ability to bind hydrophobic, unfolded

proteins, it would be stable in the presence of a hydrophobic solvent. Pure acetone was added drop-wise to crude GroEL, which was being rapidly stirred, to a final concentration of 45%, resulting in the precipitation of all proteins in the solution. Following centrifugation at 32,500 x g, 25°C for 30 minutes, the pellet was resuspended in 10 mM Tris pH 7.5, 10 mM MgAc, and 1 mM DTT. Only GroEL is able to resuspend in the buffer, whereas the contaminating proteins remain precipitated. This precipitate was removed by centrifugation at 32,500 x g, 25°C for 60 minutes and the supernatant, containing pure GroEL, was collected. To remove any trace of acetone and to concentrate the sample, saturated ammonium sulfate was added to a final concentration of 65%, followed by centrifugation at 10,000 x g, 25°C for 30 minutes. GroEL was resuspended in 10 mM Tris pH 7.5, 10 mM MgAc (and 1 mM DTT in the case of mutants containing cys residues) and de-salted on a PD-10 column (Amersham). The final product was concentrated in the Centriplus-50 concentrators, aliquotted, and frozen at -80°C. The final concentration was checked by measuring absorbance at 280 nm, using an extinction coefficient of 9600 $M^{-1}cm^{-1}$.

The purity of the GroEL preparations was confirmed by the presence of a single band on an SDS-PAGE gel (Figure 2-1), and by measuring tryptophan fluorescence in 6 M guanidine HCl. GroEL contains no native trp residues, and thus a low fluorescence emission at 350 nm following excitation at 280 nm is a good indicator of GroEL purity (57). Bovine serum albumin (4 trp/mol BSA) in 6 M guanidine HCl was used as a standard. Typically, the trp fluorescence of the GroEL preparation indicated the presence of 0.6 mols trp/mol $GroEL_{14}$. Assuming an average of about 3 trp residues in a typical protein, this gives an estimate of 0.2 SP/$GroEL_{14}$.

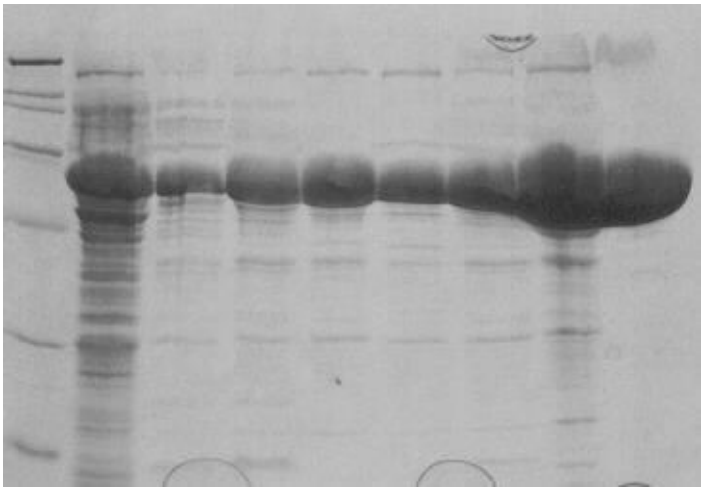

Figure 2-1: Purification of GroEL. Lane 1= MW standards. Lane 2= Crude lysate. Lanes 3-7= Fractions from DEAE column. Lane 8= Pool from S300 de-salting column. Fraction 9= Pure GroEL following acetone treatment.

Finally, it was confirmed that, under the conditions used in all experiments, GroEL was indeed a 14-mer and was not separating into either monomers or single rings. This was done for $GroEL_{WT}$, and for all GroEL mutants, using analytical gel filtration chromatography.

2.5 Purification of GroES

GroES was purified using methods modified from published protocols (58). Crude cell lysate from 4.5 L of JM105 containing plasmid pGES1 with or without mutations was prepared using the procedure described above for GroEL. This lysate was then placed in an 80°C water bath and constantly stirred until the lysate temperature was 70°C. This temperature was maintained for 10 minutes. Precipitated proteins were removed by centrifugation at 32,500 x g, 25°C for 30 minutes. Saturated ammonium sulfate was then added to the supernatant to a final concentration of 65%, and the precipitation was allowed to stir overnight at 4°C. Following centrifugation at 10,000 x

g, 4°C, for 30 minutes, the pellet was resuspended in 15-20 ml of G25 buffer (10 mM Tris pH 7.5, 0.1 mM EDTA, 0.1 mM DTT). This was de-salted on a 150 ml G25M column (Amersham) which had been equilibrated with 300 ml G25 buffer. The 60 ml of flow-through at pH 7.5 was then jumped to around pH 5.1 by the rapid addition of 80 ml 50 mM NaOAc pH 5. Three separate runs were done on a 75 ml SP Sepharose HP column (Amerhsam) equilibrated with 400 ml 50 mM NaOAc, 0.1 mM EDTA, 0.1 mM DTT. For each run, one portion of the protein solution (about 50 ml) was loaded onto the column. Following elution of the flow-through, GroES was eluted with a 750 ml gradient from 0 mM to 200 mM NaCl. Fractions containing GroES as determined by SDS-PAGE were pooled and saturated ammonium sulfate was added to a final concentration of 65%. The ammonium sulfate precipitations from all three runs were combined and allowed to stir overnight. Following centrifugation at 10,000 x g, 4°C, for 30 minutes, the pellets were resuspended in 5 ml 10 mM Tris pH 7.5 and the resulting solution was de-salted on a series of PD-10 columns equilibrated in the same buffer. This de-salted solution was concentrated on Centricon concentrators with an MW cut-off of 10,000 Da. The final concentration was determined by measuring the absorbance at 280 nm using an extinction coefficient of 1200 $M^{-1}cm^{-1}$. The final product showed a single band on an SDS-PAGE gel (Figure 2-2A).

2.6 Purification of His-Tagged GroES

1 L of JV 30 *E. coli* containing plasmid pGES1His (gift of E. Eisenstein) was grown and lysed as described above for GroEL. This crude lysate was mixed with 4 ml of Ni-NTA resin (Qiagen), (which had been equilibrated with 10 mM imidazole, 20 mM Tris pH 8, and 300 mM NaCl) for 30 minutes on ice. The lysate/resin was then loaded

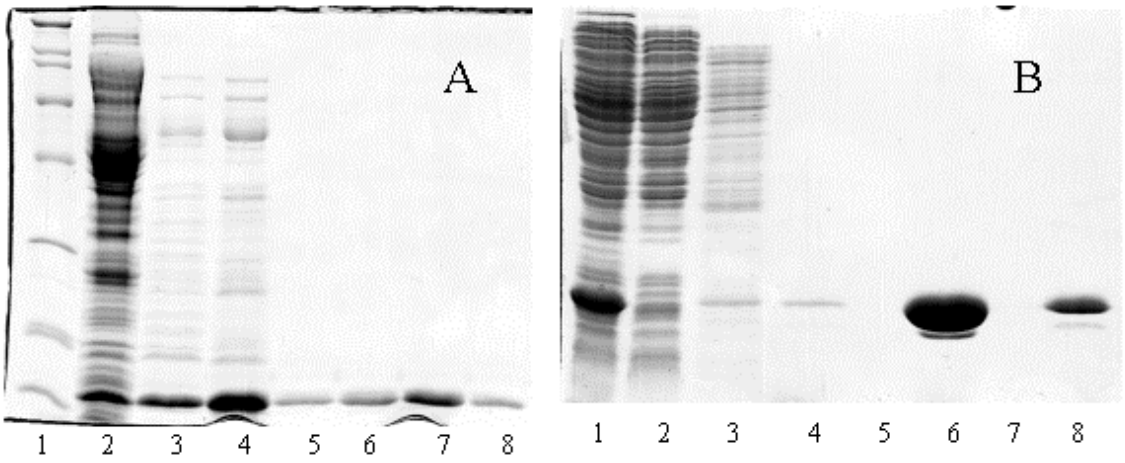

Figure 2-2: Purification of GroES. A) Purification of wild-type GroES (12% gel). Lane 1= MW standards. Lane 2= Crude lysate. Lane 3= Post-heat treatment. Lane 4= Pool from G25 de-salting column. Lane 5-7= Pools of the three SP column runs. Lane 8=Final product, pure GroES. **B**) Purification of his-tagged GroES (15% gel). Lane 1= Crude lysate. Lane 2-4= 60 mM imidazole washes. Lane 5= blank. Lane 6= 250 mM imidazole elution. Lane 7= blank. Lane 8 = Final product, pure his-tagged GroES. Note the faint, lower band of wild-type GroES which is the non-induced GroES produced normally by the cells.

into a syringe barrel and washed with 60 mM imidazole, 20 mM Tris pH 8. For the first few washes, this buffer also contained 300 mM NaCl, which was left out of the last wash. His-tagged GroES was eluted from the column with 250 mM imidazole, 20 mM Tris pH 8. The eluent was concentrated in a Centriplus-10 and then buffer exchanged on a PD-10 equilibrated in 10 mM Tris pH 7.5. The PD-10 eluent was then concentrated, aliquotted, and stored at -80°C. The final concentration was determined as above for wild-type GroES, and the final product was a single band on an SDS-PAGE gel (Figure 2-2B).

2.7 Preparing GroEL Cysteine Mutants for Cross-Linking or Labeling

In order to ensure that all thiols were fully available for cross-linking or labeling, freshly reducing pure GroEL samples was essential. This was done by adding 10-20 mM DTT to enough GroEL as was required for that day's procedure and allowing it to react

for 30 minutes. The DTT was then removed by de-salting on a PD-10 column equilibrated in 10 mM Bis-Tris pH 7.0, 10 mM MgAc, followed by concentration with a Centricon-30 (Millipore) to a useful concentration. To eliminate oxidation by any contaminating metal ions that might be present, all buffers were treated with Chelex resin (Sigma) to remove these ions (prior to Mg^{2+} addition). Under these conditions, no oxidation was detectable on a non-reducing SDS-PAGE gel.

2.8 GroEL Cross-linking

Two methods were used to induce disulfide bond formation in GroEL double cysteine mutants. The first was to use catalytic amounts of copper ($CuCl_2$), and the second was to use stoichiometric amounts of diamide, a reagent capable of forming disulfide bonds in a non-catalytic fashion (59). Unless otherwise noted, the GroEL concentration during these reactions was 40 μM. To quench these reactions, free cysteines were blocked with 40 mM N-ethylmaleimide (NEM, from Sigma) and 100 mM Tris pH 6.8. To quantitate oxidation, samples were boiled for 1 minute to expose the native, buried cys residues to NEM, and then diluted with SDS loading blue without DTT. The samples were boiled for an additional two minutes, and then loaded on the gel.

Chemical cross-linking reagents were also used in some experiments to insert irreversible cross-links of varying lengths between two cysteines (60, 61). These reagents were phenylenedimaleimides in the *ortho*, *meta*, and *para* conformations (oPDM, mPDM, and pPDM, respectively). mPDM was purchased from Sigma; oPDM and pPDM were purchased from Research Organics. 50 mM stocks of these reagents were made in DMSO and stored at -80°C. These reagents were added stoichiometrically in a volume of DMSO which did not exceed 10% of the total reaction volume. Cross-

linking was found to be complete in less than 5 seconds at room temperature. Free cysteines were blocked with NEM and cross-linking was quantitated by SDS-PAGE.

2.9 Coupled-enzyme ATPase Assay

The most commonly used method to measure ATPase activity in this dissertation makes use of a coupled-enzyme system that ties the production of ADP by GroEL to the oxidation of NADH by lactate dehydrogenase (LDH) according to the following scheme (Figure 2-3). This system has the benefit of allowing the monitoring of ATPase activity in real time, and has the added advantage of a built-in ATP regenerating system that ensures a constant ATP concentration. The system is dependent on the coupling enzymes and reagents (PK, LDH, NADH, and PEP) being in excess over GroEL to ensure an entirely coupled response. The oxidation of NADH was monitored at 340 nm in a Hewlett Packard 8453 UV/Vis spectrophotometer in kinetics mode. The system was programmed to collect data points every second for user-specified amounts of time. The cuvet holder was connected to a circulating water bath (VWR) to allow temperature regulation. This instrument does not require the cuvet to be covered during data collection, which allowed for the addition of reagents at any time during a measurement. Thus, rate changes in response to added reagents could be monitored in real time (Figure 2-4). Changes in absorbance were measured over various time intervals within a given trace. Non-linear or wavy traces were discarded. ATPase rates were calculated using the change in absorbance over a given time interval, the extinction coefficient of NADH ($6.22\ mM^{-1}cm^{-1}$), and by accounting for the GroEL concentration. Unless otherwise noted, the conditions used for all assays was 2 μM GroEL, 50 mM Tris pH 7.5, 100 mM

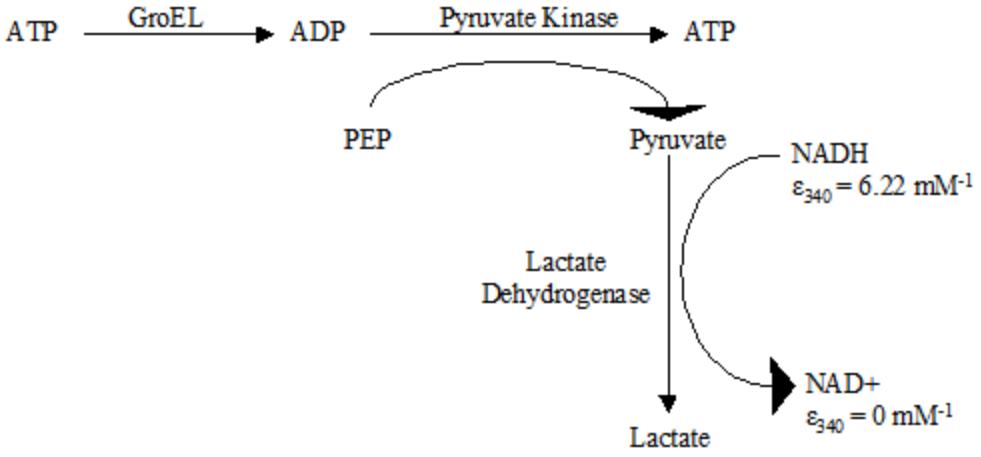

Figure 2-3: Coupled Enzyme ATPase Assay. Hydrolysis of ATP by GroEL is directly coupled to the oxidation of NADH by LDH through the intermediary enzyme, PK, which also serves to regenerate ATP. NADH oxidation is monitored at 340 nm since it absorbs at this wavelength and NAD^+ does not.

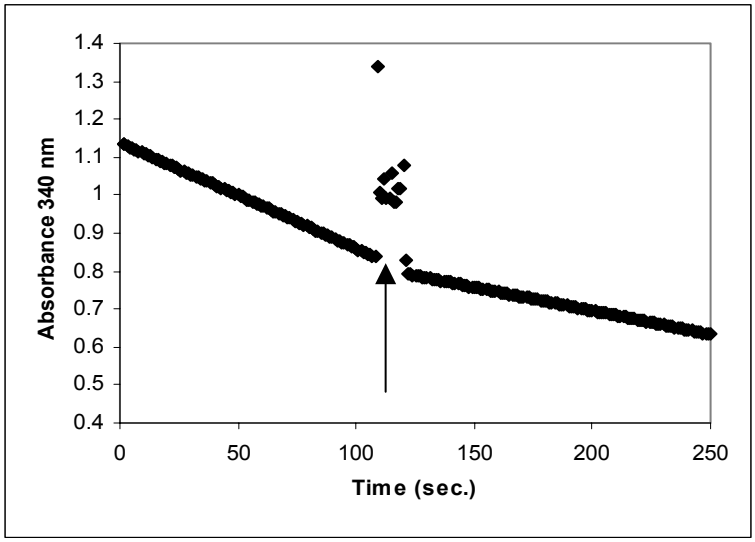

Figure 2-4: Monitoring ATPase Rate in Real Time. An example of a kinetic trace showing the decrease in absorbance at 340 nm. The trace begins by measuring the ATPase activity of GroEL alone. At the arrow, GroES was added mid-run and the rate slows. The outlying points are mixing artifacts created by the mixer interrupting the light beam.

KAc, 10 mM MgAc, 0.2 mM PEP, 0.2 mM NADH, 4 units LDH, and 5 units PK at 37°C.

2.10 Preparing Unfolded Protein Substrates

The two SPs most commonly used in these experiments were α-lactalbumin (α-LA, bovine) and malate dehydrogenase (MDH, mitochondrial, from pig heart). α-LA was purchased from Sigma and MDH from Roche, and neither was further purified before use. α-LA is known to remain unfolded in the presence of DTT and the absence of Ca^{2+} (34, 62), and therefore it was denatured in a large batch and stored at -80°C. Due to its ability to refold spontaneously (63, 64), MDH was freshly denatured before each experiment. To unfold both of these SPs, a concentrated aliquot of the protein was diluted into 2 mM Tris pH 8, 10 mM DTT and allowed to react for 10 minutes. The SPs were then diluted 5-fold into 0.01 N HCl and allowed to denature for 1 hour. MDH was used as is; α-LA was buffer exchanged on a PD-10 into 10 mM Tris pH 7.5, 10 mM MgAc and stored at -80°C until needed. Concentration was determined at 280 nm using extinction coefficients of 28,400 $M^{-1}cm^{-1}$ form α-LA and 6880 $M^{-1}cm^{-1}$ for MDH.

2.11 Computer Software

All protein structures shown in this dissertation were made with the free Protein Explorer software package at www.proteinexplorer.org (65). Unless otherwise noted, all data plotting and fitting was done with KaleidaGraph Ver. 3.5 (Synergy Software).

Chapter 3

Characterization of a GroEL Intersubunit Double Cysteine Mutant: R197C / E386C

3.1 Introduction

Like any machine, if GroEL is going to perform work, it must incorporate a "power stroke" into its mechanism of action. GroEL's power stroke is provided by the rigid body motions of its subunits when it undergoes its allosteric transitions upon binding ATP. A machine's effectiveness increases when all of its parts move in concert. Likewise, it is reasonable to assume that GroEL could exert a maximum unfolding force by having all of its subunits move in a single, concerted motion. Concerted motion has already been suggested by molecular dynamic simulations (38) and by the observation that the movement of one subunit is sterically hindered by the adjacent subunit unless the adjacent subunit is moving as well (14). Because concerted motion is a critical factor in forced unfolding, a further demonstration of its existence was sought. To accomplish this, a way of controlling the T$\rightarrow$ R and R$\rightarrow$ R' structural transitions was needed.

Extensive work in this laboratory (G. Curien, unpublished) has made use of a GroEL mutant, $GroEL_{IAX}$, in which a critical T state salt bridge, D83/K327, has been replaced by a pair of cysteine residues (51). This salt bridge connects the equatorial and apical domains within a single subunit in the T state (Figure 3-1, a and b). In the R and R' states, this salt bridge is broken. The introduction of a double cysteine pair allows for the insertion of disulfide bonds or chemical cross-linkers with the intent of tethering a subunit in the closed, T conformation. The hypothesis of this previous work was that a single disulfide bond or cross-link within a ring would be sufficient to tether the entire ring in the closed state, thus demonstrating concerted motion. This was indeed shown to be the case, and along with this, several other properties of the T and R states were discovered.

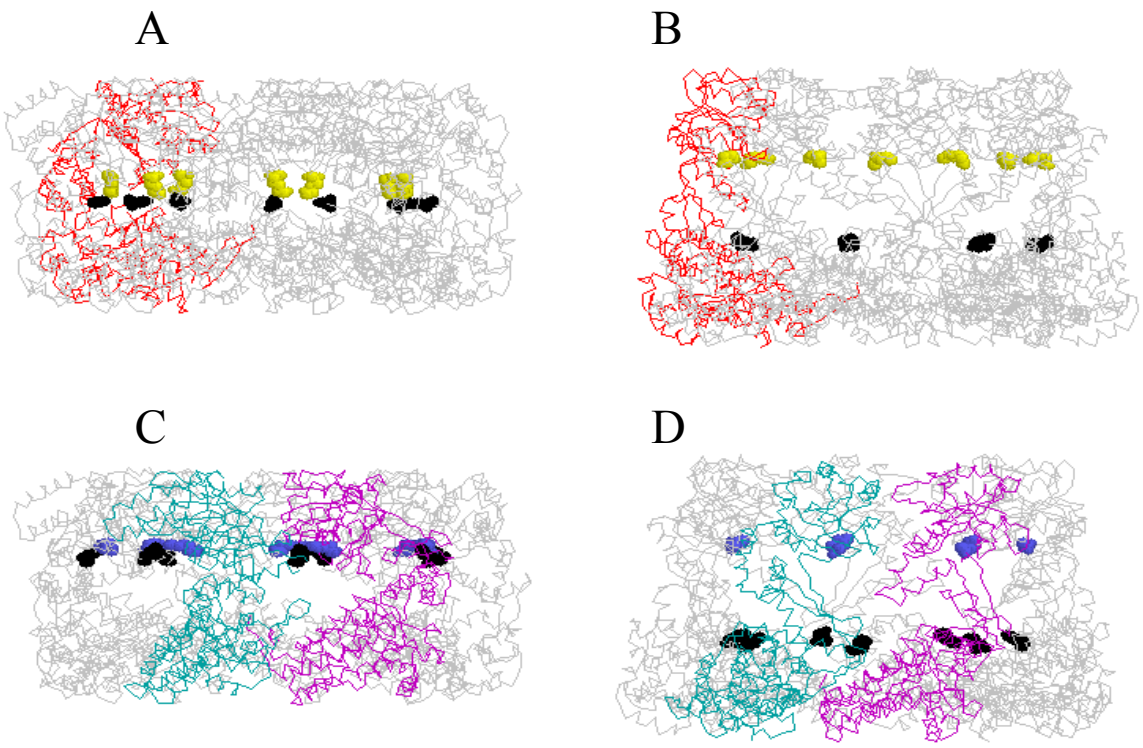

Figure 3-1: Two T State Salt Bridges Were Replaced With Cys Pairs. **A,B**) The $GroEL_{IAX}$ **D83**/K327 interdomain, intrasubunit salt bridge is present in the T state (**A**) but breaks in the R' state (**B**). The Cα-Cα distance between these two residues is 9 Å in the T state and 37 Å in the R' state. **C,D**) The $GroEL_{IRX}$ interdomain, intersubunit salt bridge **R197**/**E386** salt bridge is present in the T state (**C**) but breaks in the R' state (**D**). The Cα-Cα distance between these two residues is 12 Å in the T state and 84 Å in the R' state. These structures were made with PDB file 1aon (14).

The essential conclusions drawn from the studies with $GroEL_{IAX}$ are as follows (G. Curien, unpublished results). By carefully setting the experimental conditions, ie. eliminating contaminating metal ions, the introduction of either disulfide bonds or chemical cross-links into the double cys pair can be done in a controlled manner. $GroEL_{IAX}$ can be oxidized to any point on the reaction coordinate between 0% and 100% subunits oxidized. Previous studies with this mutant were limited to fully reduced or fully oxidized protein (51). Only one disulfide bond or cross-link is necessary to tether an entire ring in the T state and prevent GroES binding. In other words, the T→R'

transition is disallowed. Likewise, one disulfide bond or cross-link is enough to lock an entire ring closed and prevent the T→R transition upon ATP binding. Both of these findings demonstrate concerted motion within a ring. The latter observation was made possible by the finding that, unlike what the nested cooperativity model predicts, the T state does bind ATP and, in fact, hydrolyzes it at a rate that is substantially faster than the R state. The fact that cross-linking actually locks a ring in the T state is shown by Hill plots in which tethered $GroEL_{IAX}$ binds ATP with a Hill coefficient of approximately 1. Thus, tethering prevents the allosteric transitions that normally allow for positive cooperativity in ATP binding. Finally, using dimaleimide cross-linkers of different lengths, the distance the α-carbon atoms of the D83/K327 salt bridge move upon undergoing the T→R transition was measured. It is approximately 14 Å, consistent with the difference between the α-carbons distances in the T state crystal structure (10) and the R state cryo-EM structure (36).

Following the success of these studies, it was decided that a similar double cysteine mutant could be utilized to examine a different aspect of the structural transitions. The D83/K327 salt bridge is broken upon the upward motion of the apical domains during the transitions. The other major motion that occurs is the twisting of the apical domains, first 25° anticlockwise, and then 115° clockwise, relative to the equatorial domains (14). This is the motion that buries the SP binding sites and turns the inner cavity into a hydrophilic environment. An intersubunit, T state salt bridge, R197/E386, is broken during this twisting motion of the T→R→R' transitions (Figure 3-1, c and d). Thus, it was decided to replace this salt bridge with a double cys pair and characterize this new mutant ($GroEL_{IRX}$) in much the same way as $GroEL_{IAX}$. It was

expected that $GroEL_{IRX}$ would provide many of the same results as its predecessor, primarily a demonstration of concerted motion. This did not entirely turn out to be the case.

3.2 Methods Specific to Chapter 3

3.2.1 Mutagenesis The R197C and E386C mutations were inserted into the pGEL1 plasmid using the U.S.E mutagenesis kit. The mutagenic primers were as follows: R197C: GGTATGCAGTTCGACTGCGGATATCTGTCTCCTTACTTCATC, E386C: GTGGGTGCTGCTACATGTGTTGAAATGAAAGAG. R197C inserts a new EcoRV site and E386C inserts a new BspLU11I site.

It was realized at some point during these studies that wild-type GroEL subunits expressed from the native GroEL gene in the bacteria would limit the extent of cross-linking. In an attempt to overcome this, the mutant plasmid was transformed into a cell line, MGM100, in which the native GroEL gene is under the transcriptional control of a pBAD promoter (66). This promoter is activated by growing the cells in minimal media containing arabinose and suppressed by growing the cells in media containing glucose. Thus, wild-type expression could supposedly be expressed by growing the cells in glucose. This turned out to make little difference in the eventual cross-linking results, but this is noted here since much of the protein used came from this strain.

3.2.2 Gradient Gels 3-9% gradient gels were poured using a small Hoeffer gradient gel mixer with 9% resolving gel solution in the front chamber and 3% resolving gel solution in the rear chamber. The mixer was held above a magnetic stir plate and a stir bar was placed in the front chamber to ensure proper mixing. Both valves were opened and the solution was poured through rubber tubing and a thin, glass pipet into a

gel cassette 10.5 cm tall with 1.5 mm spacers. Once polymerized, a 3% stacking gel was poured on top.

3.2.3 Purification of Phosphate Binding Protein PBP A197C was purified essentially according to the published procedures with a few modifications (67, 68). A 10 ml LB starter culture containing 12.5. mg/L tetracycline was inoculated with a single colony of *E. coli* transfected with a plasmid containing the *Phos* gene. This gene expresses the PBP protein when the cells are grown under low phosphate conditions. The saturated starter culture was diluted into 100 ml LB/Tet and grown overnight. 40 ml of this LB culture was added to each of 2 flasks containing 1 L of TG Plus minimal media (67) with 640 μM phosphate. These large cultures were grown to an OD_{600} of 1.2. The cells were pelleted by centrifugation, resuspended in TG Plus media containing 64 μM phosphate, and incubated overnight at 37°C under these low phosphate conditions to produce PBP. The following day, the cells were harvested by centrifugation and resuspended in 10 mM Tris pH 7.6, 30 mM NaCl. The cells were pelleted again, washed in fresh buffer, then pelleted once again. The cells were resuspended in 50 ml 33 mM Tris pH 7.6. Then, 50 ml of 33 mM Tris pH 7.6, 0.1 mM EDTA, 40% sucrose was added rapidly, and the cells were once again pelleted. To initiate the osmotic shock which lysed the periplasm of the cells, the cells were rapidly resuspended in 100 ml 0.5 mM $MgCl_2$ and stirred. The lysed solution was then centrifuged, and the supernatant, containing PBP, was brought to 10 mM Tris pH 7.6. This solution was split into two portions. Each portion was loaded onto a 25 ml Q Sepharose HP column (Amersham) equilibrated with 10 mM Tris pH 7.6, 1 mM $MgCl_2$. A 250 ml gradient from 0 mM to 200 mM NaCl was run following elution of the flow-through. Fractions containing PBP as judged by SDS-

PAGE were pooled and concentrated in Centriplus-10 concentrators. Protein concentration was determined using an extinction coefficient at 280 nm of 60880 $M^{-1}cm^{-1}$. The protein was then aliquotted and stored at -80°C (Figure 3-2).

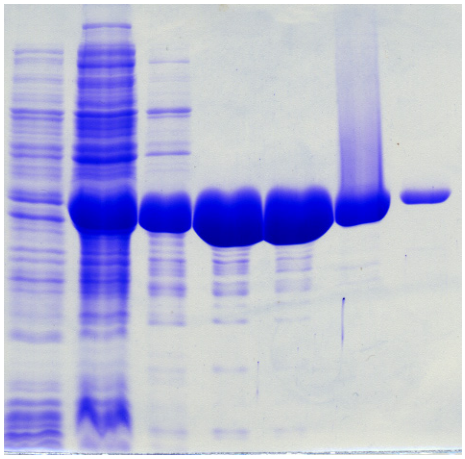

Figure 3-2: Purification of PBP. 12% SDS-PAGE gel showing results of the PBP purification. Lane 1: non-induced cell lysates Lane 2: P_i induced cell lysates Lane 3: post-osmotic shock Lanes 4 and 5: a fraction from each Q Sepharose run Lane 6: pool from both Q Sepharose runs Lane 7: final concentrated PBP product

3.2.4 Labeling of PBP 8 ml of 100 μM PBP was reacted with 150 μM MDCC (Molecular Probes) in the presence of 200 μM 7-methylguanosine (MEG) and 0.2 u/ml PNPase for 30 minutes. The latter two reagents constitute a phosphate "mop" which scavenges traces of PO_4^{2-} that can interfere with labeling, and later, with the assay (68). The labeled PBP was loaded onto a 150 ml G25 M de-salting column to separate unreacted label. The flow-through, containing the PBP-MDCC was then run on a 10 ml Q Sepharose HP column equilibrated with 10 mM Tris pH 8. A 400 ml gradient from 0-50 mM NaCl was run to separate labeled PBP from unlabeled PBP. Fractions constituting the major peak (colored yellow) were pooled, concentrated, and stored at

-80°C until used in the assay. Further purification on a MonoQ, as suggested in the published protocol (68), was found not to be necessary.

3.2.5 ATPase Assay Using PBP Labeled PBP shows a relatively strong increase in fluorescence emission upon binding phosphate. Because of the high sensitivity of PBP-MDCC fluorescence to the presence of contaminating phosphate, all buffers and ATP solutions were treated with the phosphate mop prior to use. Residual PNPase, which interfered with the signal in the assay, was removed by filtering the mopped buffers or ATP solutions on a Centricon-10. The standard conditions of this assay were 50 mM Tris pH 7.5, 100 mM KAc, 10 mM MgAc, 0.2 mM PEP, 5 units PK, 3 μM PBP, varying [ATP], and 0.05 μM GroEL. Fluorescence measurements were done in a Perkin-Elmer LS50B spectrofluorometer. The excitation wavelength was 425 nm, the emission wavelength was 463 nm with the excitation and emission monochrometer slits set to 2.5 and 15 nm respectively. Instrument response time was set to 1. Prior to each assay, a standard curve was made using known amounts of phosphate to calibrate the PBP solution for that day. To measure ATPase rates, a small volume fluorescence cuvet containing all components except GroEL was incubated in the cuvet holder for 5 minutes at 37°C. Pre-warmed GroEL was then added to a final volume of 200 μl and data collection was immediately initiated. Data points were collected every second for 200 seconds. The slope of the trace was calculated over two different intervals along the trace, and the average slope was used to calculate the change in phosphate concentration using the extinction coefficient obtained from the standard curve. From this, the ATPase rate was calculated using the GroEL concentration and sample volume.

3.2.6 Assaying GroES Release From the EL/ES Bullet Using ^{14}C-ATP This assay is based on one previously developed in our lab (G. Curien, unpublished). A GroEL/GroES bullet complex made with ^{14}C-ATP was created by mixing GroEL, GroES, and [8-^{14}C-]ATP (Amersham) in buffer at final concentrations of 10 mM Tris pH 7.5, 5 mM KAc, 10 mM MgAc, 35 μM GroEL, 35 μM GroES, and 210 μM ^{14}C-ATP at 3380 dpm/nmol ATP. Bullets were allowed to form for at least 10 minutes at which point they were diluted 1:1 with 10 mM Tris pH 7.5, 5 mM KAc, 10 mM MgAc, with or without 3 mM unlabeled ATP (final [ATP] = 1.5 mM). At various time points, the release reaction was quenched and unbound ATP was separated by loading 200 μl of the reaction on a PD-10 column equilibrated in 10 mM Tris pH 7.5, 5 mM KAc, 10 mM MgAc, 3 mM ADP. The sample was immediately chased with 2.5 ml of this buffer to bring the protein to the bottom of the column. The protein was then eluted with 1.1 ml of buffer. 500 μl of the eluent was added to a scintillation vial along with 4 ml of Scintiverse (Fisher), and counted on a Beckman scintillation counter. The number of ATP molecules retained per GroEL 14-mer was calculated using this formula:

$$ATP/14mer = (Dpm's\ Counted) * \frac{1100\,\mu l\ eluted}{500\,\mu l\ counted} * \frac{1\,nmol\ ATP}{3380\ dpm} * \frac{1}{0.25\,nmol\ GroEL\ 14mer}$$

3.2.7 Assaying GroES Release From the EL/ES Bullet Using His-tagged GroES This procedure was one created by Mark Uebel in our lab for his M.S. thesis (69). A 300 μl solution containing 10 mM Tris pH 7.5, 10 mM MgAc, 1 mM KAc, 70 μM ATP, 18 μM $GroES_{His}$, and 14 μM $GroEL_{WT}$ or $GroEL_{IRX}$ was incubated for 5 minutes at room temperature to allow bullet formation and ATP exhaustion. This solution was then loaded onto a column containing 1 ml Ni-NTA resin (Qiagen)

equilibrated with 20 mM Tris pH 7.5, 10 mM MgAc. After the sample was loaded, the column was washed three times with 0.8 ml 20 mM Tris pH 7.5, 10 mM MgAc to elute any flow-through. All three eluents were collected. To elute the GroEL, bullet dissociation was initiated by loading three separate 0.8 ml portions of a solution containing 20 mM Tris pH 7.5, 10 mM MgAc, 5 mM KAc, 7 μM $GroES_{WT}$, ± 50 μM ATP onto the column and collecting each eluent. Following a single wash with 20 mM Tris pH 7.5, 10 mM MgAc, the $GroES_{His}$ along with any undissociated GroEL was eluted with 3 separate washes with 250 mM imidazole. 60 μl of each of the 10 fractions was added to 12 μl of 6X loading blue containing BME, boiled for 2 minutes, and 18 μl of each sample was loaded on a 15% SDS-PAGE gel.

3.3 Data Analysis

It should be noted that much of the original work in developing these mathematical techniques presented in this section was done by Gilles Curien. The basic techniques for formulating the theoretical functional models (including formulating the binomial distributions and using them to produce the models, predicting populations using probabilities, and formulation of all ES binding models and the original ATPase models) were developed by Dr. Curien. The details of these are provided here for the convenience of the reader, and are cited appropriately. The development of the models and techniques used to analyze $GroEL_{IRX}$ by SDS-PAGE and the reworking and further refinement of the ATPase models was work done by this author.

3.3.1 Gel Quantitation of the Reaction Coordinate In order to characterize $GroEL_{IRX}$'s response to oxidation or cross-linking, a method is needed to quantitate the amount of cys-cys tethering that has taken place in response to some reagent. The extent

of tethering will be quantitated by SDS-PAGE, and therefore a robust method is needed to take the information from the gel and turn it into a measurement of the cross-linking reaction coordinate. This can be done using fairly simple mathematics. At first glance, adding some amount of cross-linker to a population of GroEL 14-mers seems to create a mess: some 14-mers will contain 1 tether, some will contain 2, and some will even have all 14 double cys sites tethered. It was realized during the earlier studies using $GroEL_{IAX}$ that the population of 14-mers at any point along the reaction coordinate can be described by binomial distributions (G. Curien, unpublished). These follow the general formula:

$$mole\ fraction\ of\ subnits\ containing\ x\ tethers = \frac{y!}{(y-x)!*x!} * p^x * (1-p)^{(y-x)}$$, where y is the number of subunits per oligomer (14 in the case of GroEL), x is the number of tethers in an isolated oligomer, and p is the global fraction of cys-cys sites that are tethered. The distributions are shown in Figure 3-3. This assumes that cross-linking is an entirely stochastic process, meaning that the insertion of a tether in one ring does not favor or disfavor the insertion of further tethers in the other subunits in that ring. It will be shown later experimentally that this is indeed the case.

In order for this information to be of any use, the reaction coordinate must be defined by direct measurement. A clearer way of referring to this coordinate is by calling it the fraction of subunits tethered. In the case of $GroEL_{IAX}$, where the cys-cys pairs are intrasubunit, a tether causes a GroEL subunit to run with reduced mobility on an SDS-PAGE gel (Figure 3-4). The fraction tethered can be calculated simply by dividing the intensity of the upper band by the combined intensities of the upper and lower bands. Simplifying the situation even further is that the measurement in each lane of the gel is

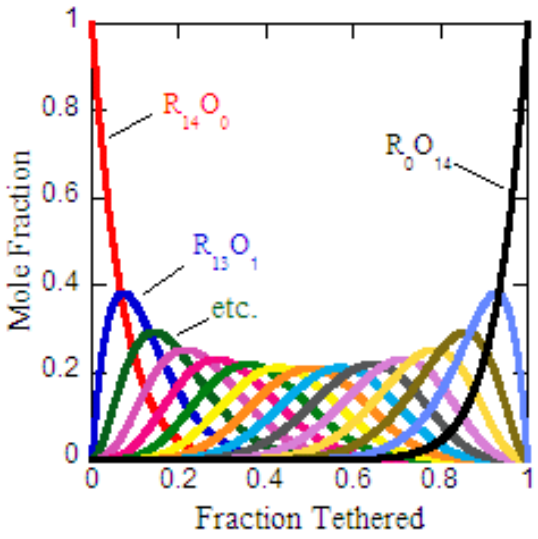

Figure 3-3: Binomial Distributions Define Population of 14-mers Containing 0,1,2...etc Tethers at Any Point on the Reaction Coordinate. (G. Curien, unpublished) Formulated using the equation given in the text, these traces show the fraction of 14-mers containing 0, 1 or more tethers. The numbers of **R**educed and **O**xidized (or cross-linked) subunits are noted for some of the traces.

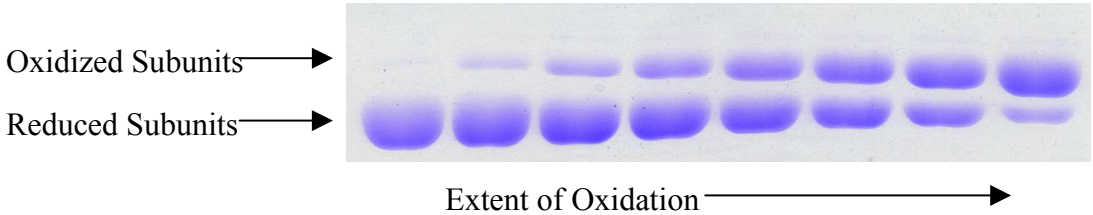

Figure 3-4: Quantitation of GroEL$_{IAX}$ Oxidation. (G. Curien, unpublished) Oxidation of GroEL$_{IAX}$, which contains intrasubunit cys-cys pairs. A intrasubunit disulfide bond causes a GroEL$_{IAX}$ subunit to run with reduced mobility on a 12% SDS-PAGE gel. Fraction tethered is quantitated by dividing the intensity of the upper band by the total intensity of both bands in each lane.

independent of the other lanes; thus, sample load is not required to be the same in each lane (G. Curien, unpublished).

Quantitating the fraction of subunits tethered when working with $GroEL_{IRX}$ is considerably more complicated. This is due to the cys-cys pairs being intersubunit rather than intrasubunit. A single tether between two subunits results in the formation of a dimer. Further addition of tethers results in the formation of more dimers and eventually trimers, tetramers, pentamers, hexamers, and heptamers. A heavily tethered sample of $GroEL_{IRX}$ produces a ladder when run on a gel (see section 3.4.1). In order to quantitate the fraction of subunits tethered, the appearance and disappearance of each of these multi-subunit species must be defined as the reaction coordinate progresses. This was done according to the scheme shown in (Figure 3-5). Beginning with a 14-mer containing no tethers, the insertion of a single tether has a 1/1 probability of causing a dimer to form. The insertion of a second tether has a 2/13 chance of producing a trimer, and an 11/13 chance of producing a second dimer. Insertion of a third tether results in the species and probabilities shown in the figure. This mathematical analysis was continued for the fourth through fourteenth tether, and a series of probability equations was constructed (see Appendix). These equations produce the mole fraction of a given species (monomer, dimer, etc.) at any value along the reaction coordinate by multiplying the fraction of 14-mers with a given number of tethers (the rxn coordinate) by the probability that those 14-mers contain that particular species, by the number of that species the 14-mer is predicted to contain. This results in the plot shown in Figure 3-6. The key features of this plot to note are the decrease in the mole fraction of monomers,

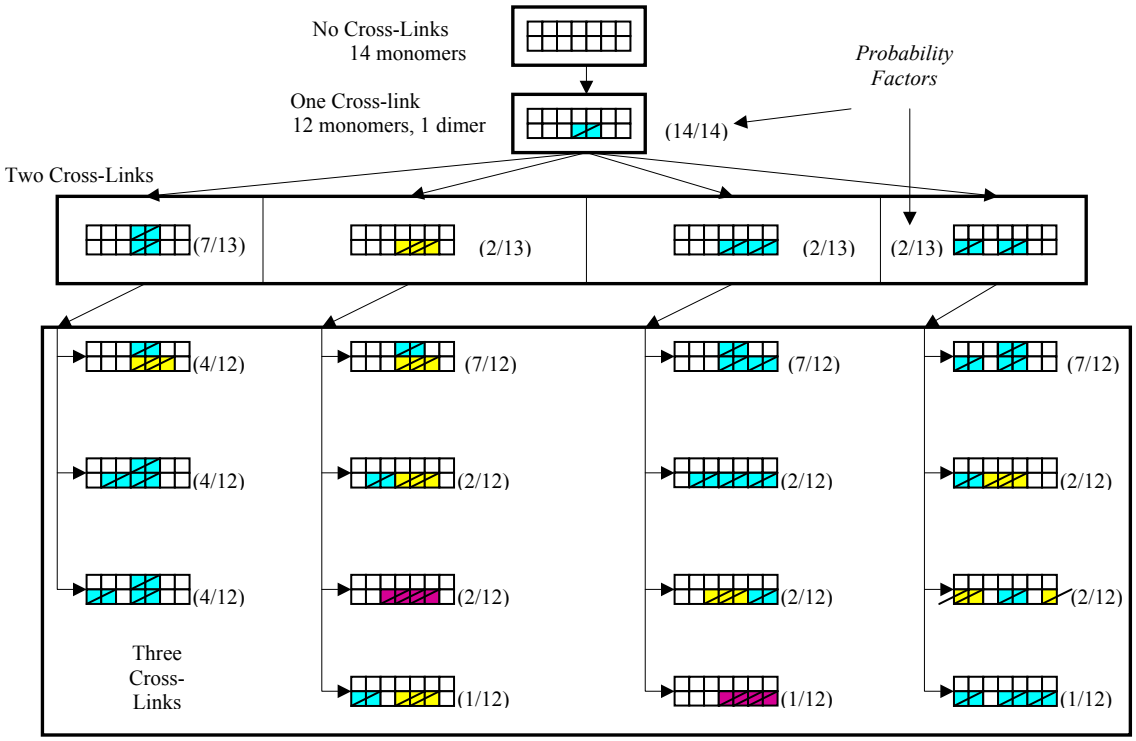

Figure 3-5: Scheme for Modeling the Cross-linking of GroEL$_{IRX}$. The disappearance of monomers and appearance of dimers, trimers, etc. in response to inserted intersubunit tethers in the case of GroEL$_{IRX}$ can be modeled using simple probabilities. GroEL is represented by 14 blocks with each row of blocks representing a ring. One inserted tether has a 14/14 chance of causing a dimer to form. The next inserted tether has a 2/13 chance of causing a trimer to form and an 11/13 chance of forming another dimer. This analysis can be continued for 3,4,…,14 tethers per 14-mer.

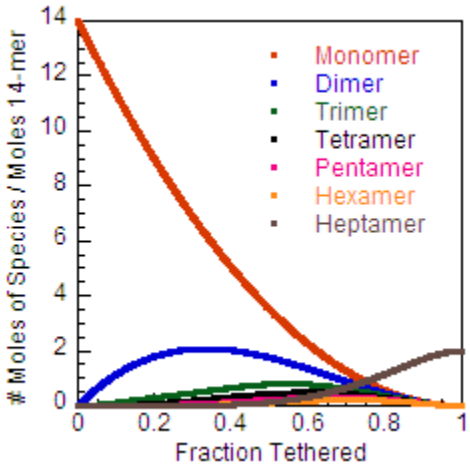

Figure 3-6: Cross-linking Model of GroEL$_{IRX}$. Beginning with 14 monomers at 0% cross-linked, and ending with 2 heptamers at 100% cross-linked, this plot shows the number of moles of each GroEL$_{IRX}$ monomer or multimeric species that are present at all points on the reaction coordinate. These traces were formulated using the methods described in the text and depicted in Figure 3-5.

the relatively significant increase and then decrease in the dimers, and the eventual takeover by the heptamers when everything is nearly fully tethered.

This information now allows for the quantitation of the fraction tethered using SDS-PAGE. The easiest way to accomplish this is by concentrating on the disappearance of the monomer (see section 3.4.1). Each point on the reaction coordinate shows a unique amount of monomers (unlike the dimer which occurs in the same amount at two points on the coordinate) and this amount decreases as the fraction tethered increases. The monomer curve can be fit to a polynomial equation (Figure 3-7). This allows for the

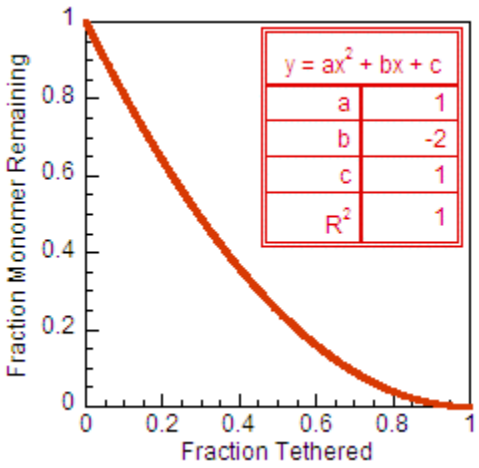

Figure 3-7: Extent of Tethering is Quantitated Using Disappearance of Monomers. The monomer trace from the $GroEL_{IRX}$ cross-linking model is plotted as the fraction of monomers remaining and fit to a 2nd degree polynomial equation. The trace fits perfectly to the equation: $y = x^2 - 2x + 1$. This equation can be used to relate the fraction of monomer remaining (vs. the uncross-linked control) on an SDS-PAGE gel to the overall fraction tethered of the reaction.

conversion of the fraction of monomer remaining in a lane to the fraction tethered. The gel is run with an untreated control sample that is assumed to have undergone no cross-linking. The intensities of the monomer bands in the other lanes are then divided into the intensity of the monomer band in the control lane to obtain the fractions of monomer remaining. These are then converted to the fractions tethered using the polynomial equation. Overall: $Fraction\ Tethered = 1 - \sqrt{Fraction\ \ Monomer}$. One further note: because the intensity of a band in one gel lane is being compared with the band intensity in another lane, the loading needs to be normalized. This was done by including an

internal protein standard, carbonic anhydrase, CbAn (Sigma), which is about 30 kDa. All other lanes were normalized to the control lane using this equation:

$$Corrected\ \ Monomer\ Int = Monomer\ Intensity\ Lane\ X * \frac{CbAn\ Intensity\ Control\ \ Lane}{CbAn\ \ Intensity\ \ Lane\ \ X}$$

3.3.2 Developing Models that Predict GroEL$_{IRX}$'s Response to Cross-Linking

The goal of several of these experiments was to determine the number of tethers per ring necessary to prevent conformational changes. As stated above, this analysis was also performed on GroEL$_{IAX}$ prior to the studies with GroEL$_{IRX}$. As part of the previous studies a method was developed to predict the response of GroEL$_{IAX}$ to cross-linking (G. Curien, unpublished). This method involves determining the number of tethers in each ring using probabilities, and then predicting a property of that ring in response to the number of tethers. The result is a theoretical plot that the real data should closely match if the prediction is correct. For example, it was predicted that one tether per ring would lock that ring in the T state and prevent GroES binding. To build the model, an analysis was done to determine the probability that 14-mers at any point on the reaction coordinate contained one ring that was not tethered. These 14-mers would still be able to bind GroES. The analysis was as follows: insertion of the first tether has a 1/1 probability of tethering one ring. A second tether then has a 6/13 chance of tethering another subunit in the same ring and a 7/13 chance of inserting into the other ring. Thus, after only two inserted tethers, 7/13 of the GroEL 14-mers will not be able to bind GroES. This analysis is continued for the tethers beyond 2 up to 14, although by the time the eighth tether is inserted, all GroEL would be predicted to be unable to bind GroES. A similar analysis can be done in which it is predicted that two tethers are required per ring to prevent GroES binding. The probability of a 14-mer containing a given number of

tethers in each ring is multiplied by the fraction of the GroEL population containing the total number of tethers in both rings (known from the binomial distributions), which is then multiplied by a number representing the function of the tethered species. In this case, a 14-mer that can bind GroES is assigned '1' and a 14-mer that cannot is assigned '0'. The theoretical plot is shown in Figure 3-8 (Curien, unpublished).

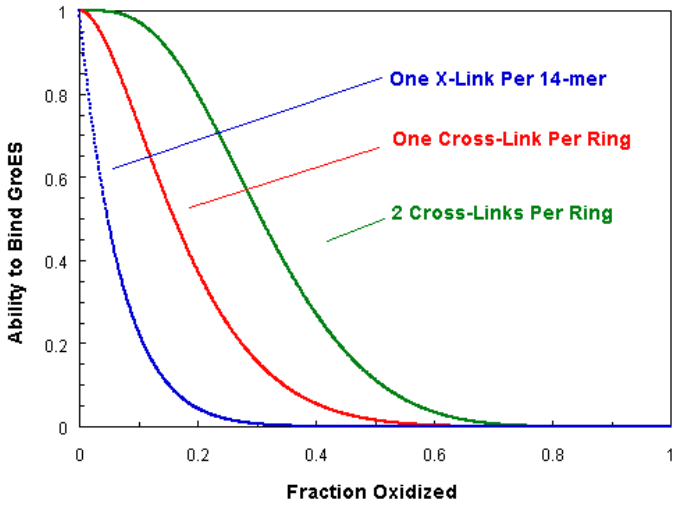

Figure 3-8: Modeling the Effect of Cross-links on GroEL's Ability to Bind GroES. (G. Curien, unpublished). Formulated using simple probabilities and the binomial distributions as described in the text, the theoretical models shown here predict the number of tethers necessary to prevent GroES from binding to GroEL (the number of tethers necessary to prevent the T→R' transition). Data obtained with both $GroEL_{IAX}$ (G. Curien, unpublished) and $GroEL_{IRX}$ (Figure 3-16c) follow closely the trace in which 1 cross-link per ring eliminates GroES binding to that ring.

A similar analysis was done to draw theoretical models that predict the response of the ATPase activity of a given GroEL mutant to cross-linking. Again, the goal was to demonstrate the number of cross-links necessary to lock a ring in the T state. These models were formulated by predicting a V_{max} for both the T and R states and using these numbers in the same way that the functional number was used in the ES binding models. One surprising result obtained with $GroEL_{IAX}$ was that the ATPase activity increased at

low levels of cross-linking but then decreased to zero at high levels (Curien, unpublished). Thus, another feature was incorporated into the model that accounted for this by hypothesizing that a tether inserted into a subunit destroyed the ATPase activity of that subunit. However, subsequent work with a single-ringed version of GroEL done well after the original $GroEL_{IAX}$ studies showed that this model is probably not correct (J. Gresham, unpublished). Collectively, a new model was formulated by the lab that accounted for the decrease in activity by stating that a ring remains fully active until a certain number of subunits in a ring are tethered. After that many tethers are inserted, the ring becomes inactive; a so-called "X strikes and you're out" model (J. Gresham, unpublished). This new model satisfactorily fit the data for both $GroEL_{IAX}$ and single-ringed GroEL.

Further refinement of the ATPase model is necessary when considering $GroEL_{IRX}$, due to the fact that the ATPase activity of $GroEL_{IRX}$ decreases at high levels of cross-linking, but does not disappear completely. A new model was developed to account for this by including another V_{max} in the analysis (Figure 3-9). This value is assigned to a GroEL ring with X cross-links in it, and represents the residual activity that the ring retains upon receiving X tethers. In the case of $GroEL_{IAX}$, this residual V_{max} would be 0. This number, along with $V_{max}T$, $V_{max}R$, and X (the number of "strikes") can be varied to obtain the best fit for the data (Figure 3-10). This more robust model is new work presented in this dissertation.

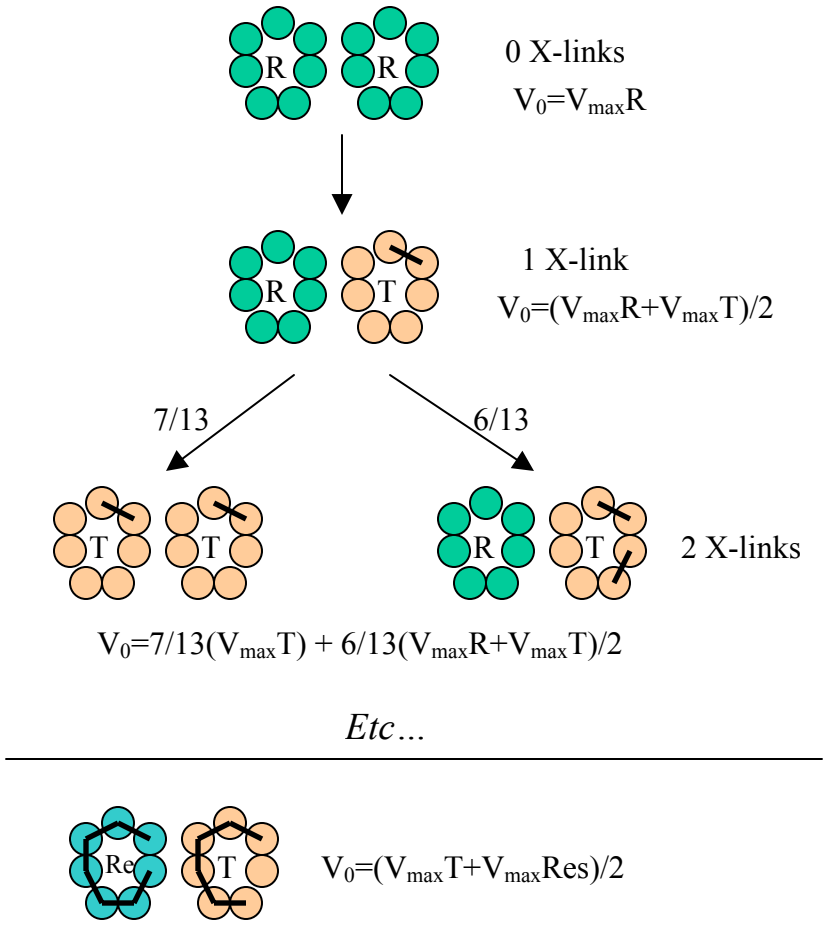

Figure 3-9: Scheme for Developing Models Which Predict the Response of GroEL ATPase Activity to Cross-linking. This general scheme is used to model the ATPase activity of GroEL as cross-linking increases. This figure depicts the partial formulation of a model in which one cross-link per ring locks that ring in the closed, T state. When no cross-linking has occurred, both rings will be in the open, R state, and the rate (calculated on a per subunit basis) will be $V_0[0]=V_{max}R$. Upon the insertion of one cross-link, there is a 14/14 chance that one will be locked in the T state. The rate/subunit ($V_0[1]$) will now be the average of $V_{max}R$ and $V_{max}T$. Upon the insertion of the second cross-link 7/13 14-mers will be in the TT state and 6/13 will remain in the TR state. The rate/subunit of 14-mers with 3 cross-links will be $V_0[2] = 7/13(V_{max}T) + 6/13(V_{max}R+V_{max}T)/2$. If it were the case that only two cross-links could be placed in GroEL, the overall rate would be calculated by multiplying the rate equation for 0,1, and 2 cross-links by the mole fraction of 14-mers ($\chi[y]$) containing *y* cross-links, as determined by the binomial distribution, and adding them together:
Overall Rate=$\chi[0]*V_0[0] + \chi[1]*V_0[1] + \chi[2]*V_0[2]$. Of course, more than two cross-links can be placed in GroEL, and the real equation is much longer.

At the bottom of the figure is a 14-mer that has received the requisite number of "strikes" in one ring, which means the activity of the subunits in that ring will decrease to $V_{max}Res$. The activity per subunit is then the weighted average of $V_{max}T$ and $V_{max}Res$.

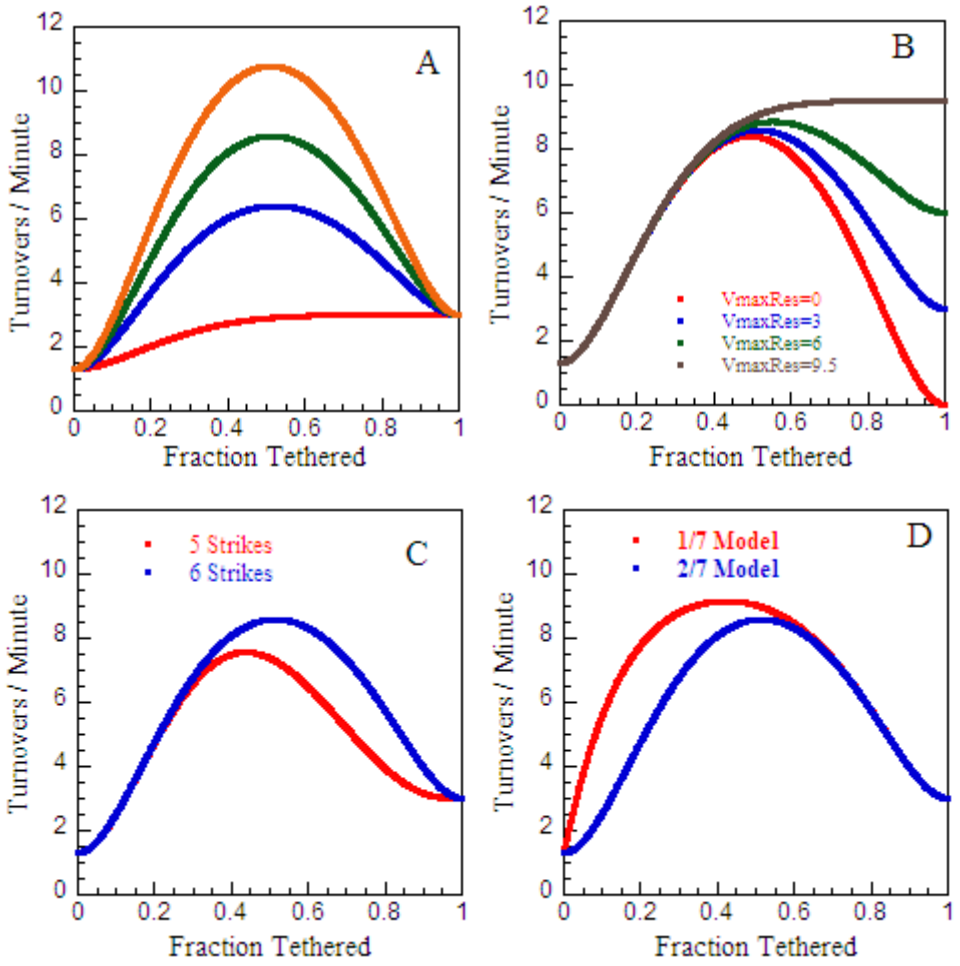

Figure 3-10: Varying the Input Parameters Affects the Shape of the Theoretical ATPase Traces in Different Ways. In order to find a model that best matches an obtained data set, several parameters ($V_{max}T$, $V_{max}Res$, # of strikes, and number of cross-links needed per ring to lock a ring in the T state) must be varied and the best model is then determined empirically. Shown here are the effects of varying those 4 parameters. $V_{max}R$ is fixed at 1.3 turnovers/min. for all plot shown. **A**) Varying $V_{max}T$. $V_{max}Res$ fixed at 3, 6 strikes and injured, 2/7 model. $V_{max}T$= 3, 7, 9.5, 12. **B**) Varying $V_{max}Res$. $V_{max}T$=9.5, 6 strikes, 2/7 model. **C**) Varying number of strikes needed to "injure" a ring. $V_{max}T$=9.5, $V_{max}Res$=3, 2/7 model. **D**) Varying number of cross-links needed per ring to lock it in the T state. $V_{max}T$=9.5, $V_{max}Res$=3, 6 strikes.

3.4 Results

3.4.1 Cross-linking of GroEL$_{IRX}$ Since the R197C/E386C cysteine pair replaces an *inter*subunit salt bridge, the introduction of a disulfide bond or cross-link between these residues would produce a GroEL dimer. Further cross-linking would produce higher-order multimers. Run on an SDS-PAGE gel, cross-linked GroEL$_{IRX}$ would be expected to produce a ladder in which everything from monomers to heptamers should be visible. To confirm this, GroEL$_{IRX}$ was oxidized to various extents using stoichiometric amounts of diamide. Diamide has the chemical formula $(CH_3)_2NCON{=}{=}NCON(CH_3)_2$ and adds disulfide bonds to free thiol pairs using a two-step reaction mechanism (59). Varying amounts of diamide were added to a 40 μM dilution of GroEL$_{IRX}$ in 10 mM Tris pH 8, 10 mM MgAc. The solution also contained 30 μM CbAn to use as the internal standard during quantitation. After 30 minutes at 37°C, free thiols were blocked by the addition of NEM (see section 2.6) and denatured by the addition of SDS loading blue without DTT. To best visualize the ladder, the oxidized GroEL was loaded onto a 3%-9% gradient gel (section 3.2.2). This type of gel (Figure 3-11a) clearly shows an increasing amount of higher-order multimers as the diamide amount is increased. Eight distinct bands, representing monomers through the two forms of heptamers (six or seven tethers leading to open or closed rings, respectively), can be distinguished.

The decrease in the amount of monomers as oxidation increased was used to determine the extent of oxidation (see section 3.3.1). Diamide-oxidized GroEL was run on 12% SDS-PAGE gels on which the monomer band can be easily quantified (Figure 3-11b). These gels also allowed for the quantitation of the carbonic anhydrase internal

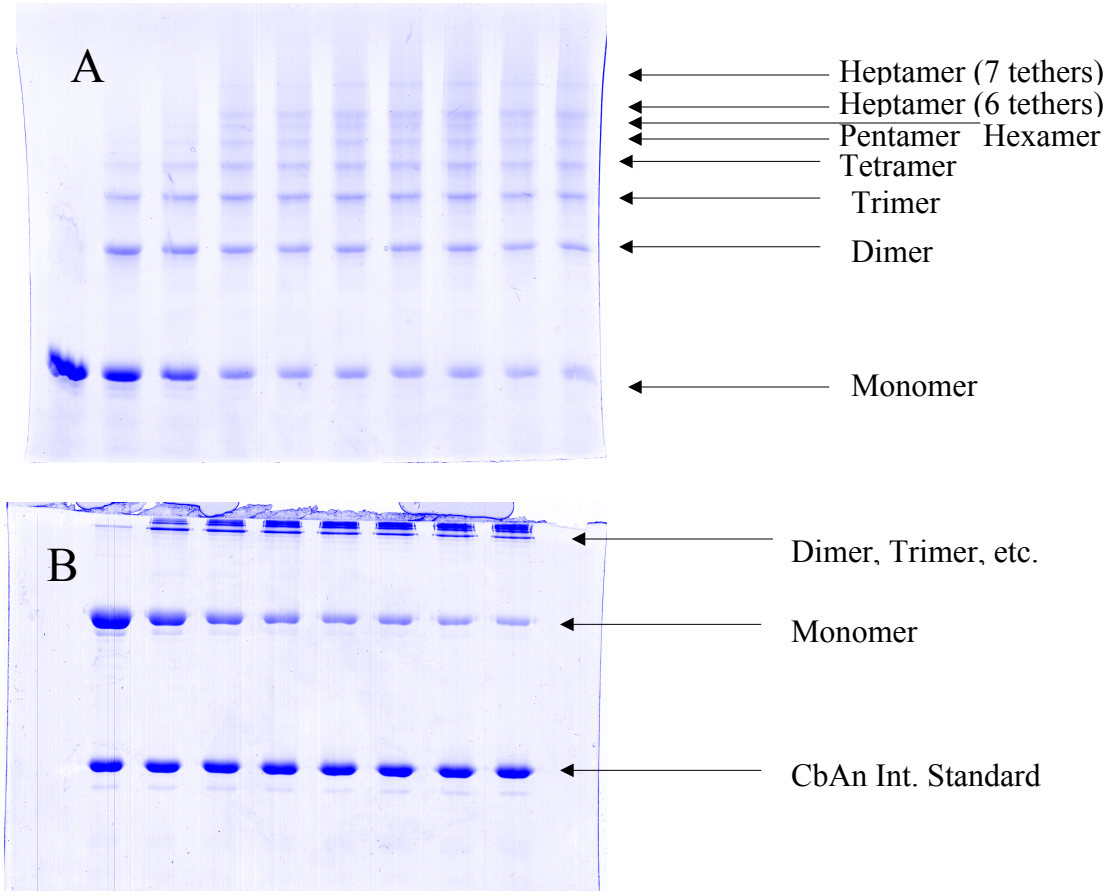

Figure 3-11: Cross-linking of GroEL$_{IRX}$ Can Be Visualized Using SDS-PAGE. GroEL$_{IRX}$ was oxidized with diamide, blocked with NEM, and loaded on gels using non-reducing loading buffer. [Diamide] increases left to right. **A**) 3%-9% Gradient Gel. This depicts the ladder that was expected from forming intersubunit disulfide bonds. All species from monomers to heptamers can be distinguished on the gel and are labeled. The less mobile heptamer band may be the GroEL species in which all possible tethers have been inserted into a ring, so that the ring cannot linearize upon denaturation. The other heptameric species contains only six tethers and can therefore linearize upon denaturation, causing it to run with a higher mobility **B**) 12% Linear Gel. This gel clearly shows the decreasing intensity of the monomer band as oxidation increases. This decrease in intensity can be converted to the overall "fraction oxidized" of the reaction: dividing the monomer intensity by the intensity of the monomer in the unoxidized sample (lane 1) gives the fraction of monomer remaining. This is then converted to the value of the reaction coordinate using the equation obtained from the fit in Figure 3-7.

standard. Similar oxidation experiments were done with $GroEL_{WT}$. No oxidation was detected (not shown).

3.4.2 Native Cysteines are Non-reactive GroEL contains three native cysteine residues. These create a potential risk for side reactions when working with double-cysteine mutants, although the crystal structure seems to indicate that the native cys residues are buried. When others have used GroEL mutants with inserted cysteines, they have first mutated the native cys residues to alanine (17, 51). It has also been reported that the native cysteines are indeed reactive to sulfhydryl labels under certain conditions (70). However, we and others have found that cysteine-less GroEL shows a marked decrease in ATPase activity (G. Curien, unpublished, and (17)). In fact, $GroEL_{IRX}$ constructed in a cysteine-less background is extremely unstable and difficult to purify (data not shown). Therefore, it was decided to construct the double cysteine mutants used in this laboratory exclusively in wild-type backgrounds.

To determine the extent of any side reactions that may take place with the native cysteines, a diamide and dimaleimide titration was performed with $GroEL_{IRX}$. Increasing amounts of either diamide or oPDM were added to 40 μM $GroEL_{IRX}$ at 10 mM Tris, 10 mM MgAc pH 8 and pH 7.5 respectively. The reaction was allowed to run for 30 minutes, and free thiols were then blocked with NEM. Extent of oxidation and cross-linking were quantitated by SDS-PAGE. The results show that both diamide and oPDM react in a directly proportional manner until the reagent concentration reaches approximately the GroEL site concentration (40 μM), after which no further increase in the reaction extent is seen (Figure 3-12a,b). Because the titration curve breaks almost exactly at the site concentration, it is reasonable to conclude that the other cysteines are

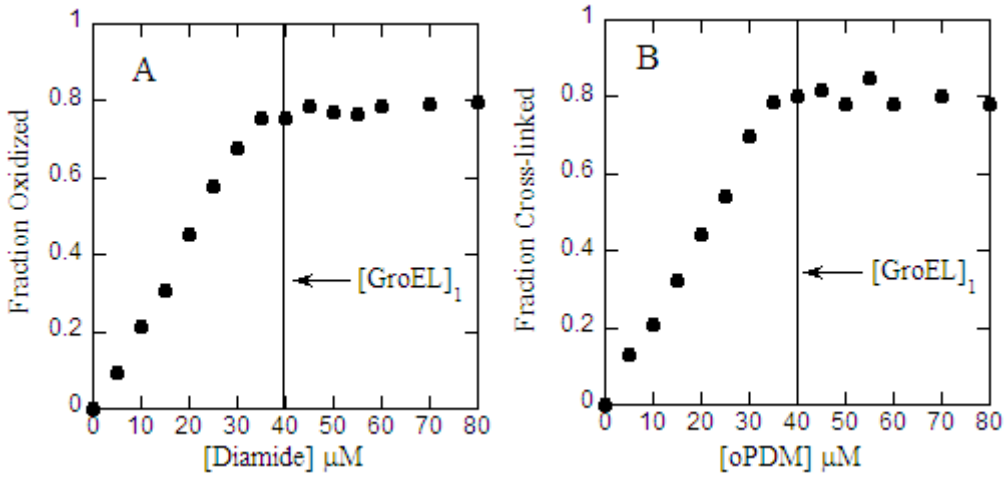

Figure 3-12: Stoichiometric Cross-linking of GroEL$_{IRX}$ Indicates No Reaction With Native Cysteines. 40 μM GroEL$_{IRX}$ (along with 30 μM CbAn) was reacted with the indicated amounts of either diamide (**A**) or oPDM (**B**). Extent of cross-linking was measured by SDS-PAGE. The vertical black line in both plots indicates site concentration.

non-reactive, at least to these reagents. GroEL$_{WT}$ is unaffected by oxidation or cross-linking (data not shown).

3.4.3 Kinetics of Diamide Oxidation and DTT Reduction Demonstrate that Oxidation is Stochastic

A critical assumption in being able to use the mathematics discussed in section 3.3 is that the insertion of disulfide bonds or cross-links into a 14-mer is stochastic. The insertion of a tether into one ring does not favor or disfavor the insertion of a second tether into the same ring. To demonstrate that this is indeed the case with GroEL$_{IRX}$, a detailed examination of its oxidation and reduction kinetics was undertaken. If oxidation is indeed stochastic, then oxidation kinetics are expected to be single exponential. Furthermore, the kinetics of reduction of fully oxidized GroEL$_{IRX}$ by DTT should also be single exponential with the rates having a linear dependence on DTT concentration. A similar analysis to this was used in the earlier work with GroEL$_{IAX}$, but

those studies relied on copper oxidation, which has a relatively complicated reaction mechanism (G. Curien, unpublished). Diamide uses a much simpler two-step mechanism to form disulfide bonds:

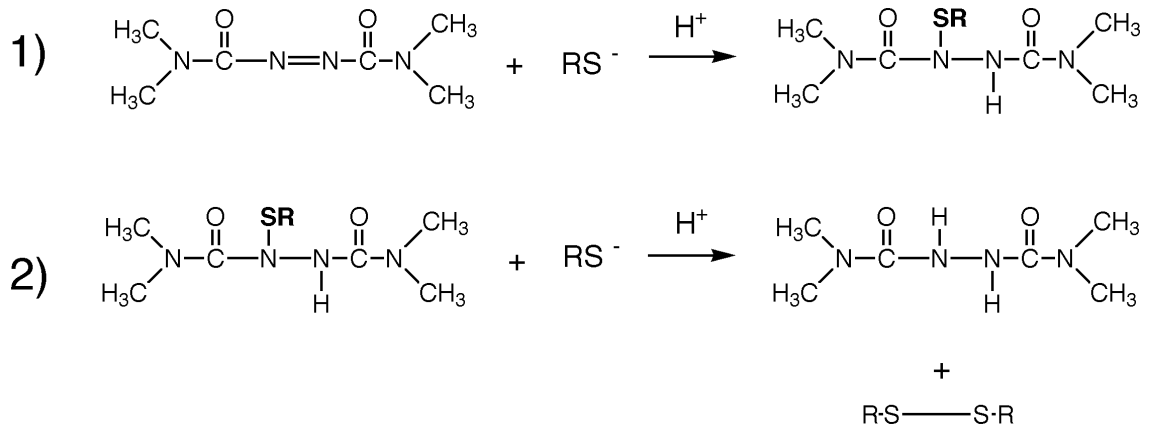

In the first step, diamide reacts with a free cysteine thiol. This step is expected to be concentration dependent. In the second step, the attached diamide reacts with the other free cysteine in the pair. The product of this second step is a disulfide bond and a reduced diamide molecule (59).

To confirm the kinetics of this reaction, various amounts of diamide were added to 40 μM $GroEL_{IRX}$ at 37°C in 10 mM Tris pH 8, 10 mM MgAc. The rate of disulfide formation was monitored by quenching the reaction at certain times with NEM. Extent of oxidation was quantitated by SDS-PAGE. The kinetics of oxidation were found to be single exponential with a rate constant that is independent of diamide concentration (Figure 3-13 a,b). This implies that the rate-limiting step in the reaction is the second step, the formation of the disulfide bond, which the reaction mechanism predicts is concentration independent.

The reduction of fully oxidized $GroEL_{IRX}$ by DTT was also monitored. A 40 μM sample of diamide-oxidized $GroEL_{IRX}$ was reacted with various concentrations of DTT in

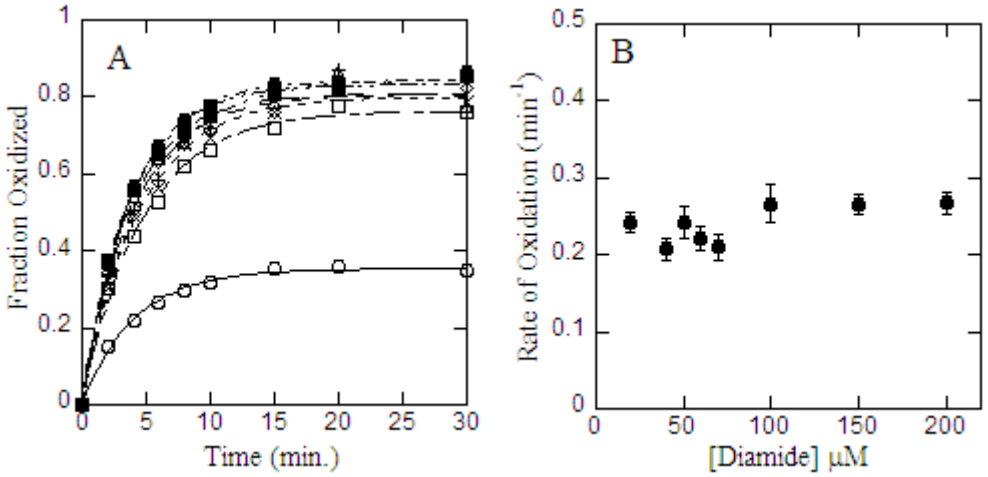

Figure 3-13: Oxidation Kinetics of GroEL$_{IRX}$ Using Diamide. 40 μM GroEL$_{IRX}$ was oxidized with various amounts of diamide at 37°C in 10 mM Tris pH8, 10 mM MgAc. The reactions were quenched by blocking unreacted cysteines with NEM, and quantitated by SDS-PAGE. **A**) Data at all diamide concentrations fit to single exponentials. The open circle data was collected using a sub-stoichiometric amount of diamide (20 μM). All other data was collected with [diamide] ≥ 40 μM. **B**) Re-plot of the rates obtained from the single exponential fits of the data from A. The error bars represent the uncertainty of the fit.

10 mM Tris pH 8, 10 mM MgAc, and the kinetics of reduction were monitored at 37°C. The reaction was quenched at various time points by NEM, and the extent of reduction was quantitated by SDS-PAGE. Reduction kinetics were single exponential with a rate constant that is [DTT] dependent (Figure 3-14a). A re-plot of these rate constants vs. [DTT] shows a linear dependence with a slope that is the bi-molecular rate constant of DTT reduction (Figure 3-14b). Taken together, these kinetics demonstrate that oxidation is indeed stochastic. A similar analysis was not possible with dimaleimide cross-linkers since the kinetics of cross-linking are too fast to measure, and the reaction is irreversible.

3.4.4 GroEL$_{IRX}$ Has Reduced Overall Cooperativity Compared to GroEL$_{WT}$

GroEL$_{WT}$ shows an unusual ATPase activity dependence on ATP concentration (Figure 1-4). This observation prompted the formulation of the nested cooperativity model (33).

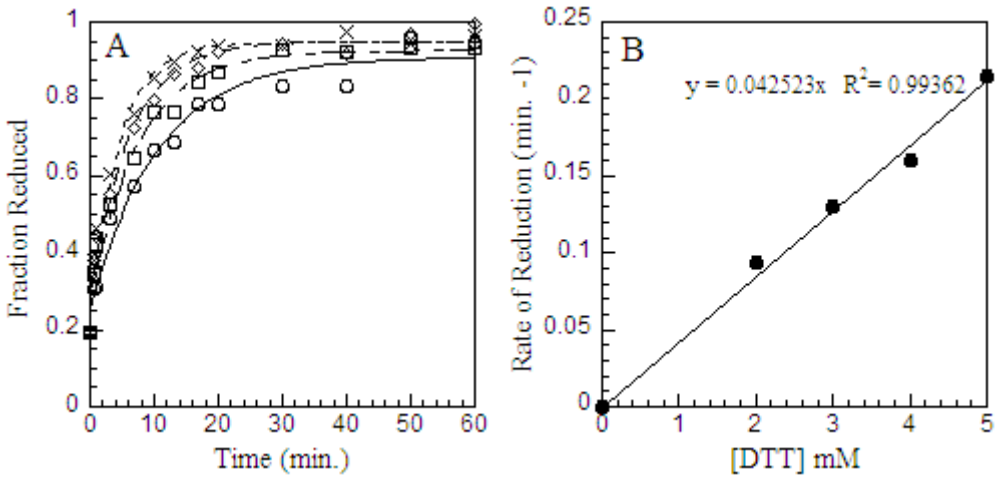

Figure 3-14: Reduction Kinetics of Oxidized GroEL$_{IRX}$ Using DTT. Diamide-oxidized GroEL$_{IRX}$ at 40 μM was reduced with various concentrations of DTT at 37°C in 10 mM Tris pH 8, 10 mM MgAc. **A**) The data were fit to single exponentials. **B**) Re-plot of the reduction rates obtained from the fits in **A**. These rates were fit to a linear equation, the slope of which is the second order rate constant of the reaction, 0.043 $mM^{-1}min^{-1}$.

This experiment was repeated using the coupled-enzyme assay under the conditions listed in section 2.9 at 37°C with 2 μM GroEL$_{WT}$. The results (Figure 3-15a) are similar, but not identical, to Yifrach and Horovitz's (33), showing the two breakpoints at 5 μM and 30 μM ATP. The [ATP] dependence of GroEL$_{IRX}$'s activity was also measured using the coupled-enzyme assay under the same conditions. The results in Figure 3-15b show that the first transition is occurring at ATP concentrations below site concentration (2 μM), where any rate measurement violates steady-state assumptions. In order to accurately measure the [ATP] dependence of this mutant, another method was needed that could measure ATPase activity at GroEL concentrations significantly lower than 2 μM (the lower limit of the coupled-enzyme assay is about 1 μM).

Martin Webb and colleagues have developed a method of measuring inorganic phosphate release that relies on a mutant of a periplasmic bacterial protein called

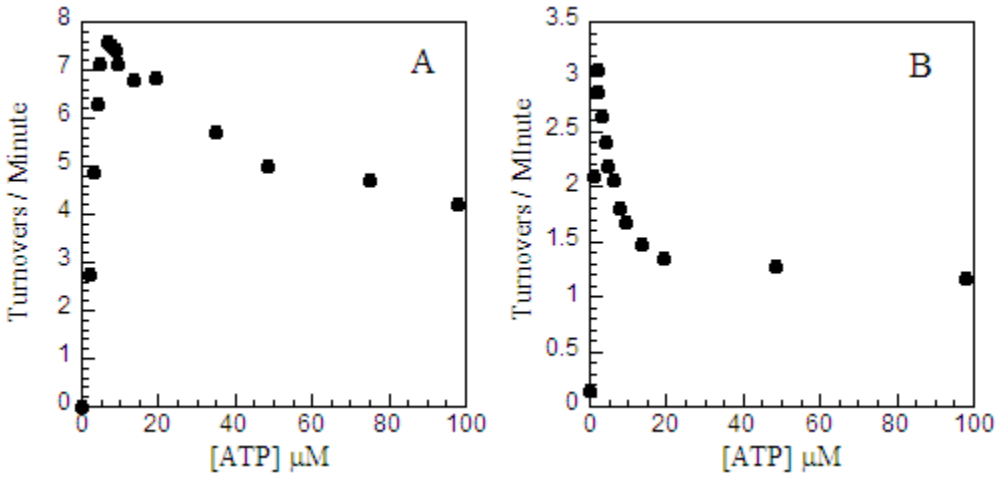

Figure 3-15: Dependence of GroEL ATPase Activity on [ATP]. The ATPase activity at 37°C of $GroEL_{WT}$ (**A**) and $GroEL_{IRX}$ (**B**) was determined with the coupled-enzyme assay using a subunit concentration of 2 μM. The [ATP] concentration at which the first transition occurs is too low to be measured with this assay in the case of $GroEL_{IRX}$.

phosphate binding protein (PBP) (67, 68). PBP is a phosphate scavenger that binds inorganic phosphate with very high affinity. Webb and colleagues constructed a single cysteine mutant of PBP (A197C) and labeled it with a thiol-specific fluorescent probe, MDCC. They found that the fluorescence emission of PBP-MDCC was extremely sensitive to very low concentrations of phosphate, able to detect nanomolar amounts. PBP-A197C was obtained from Dr. Webb, purified and labeled with MDCC as described in sections 3.2.3 and 3.2.4. An ATPase assay loosely based on a published protocol (71) was then developed using PBP-MDCC as its indicator (section 3.2.5).

The ATPase activity of $GroEL_{IRX}$ was measured using a GroEL concentration of 0.05 μM, 40-fold less than in the coupled-enzyme assay. This was done using PBP-MDCC at a concentration of 3 μM, where its fluorescence emission following excitation at 425 nm had a linear dependence on phosphate concentration over a useful range of $[P_i]$ (Figure 3-16a). Measurements were done at 37°C in 50 mM Tris pH 7.5, 100 mM KAc,

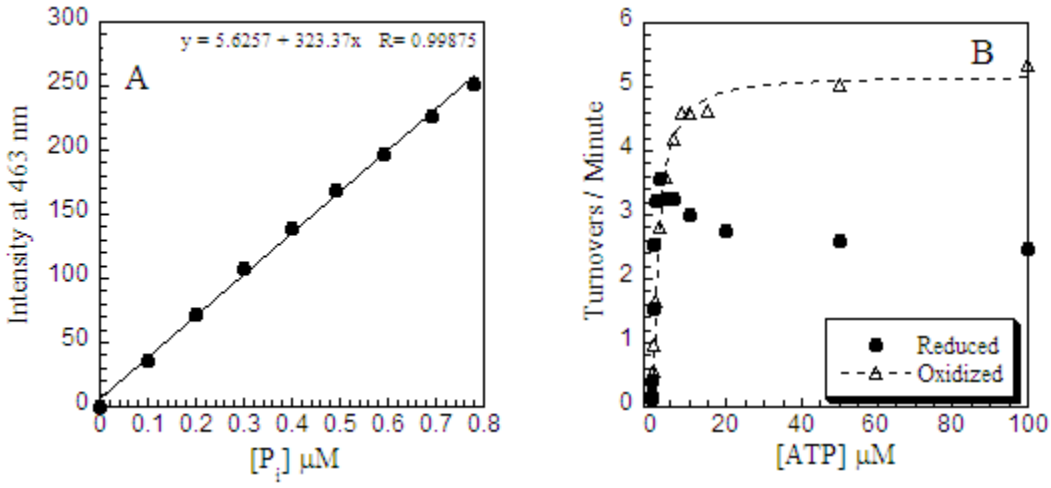

Figure 3-16: Determination of GroEL$_{IRX}$'s ATPase Activity Using the PBP Assay. In order to use a lower [GroEL], the more sensitive fluorescent PBP assay was used to measure activity. **A)** The fluorescence response to increasing amounts of inorganic phosphate was standardized before every experiment using a phosphate standard curve, an example of which is shown here. **B)** ATPase activity of both reduced (closed circles) and 50% oxidized (open triangles) GroEL$_{IRX}$ was determined with the PBP assay at 37°C using 0.05 μM GroEL. The oxidized GroEL data were fit to the Hill equation giving values: Vmax=5.2 turnovers/min., K=0.44 μM, n_H=1.3.

10 mM MgAc, 0.2 mM PEP, and 5 u PK. The latter two were included to ensure a constant [ATP]. Great care was taken to eliminate contaminating phosphate from all solutions by making use of a enzymatic phosphate "mop" developed by the Webb group (see section 3.2.4) (68). The results in Figure 3-16b show that both breakpoints now occur above site concentration, at about 1 μM and 10 μM. All transitions are shifted to lower [ATP] compared to GroEL$_{WT}$, indicating a reduction in the overall cooperativity with respect to ATP binding. The shifting of the transition to lower [ATP] is consistent with the absence of a salt-bridge that stabilizes the T state, which R197/E386 does. The rates overall are about half that of GroEL$_{WT}$. Rates obtained using PBP as an indicator are very close to those obtained with the coupled-enzyme assay, demonstrating the usefulness of the PBP assay.

3.4.5 Locking GroEL$_{IRX}$ Into the TT State Eliminates Cooperativity Inserting a disulfide bond or cross-link into a GroEL$_{IRX}$ ring presumably locks it into the closed, T state conformation. GroEL$_{IRX}$ that is 50% oxidized should contain more than enough tethers per ring to lock it in a TT conformation (see next section). An allosteric protein that cannot undergo a T→R transition should display no cooperativity. GroEL$_{IRX}$ was oxidized with diamide to an extent of about 50% (confirmed by SDS-PAGE) and was assayed using the PBP method. The results (Figure 3-16b) show standard saturation kinetics, and when fit to the Hill equation ($V_0=V_{max}K[S]^n/(1+K[S]^n)$) (33), have a Hill coefficient of 1.3, close to 1. Thus, cooperativity is eliminated when GroEL$_{IRX}$ is heavily oxidized, confirming that cross-linking locks the rings in the T state.

3.4.6 Two Cross-links Are Needed in a GroEL$_{IRX}$ Ring to Lock it in the T State If the T→R→R' transitions are truly concerted, then one cross-link per GroEL ring should be sufficient to lock the entire ring in the T state. This was successfully demonstrated with GroEL$_{IAX}$ (G. Curien, unpublished), as has been discussed. It was expected that GroEL$_{IRX}$ would exhibit the same properties. To determine this, the ATPase activity of GroEL$_{IRX}$ was measured at different extents of oxidation. Varying amounts of diamide were added to 40 μM GroEL$_{IRX}$ in 10 mM Tris pH 8, 10 mM MgAc, 30 μM CbAn at 37°C, and the reaction was allowed to proceed for at least 30 minutes. To quantitate the extent of oxidation, a small aliquot of the oxidized GroEL$_{IRX}$ was removed, added to NEM to block unreacted cysteines, denatured in SDS loading buffer, and run on a 12 % SDS-PAGE gel as has been described. The remaining oxidized GroEL$_{IRX}$ was added to the ATPase assay cuvet, obtaining a final concentration of 2 μM. The reaction conditions were so-called "RR" conditions, conditions under which both

rings are known to be in the R state. High ATP concentrations are known to create the RR state (33), and a high potassium concentration is thought to do the same (72). Thus, the conditions used in these assays are 50 mM Tris pH 7.5, 100 mM KAc, 10 mM MgAc, 1 mM ATP, 0.2 mM PEP, 0.2 mM NADH, along with LDH and PK. After collecting data for 150 seconds, GroES was added to a final concentration of 2 μM, and data collection was continued for another 150 seconds. Rates were calculated from the data both before and after GroES addition, and plotted vs. the fraction oxidized obtained from the gel quantitation (Figure 3-17a). As was the case with $GroEL_{IAX}$, activity rises as oxidation increases, indicating that the T state has a higher activity than the R state. As was also the case with $GroEL_{IAX}$, activity decreases at higher levels of oxidation, although, unlike $GroEL_{IAX}$, the activity does not appear to extrapolate to zero at 100% oxidation. As would be expected, at higher levels of oxidation, GroES has no effect on the activity, since all rings are presumably locked in the T state at this point and cannot bind GroES.

In order to determine the number of disulfide bonds required to lock a ring in the T state and prevent the transition to the less active R state, theoretical models of the ATPase activity response to oxidation were formulated using the methods that are described in section 3.3.2. The data are then compared empirically to these models, and conclusions are drawn depending on which model follows the data the closest. These models require the input of several parameters: the V_{max} of the R state, the V_{max} of the T state, the number of subunits in a ring that need to be oxidized in order for the ring's activity to decrease (the number of "strikes"), and the residual V_{max} of a subunit in a ring that has been hit with that many "strikes." Finally, the number of cross-links per ring

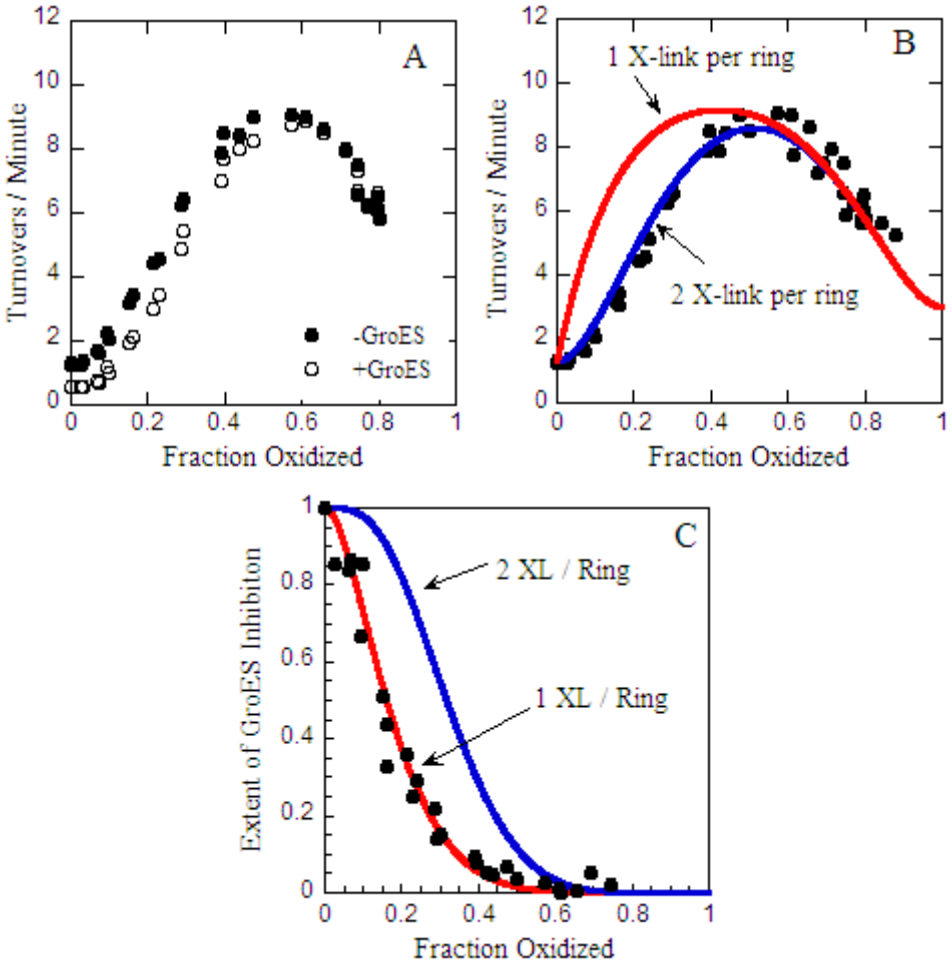

Figure 3-17: Response of GroEL$_{IRX}$ ATPase Activity to Oxidation. GroEL$_{IRX}$ activity was measured at 37°C, 2 μM subunits using the coupled enzyme assay. Fraction oxidized was quantitated by removing a small sample of the diamide-oxidized GroEL and blocking it with NEM for later use on a SDS-PAGE gel. **A**) ATPase activity with (open circles) and without (closed circles) 2 μM GroES. **B**) Data without GroEL were plotted against theoretical models in which one or two cross-links in a ring are required to lock the ring in the T state and prevent the T→R transition. The models were formulated using the methods described in Figure 3-9 and in the text. The models here were formulated using $V_{max}R$=1.3, $V_{max}T$=9.5, $V_{max}Res$=3, and assuming that 6 strikes in a ring were required to reduce its activity to $V_{max}Res$. **C**) The ability of GroES to inhibit ATPase activity (as calculated in the text) was plotted against two theoretical models which predict that one or two cross-links in a ring are required to prevent that ring from binding GroES (undergoing the T→R' transition).

required to lock it in the T state must be included. Two of these parameters are known from inspection of the data. $V_{max}R$ is the rate measured when the GroEL is fully reduced, since the assay is done under RR conditions. $V_{max}Res$ is the rate that the data appear to extrapolate to at a fraction oxidized of 1. The data show that these values are approximately 1.3 and 3 turnovers per minute, respectively. The other parameters must be determined empirically simply by comparing many different traces to the data. It should be noted that $V_{max}T$ is *not* the activity at the peak of the data curve, since some rings will already have begun to lose their activity at this point on the reaction coordinate. For all experiments such as this, two models were simulated, one in which 1 cross-link locked a ring into the T state (a 1/7 model), and one in which 2 cross-links were needed (a 2/7 model). Equations used to produce these models assuming 6 strikes are given in the Appendix. Data obtained with the single-ring version of GroEL suggest that the number of strikes needed in a ring to reduce the activity was 6 (J. Gresham, unpublished). Therefore, the only parameter left to be determined was $V_{max}T$. Through trial and error, it was determined that a model in which $V_{max}T$ was set to 9.5 fit the data the best (Figure 3-17b). This is about half of the empirically determined $V_{max}T$ for $GroEL_{IAX}$ (see Chapter 4). What was unexpected was that this model was a 2/7 model, one in which *2* cross-links were needed per ring in order to lock it in the T state, not 1 as would have been expected if the subunits moved in a concerted fashion.

It should be noted that several other models were considered to explain the data. A model in which 1 cross-link locked both rings in the T state (a 1/14 model), or one in which one cross-link locked a ring in the T state, but destroyed the activity in the two subunits that were cross-linked together were formulated and discarded. There are

several other examples that need not be noted here. The only model that satisfactorily described the data was the 2/7 model, primarily due to the lag seen in the data at low levels of oxidation.

3.4.7 One Cross-link Per GroEL$_{IRX}$ Ring is Sufficient to Prevent GroES Binding The same set of data can be used to examine the effect of oxidation on GroEL$_{IRX}$'s ability to bind GroES by examining the effect of GroES addition on ATPase activity. GroES inhibition of ATPase activity was quantitated by dividing the rate measured without GroES by the rate measured with GroES to obtain the fraction of activity inhibited by GroES. This number was normalized using the following equation:

$$Inhibition\ Factor_{Normalized} = \frac{(1 - ES\ Inhibition_{GroEL\ At\ 0\%\ Oxidized})}{(1 - ES\ Inhibition_{GroEL\ Oxidized\ to\ X\ Extent})}.$$ Presented in this way, an inhibition factor of 1 means that GroES is having its maximal effect on GroEL ATPase activity (usually reducing the activity to half of what it is without GroES), and an inhibition factor of 0 means GroES has no effect on the activity. The normalized data are plotted in Figure 3-17c. Theoretical models are also plotted which predict that either 1 or 2 cross-links per ring are necessary to prevent GroES binding (section 3.2.2). The data points clearly follow the model in which 1 cross-link per ring prevents GroES binding, or put another way, 1 cross-link per ring prevents the T$\rightarrow$R' transition. At least in the case of this transition, conformational changes appear to be concerted.

3.4.8 GroEL$_{IRX}$'s Ability to Release GroES is Compromised Binding of ATP to the *trans* ring of a GroEL/GroES bullet complex causes GroES and trapped ADP to be released from the opposite *cis* ring. Studies with GroEL$_{WT}$ and GroEL$_{IAX}$ bullets indicate that ADP is completely released within 1 minute of ATP addition (G. Curien, unpublished). Studies with GroEL and GroES labeled with fluorescent probes that

constitute a FRET pair show that GroES release takes place anywhere from 40 seconds down to <1 second depending on conditions (see Chapter 5). The release rate of GroES from reduced $GroEL_{IRX}$ was measured using the assay described in section 3.2.6 in which the GroEL/GroES bullet is made using a small excess of ^{14}C-labeled ATP, which is allowed sufficient time to exhaust. Following the addition of a large excess of unlabeled ATP to cause release, the remaining bound ^{14}C is measured at several time points. The results in Figure 3-18 show that release of ^{14}C-ADP occurs with a half time of 8-10 minutes, much slower than in similar experiments with $GroEL_{WT}$ or $GroEL_{IAX}$.

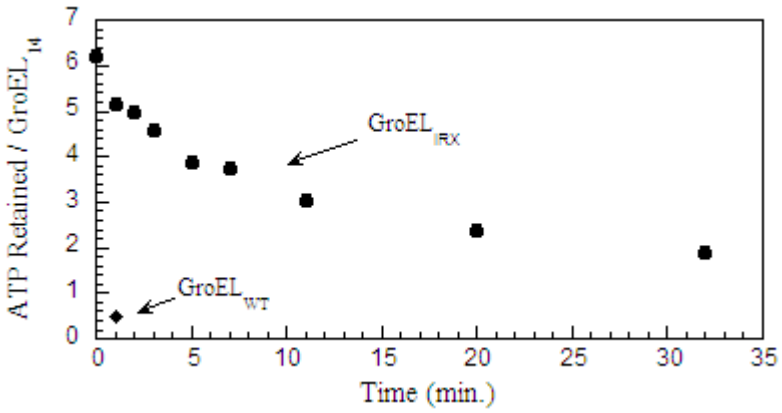

Figure 3-18: Kinetics of GroES Release from $GroEL_{IRX}$ in Response to ATP Binding to the *Trans* Ring. The release of GroES from the $GroEL_{IRX}$/GroES/ADP bullet was quantitated by measuring the amount of trapped ^{14}C-ADP left bound to GroEL underneath the GroES cap at various times following the addition of a large excess of cold ATP. The reaction was quenched by loading the solution on a PD-10 column and separating free ATP from the GroEL. ^{14}C-ADP co-eluting with GroEL was measured by scintillation counting.

Since the assay using ^{14}C-ATP actually measures the release of ADP from the bullet complex and not GroES release, it was possible that GroES was being released but not ADP. To confirm the results of the ^{14}C-ATP assay, GroES release was measured by another method (section 3.2.7) (69) in which the GroEL/GroES bullet is made using his-tagged GroES ($GroES_{His}$). The complex is then loaded onto Ni-NTA resin. Following a

wash with buffer to elute unbound protein, ATP and excess wild-type GroES are added to the resin to initiate bullet dissociation and cause GroES exchange. His-tagged GroES and any remaining complexed GroEL are then eluted with an imidazole wash. All elutions from the column are collected and run on an SDS-PAGE gel. As is seen in Figure 3-19, a control experiment with $GroEL_{WT}$ shows complete release of GroEL from $GroES_{His}$ within the time span of the experiment (about 5 minutes). However, the same experiment with reduced $GroEL_{IRX}$ shows that only about 50% of the $GroES_{His}$ has been released over the same time span. This confirms that $GroEL_{IRX}$ is somehow deficient in its ability to signal bullet dissociation following ATP binding to the *trans* ring.

Section 3.4.9 Unfolded SP Does Not Stimulate $GroEL_{IRX}$ ATPase Activity The ATPase activity of $GroEL_{WT}$ is stimulated approximately 6-7-fold in the presence of unfolded SP (34). The ATPase activity of $GroEL_{IRX}$ was measured in the presence two acid-denatured SPs, α-lactalbumin and malate dehydrogenase. In neither case was any stimulation of activity seen (Figure 3-20a). $GroEL_{WT}$ in the same experiment was stimulated 6-7 fold by both SPs.

It is possible that $GroEL_{IRX}$ does not show any rate enhancement in the presence of SP because it cannot bind unfolded SPs. To make sure that $GroEL_{IRX}$ is binding SP, 80 μM $GroEL_{IRX}$ was reacted with 22 μM folded or unfolded MDH in 20 mM Tris pH 7.5, 100 mM KAc, 10 mM MgAc, 0.2 mM PEP, 100 μM ATP, 2 units PK. The GroEL/MDH solution was loaded onto a S3000 analytical gel filtration column (Phenomenex) equilibrated in 20 mM Tris pH 7.5, 10 mM MgAc, 100 μM ATP, 50 mM NaCl, 0.05% NaN_3. This column can separate GroEL/MDH complex from free MDH. The GroEL and MDH peaks were collected, precipitated with trichloroacetic acid,

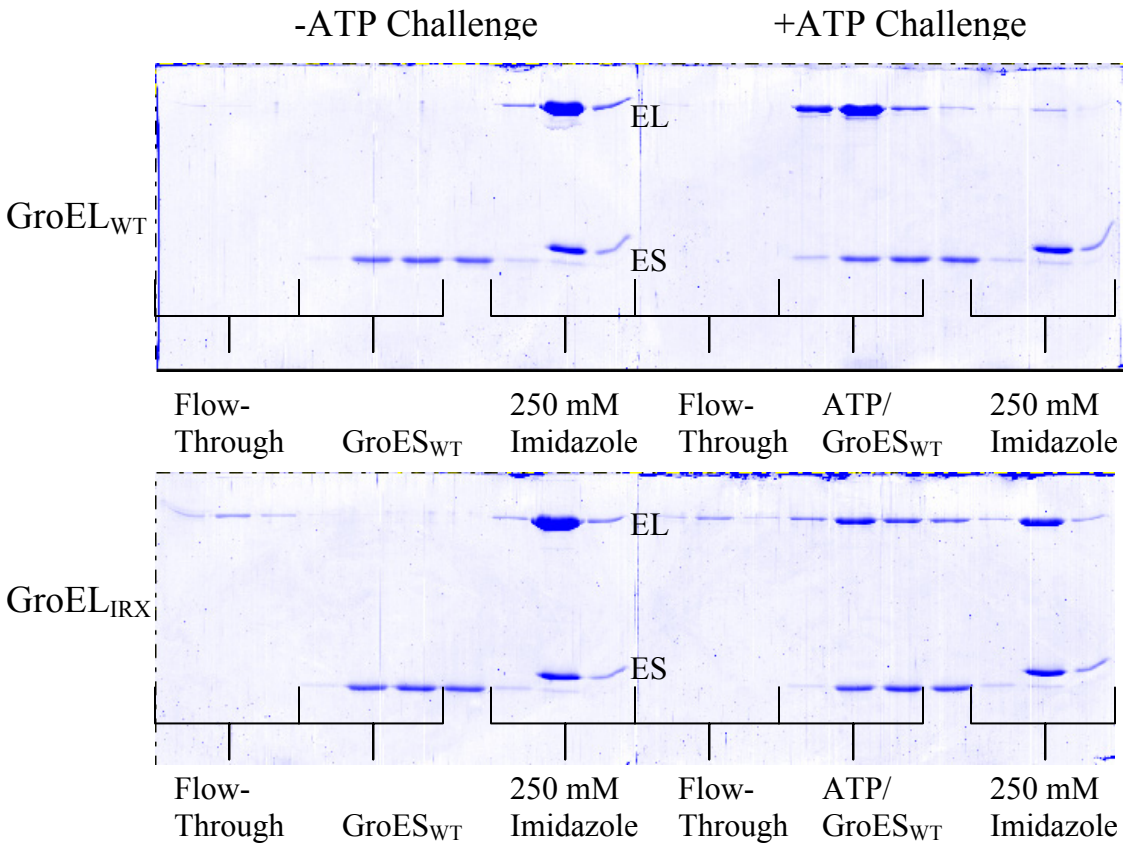

Figure 3-19: GroES Release from GroEL$_{IRX}$ as Measured Using GroES$_{His}$. As described in section 3.2.7, the bullet complex was made with 14 μM GroEL (WT or IRX) and GroES$_{His}$, and loaded onto a Ni-NTA column. The column was washed 3 times with buffer, with the washes collected as the flow-through. Next, GroES$_{WT}$/±ATP was applied to the column in 3 portions to initiate GroEL release from GroES$_{His}$ in exchange for GroES$_{WT}$. Following 1 wash with buffer to remove remaining GroES$_{WT}$, GroES$_{His}$ was released from the column with 3 washes of 250 mM imidazole. All 10 fractions were run on 15% SDS-PAGE gels, loaded in order of elution. On each gel, the first three lanes are the flow-through, showing GroEL which was not retained on the column, presumably because it never bound GroES$_{His}$. The next four lanes contain the GroEL (upper band) eluted by GroES$_{WT}$ ± ATP, along with the GroES$_{WT}$ (lower band). The last three lanes contain the GroEL which elutes with GroES$_{His}$, presumably because it did not release from GroES$_{His}$ upon addition of ATP. GroES$_{His}$ runs with a slightly reduced mobility compared to GroES$_{WT}$.

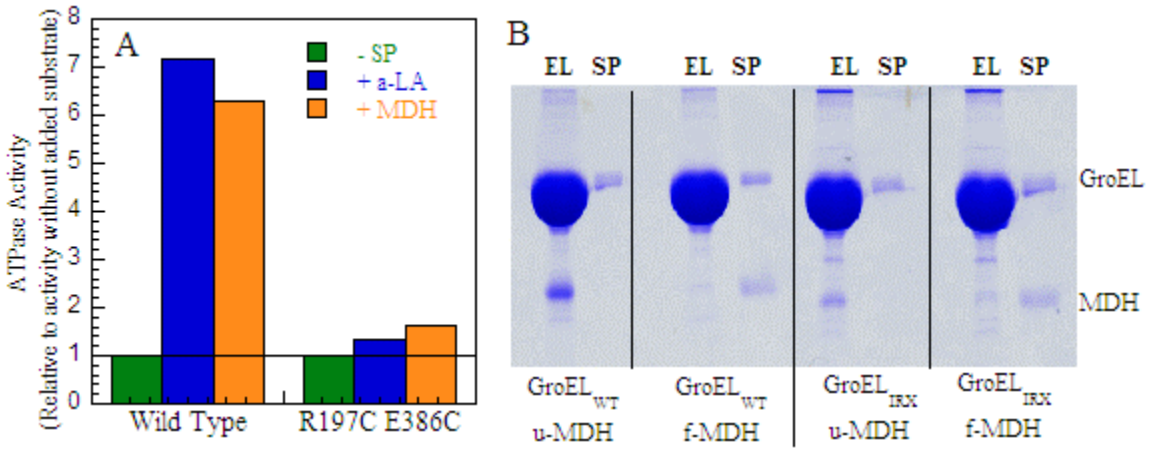

Figure 3-20: $GroEL_{IRX}$ Binds Unfolded SP but its ATPase Activity is Not Enhanced by it. **A**) The ATPase activity of $GroEL_{WT}$ and reduced $GroEL_{IRX}$ was measured in the presence of acid-denatured α-lactalbumin or malate dehydrogenase (50-fold excess and 4-fold excess over GroEL rings respectively). ATPase rates are plotted relative to the activity of GroEL without added SP. **B**) The binding of folded and unfolded MDH to $GroEL_{WT}$ or reduced $GroEL_{IRX}$ was examined. Native or acid-denatured MDH was mixed with GroEL in the presence of ATP and loaded on an S3000 analytical gel filtration column to separate unbound MDH from GroEL and any bound MDH. The GroEL and MDH peaks were collected and run on 12% SDS-PAGE gels.

dissolved in loading blue, and samples of each were loaded onto an SDS-PAGE gel (Figure 3-20b). Folded MDH eluted entirely as free MDH, but unfolded MDH eluted both as free MDH and also co-eluted with the GroEL, indicating that unfolded MDH does indeed bind to $GroEL_{IRX}$. A control experiment with $GroEL_{WT}$ showed the same result with a comparable amount of MDH binding. These results seem to show that $GroEL_{IRX}$ can bind unfolded SP, but for some reason its ATPase activity is not enhanced by it.

Section 3.5 Discussion

The earlier studies done with $GroEL_{IAX}$ provided straightforward answers as to the effect of adding cross-linkers to a GroEL ring. In the cases of both the T→R and T→R' transitions, one cross-link within a ring was sufficient to lock that ring in the T

state (G. Curien, unpublished). If one cross-link is enough to lock a ring in the T state, then it can be inferred that all subunits are moving in a concerted fashion as a ring opens and closes. This concerted motion would seem to be a favorable mechanism for providing the maximum unfolding force if GroEL does actively unfold proteins. It was expected that $GroEL_{IRX}$ would closely mimic those results, but this did not prove to be the case. The studies presented here with $GroEL_{IRX}$ reveal some important limitations of the sort of analysis used here, and they provide some evidence that the allosteric mechanism is more complicated than was previously thought.

Before discussing allostery, there is one unusual, but consistent, result seen in all cross-linking experiments done with $GroEL_{IRX}$. It may have been noticed that in all cross-linking experiments, $GroEL_{IRX}$ is never oxidized or cross-linked beyond about 80%. $GroEL_{IAX}$ could be cross-linked to at least 95%. There are several reasons why this may be so. The first is the presence of $GroEL_{WT}$ subunits in all 14-mers. $GroEL_{WT}$ is produced from the native *E. coli* GroE operon in an unknown amount during bacterial growth and during induction. The presence of even one $GroEL_{WT}$ subunit in a mostly $GroEL_{IRX}$ 14-mer will reduce the number of possible tethers in that 14-mer from 14 to 12, since the double cysteine pair in this mutant is intersubunit. This means that the reaction coordinate can never exceed 85%. The presence of a second wild-type subunit would reduce this number even further. Eliminating all $GroEL_{WT}$ subunits requires advanced molecular biology techniques, made more difficult by the fact that GroEL is absolutely required for cell growth. This was not deemed to be necessary for these experiments, and a maximum extent of cross-linking of 80% proved to be sufficient to obtain the necessary results.

The most surprising result obtained with $GroEL_{IRX}$ was that 2 cross-links per ring are required to lock a ring in the T state and prevent the T→R transition. This result is difficult to interpret in the face of all of the other results from these types of experiments, which have suggested that all subunits move in a concerted motion. The T→R' transition in this mutant appears to be concerted, and both transitions are concerted in $GroEL_{IAX}$. However, it does seem possible that one transition only requires one cross-link to prevent it from occurring whereas the other requires two. The two transitions involve different conformational changes. The T→R transition is only a partial opening of the ring, involving the movement of the apical domains upwards and twisting anticlockwise 25° in response to ATP binding in the absence of GroES. The T→R' transition requires a more dramatic upward motion of the apical domains, and a 90° clockwise twist (relative to the T conformation). It is possible that the elimination of the R197/E386 salt bridge allows enough flexibility in the motion of the ring to allow the T→R transition to occur more freely, and additional tethers may be required to hold the ring in the T state. Complicating the situation further is a recent cryo-EM structure of ATP-bound GroEL produced by Helen Saibil and co-workers, which presumably mimics the R state (36). In this structure, a salt bridge is postulated to exist between K80 and E386. Thus, the E386C mutation in $GroEL_{IRX}$ may not only remove a T state salt bridge, but an R state one as well. Both the T and R states may be destabilized by this mutation. It is, therefore, possible that the motion of a $GroEL_{WT}$ ring is indeed concerted, and the unusual result seen with this mutant is an artifact of the mutations. There has also been a recent observation that the energy of the R197/E386 salt bridge is possibly coupled to the energy of a salt bridge involving D155 (73). The weakening of one salt bridge leads to

the weakening of the other. A GroEL mutant, D155A, remarkably undergoes *sequential* structural transitions rather than concerted ones, for an unknown reason (73). It is possible that the structural transitions of $GroEL_{IRX}$ are less concerted due to a weakening of the D155/R395 salt bridge, leading to a partially sequential transition, and this may be why two cross-links rather than one are required to prevent the T→R transition.

The observation that the structural transitions of $GroEL_{IRX}$ occur at lower ATP concentrations than observed with $GroEL_{WT}$ is more readily explained. The removal of a salt bridge that stabilizes the T state would be expected to allow an easier transition to the R state (although this is complicated by the E386 mutation potentially removing both a T and R state salt bridge). The shifting of the transitions to lower ATP concentrations also raises the values of the allosteric constants L_1 and L_2. The Hill coefficient describing the interaction between the two rings can be calculated using the following equation: $n_H = 2/[1+(L_1/L_2)^{1/2}]$ (33). The values of L_1 and L_2 were not explicitly determined in these studies due to the necessity of eliminating the exclusive binding assumption (see sec. 1.6) from the complex equation needed to fit these data. This is work ongoing in the lab (J. Gresham, unpublished). However, published work with a similar mutant, R197A (33, 74), is entirely consistent with the results obtained here, in that the values of the allosteric constants were higher than those for wild-type. In the case of the R197A mutant, the Hill coefficient as calculated above was higher compared to wild-type (0.07 vs. 0.003 respectively) (33). Since these numbers are less than one and describe negative cooperativity, an increase in n_H compared to wild-type means that negative cooperativity is reduced in the mutant. It may then be assumed that negative cooperativity in $GroEL_{IRX}$ is reduced as well, based on the similar results to R197A.

This reduction in negative cooperativity may provide an explanation for another unusual result obtained with $GroEL_{IRX}$. As has been shown, the ability of $GroEL_{IRX}$ to release GroES upon binding ATP to the *trans* ring is somehow deficient compared to $GroEL_{WT}$. This event requires communication of an unknown, probably subtle, structural signal from the *trans* ring to the *cis* ring. A reduction in negative cooperativity implies that the two rings are not communicating properly in $GroEL_{IRX}$, and thus the release signal is possibly not being sent efficiently. The structural basis for the R197C/E386C mutations affecting negative cooperativity, which is almost certainly controlled primarily by interactions at the equatorial plate, remains unknown.

The observation that unfolded SP does not stimulate ATPase activity in $GroEL_{IRX}$ as it does in $GroEL_{WT}$ is more difficult to explain, although the reason may also involve the reduction in negative cooperativity. It has been observed that the single-ring variant of GroEL, SR1, is also not stimulated by SP (J. Gresham, unpublished). In this mutant, negative cooperativity clearly cannot exist. It is therefore possible that stimulation by SP somehow depends on negative cooperativity, or more accurately, depends on efficient inter-ring communication. Stimulation by SP will be covered in more detail in the next chapter, and its possible dependence on inter-ring communication will be discussed in Chapter 6. These studies with $GroEL_{IRX}$ highlight the potential importance of inter-ring communication in events in which this type of signaling has previously not been implicated.

Chapter 4

Allosteric Basis for the Actions of SP on GroEL ATPase Activity: Evidence for Active Unfolding

4.1 Introduction

It is difficult to demonstrate that GroEL exerts a mechanical force on bound SP. Short of an atomic force microscopy experiment, the only ways currently available to demonstrate the existence of active work on SPs are by indirect methods. The following argument can be considered: if GroEL exerts force on an SP and pulls it apart, then the SP must exert a reciprocal force on GroEL.

GroEL would exert its pulling force during the separation of its SP binding sites while undergoing its allosteric transitions (Figure 1-2). Adjacent binding sites move from being 23 Å apart in the T to state to 29 Å apart in the R state, to an even larger 36 Å in the R' state. The presence of SP would tend to counteract the displacement of the binding sites. Since the SP binding sites are most exposed in the T state, SP preferentially binds to the T state. SP bound to these sites will thus tend to hold a ring in the T conformation, affecting the T→R equilibrium in favor of the T state (34).

But, does SP actually pull on the SP binding sites, holding a ring in the T state? A clue is provided by the observation that unfolded substrate stimulates the ATPase activity of $GroEL_{WT}$ (34). At the time this was discovered, it was postulated that the stimulation was the result of a shift in the overall equilibrium from the RR state to the TR state. According to the original nested cooperativity model, the TR state is the most active state, due to the highly active R ring (33). This model, however, contains the exclusive binding assumption. From the results with $GroEL_{IAX}$, and the results presented in Chapter 3 with $GroEL_{IRX}$, it is now known that the exclusive binding assumption is invalid. The T state does bind ATP and hydrolyzes it at a faster rate than the R state. The reasons behind ATPase stimulation by SP must therefore be revisited.

Since the presence of SP shifts the T→R equilibrium in favor of the T state, and since we now know that the T state has a higher ATPase activity than the R state, it is tempting to speculate that ATPase activity is stimulated because SP is holding one or both rings in the T conformation. In effect, the SP is acting as a tether, similar to the tethers provided by the disulfide bonds or chemical cross-links in the studies with $GroEL_{IAX}$ and $GroEL_{IRX}$. The latter two are covalent linkages; mechanical constraints that lock a ring in the T state by counteracting the force of the structural transition. If SP is mimicking a covalent tether, then it must also be counteracting the motion of the subunits, and it must do this by exerting its own force on the subunits. This is what would be predicted if active unfolding occurs in the GroE system. In order for GroEL to encapsulate the SP, it must overcome the force of the SP and undergo the T→R→R' transitions, binding GroES and burying the SP binding sites. If the binding of SP is tight, then bound SP will be stretched as the subunits move, and will be actively unfolded. Therefore, a demonstration that SP mimics the effect of a covalent tether will provide further evidence that active unfolding by GroEL is a real process.

If SP is mimicking a covalent bond, then certain predictions can be made about the effect of SP on the behavior of GroEL. If SP is locking, or holding, a ring in the T state, then the measured ATPase activity in the presence of SP should be approximately the V_{max} of the T state. $V_{max}T$ cannot be measured directly, but can be estimated using the ATPase models described in the previous chapter if the experiments are performed with a double cysteine mutant, such as $GroEL_{IAX}$. Furthermore, SP should have no additional effect on the ATPase activity of $GroEL_{IAX}$ that has already been locked in the T state. Finally, if SP is acting as a tether, then it must be acting as an intersubunit tether,

connecting two or more SP binding sites. These binding sites need not necessarily be on adjacent subunits. This would depend on the conformation of the highly variable unfolded substrate. But, the SP would necessarily have to be large enough to span at least two adjacent subunits in order to act as a tether, a distance of approximately 23 Å. A small substrate such as a short peptide should not be able to form a tether, and therefore should not affect the ATPase activity. Here, these predictions are tested experimentally using two different SPs and by making use of $GroEL_{IAX}$, the intrasubunit double cysteine mutant.

4.2 Methods Specific to Chapter 4

4.2.1 Assay for MDH Activity During Re-folding by GroEL The recovery of activity by MDH during re-folding by GroEL was monitored spectroscopically. Acid-denatured MDH was added to a solution containing 50 mM Tris pH 7.5, 100 mM KAc, 10 mM MgAc, 0.2 mM PEP, 0.2 mM NADH, 1 mM DTT, 1 mM ATP, 5 units PK, 2 μM $GroEL_{WT}$, and 2 μM GroES, with a final MDH concentration of 0.4 μM at 30°C. At various times after MDH addition, 30 μl of this refolding reaction was removed and added to a cuvet containing 900 μl 50 mM Tris pH 7.5, 100 mM KAc, 10 mM MgAc, 0.2 mM NADH, 1 mM DTT and 1 mM oxaloacetate. The final [MDH] was 14 nM. The decrease in absorbance at 340 nm was monitored over 30 seconds, and the rate was calculated using the ΔAU and the [MDH].

4.3 Results

4.3.1 Effect of SPs on GroEL ATPase Activity The ATPase activity of $GroEL_{WT}$ and $GroEL_{IAX}$ was measured in the presence of acid-denatured α-lactalbumin (α-LA) and malate dehydrogenase (MDH) using the coupled enzyme assay at 37°C. α-

LA is a convenient SP to use in these experiments, because it is stable at all temperatures used and will not refold even in the presence of GroEL/GroES. MDH is less convenient, because it is somewhat unstable at 37°C, tends to aggregate, and will refold in the presence of both GroEL and GroES (but, not GroEL alone). Representative data are shown in Figure 4-1. In all cases, the GroEL concentration was 2 μM. A 25-fold excess

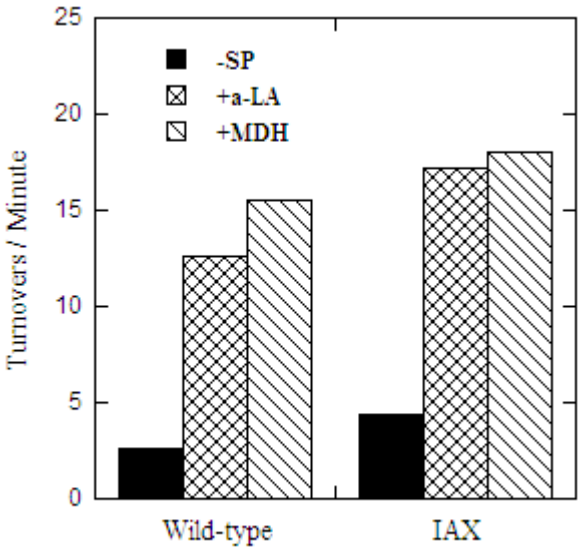

Figure 4-1: Stimulation of ATPase Activity by Unfolded SP. A 25-fold excess of acid-denatured α-LA or a 2-3-fold excess of acid-denatured MDH (see section 2.10) was added to a GroEL ATPase reaction with 2 μM GroEL at 37°C. $GroEL_{WT}$ consistently showed slightly slower rates than $GroEL_{IAX}$ but was stimulated by SP to a greater extent. Controls using folded α-LA and MDH showed slight stimulations (about 1.5-fold), probably due to the presence of unfolded protein in these commercial preparations.

of α-LA or a 2-3 fold excess of MDH over GroEL rings was used to obtain the rates shown. $GroEL_{WT}$ was typically stimulated 5-7 fold by SP, and $GroEL_{IAX}$ about 3-4 fold. $GroEL_{IAX}$ consistently shows a higher basal ATPase rate than $GroEL_{WT}$, which explains why it did not undergo the same degree of stimulation. The absolute rates and the degree of stimulation obtained with unfolded SPs tended to vary from experiment to experiment, depending on the preparation of GroEL that was used. This most likely reflected the

small amount of contamination that remained even after the acetone precipitation was used to purify the GroEL. Controls with folded SP typically showed about a 1.5-fold stimulation of activity, presumably due to unfolded SP present in the solution (data not shown).

4.3.2 Titration of Unfolded SP To determine the amount of SP required for maximal stimulation of $GroEL_{WT}$ and $GroEL_{IAX}$, increasing amounts of unfolded α-LA or MDH were added to 2 μM GroEL (0.14 μM $GroEL_{14}$) and activity was measured at 37°C. The results are presented in Figure 4-2. The SPs appear to bind less efficiently to $GroEL_{IAX}$. This is probably due to the absence of the T state salt bridge causing a shift of the T→R intra-ring equilibrium towards the R state, making the SP binding sites less accessible. A 50-fold excess of the weak-binding α-LA over rings is needed to cause maximum rate stimulation, but in the case of the tight-binding MDH, only a 3-fold excess is required.

4.3.3 Refolding of MDH by GroEL/GroES The re-folding of MDH is accelerated by the complete GroE system (GroEL, GroES, ATP) (64). It was noticed that upon addition of MDH to an ATPase reaction containing both GroEL and GroES, that there is an initial rate stimulation, followed by a slow decrease back to approximately the rate measured without added MDH. No such observation is made with α-LA, which, once added, continues to stimulate the rate to the same extent for the entire measurement (Figure 4-3). Once decalcified, reduced, and denatured, α-LA cannot refold to the native state (34) even in the presence of GroE, whereas MDH can. The burst of activity seen with MDH followed by the relaxation to the initial rate must represent the refolding of the SP, which no longer stimulates GroEL's ATPase activity once refolded. The

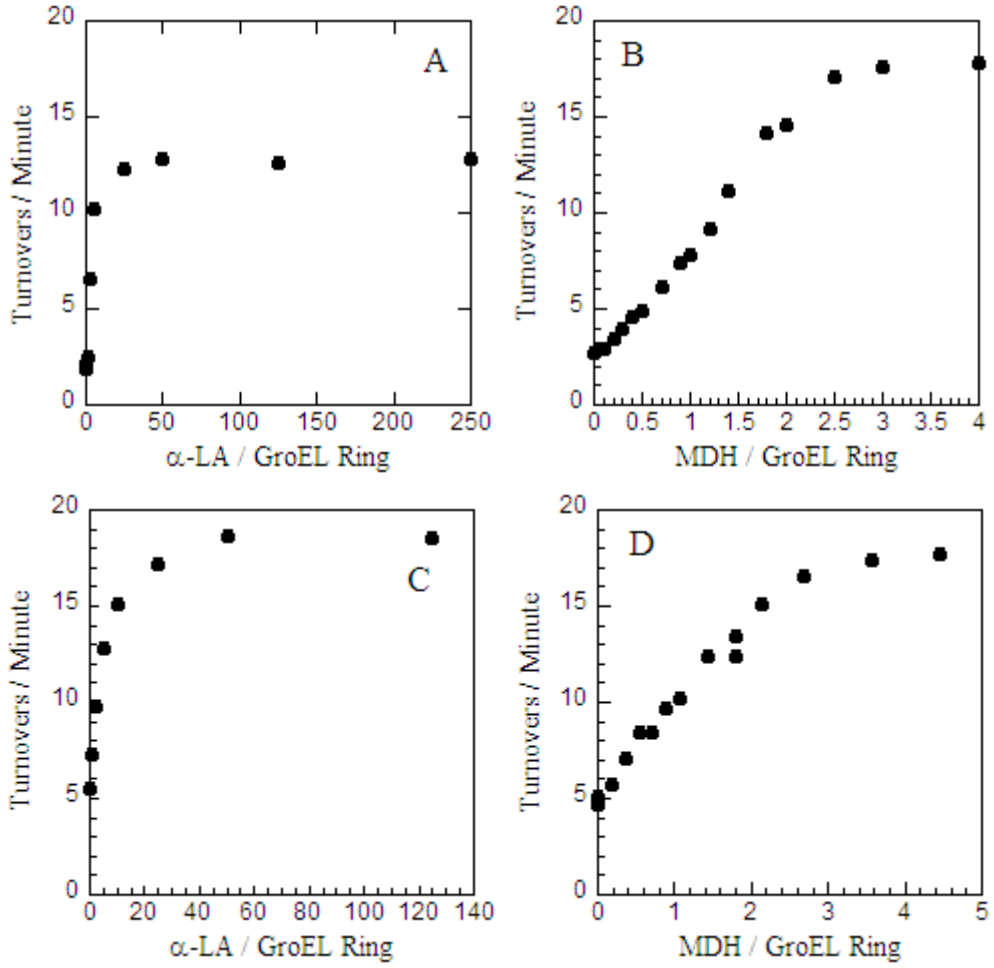

Figure 4-2: Titration of unfolded SP into GroEL ATPase Reactions. Increasing amounts of α-LA or MDH were added to GroEL ATPase reactions with 2 μM GroEL (0.29 μM GroEL rings) at 37°C. **A**) $GroEL_{WT}$ with α-LA **B**) $GroEL_{WT}$ with MDH **C**) $GroEL_{IAX}$ with α-LA, **D**) $GroEL_{IAX}$ with MDH.

amplitude of the burst is dependent upon the concentration of MDH added, and the rate of refolding is approximately constant at all [MDH] (Figure 4-4a,b,c).

To confirm that MDH is refolded under the conditions of the ATPase assay, unfolded MDH was added to a solution containing the complete GroE system in the same buffer as was used in the coupled-enzyme assay (Figure 4-4d). At various times, MDH activity was measured by removing an aliquot of this reaction and adding it to a cuvet

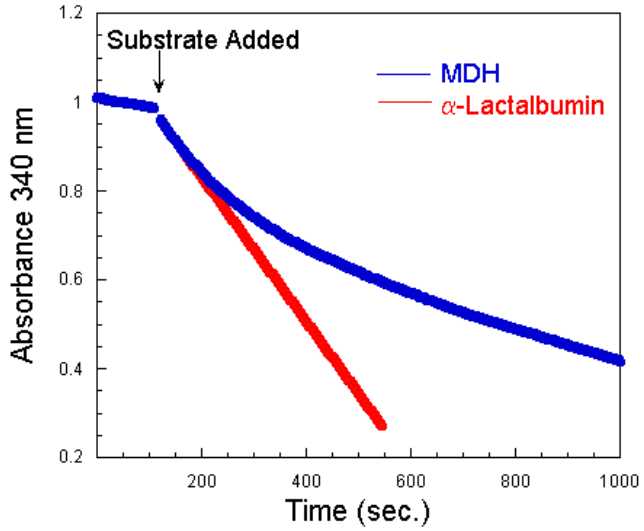

Figure 4-3: Addition of SP to GroEL/GroES ATPase Reaction. The change in rate upon addition of α-LA or MDH to an ATPase reaction was monitored in real-time using the coupled-enzyme assay. The absorbance readings at 340 nm are shown, with SP added at the arrow, and rate can be inferred by considering the slope of the trace. Addition of a 25-fold excess of α-LA over $GroEL_{WT}$ rings in the presence of 2 μM GroES at 37°C causes constant stimulation over the course of the measurement. Addition of a 2-fold excess of MDH to $GroEL_{WT}$/GroES causes an initial rapid decrease in absorbance followed by a slow return to approximately the same slope as before the SP was added. The mixing points are masked for clarity.

containing oxaloacetate and NADH (section 4.2.1). This experiment was carried out at 30°C due to the instability of MDH at 37°C (63). The kinetics of the ATPase burst and that of the MDH re-folding cannot be directly compared due to a dimerization step that must take place in order for MDH to regain full activity (50).

4.3.4 X-linked $GroEL_{IAX}$ is not Affected by SP The simplest explanation for why SP stimulates activity is that SP is forcing the GroEL ring to maintain the more active T conformation. If this is true, then SP should not affect the ATPase activity of a ring that is already locked in the T state by a cross-link. To test this, $GroEL_{IAX}$ was cross-linked to an extent of about 25% and assayed with and without SP. An extent of

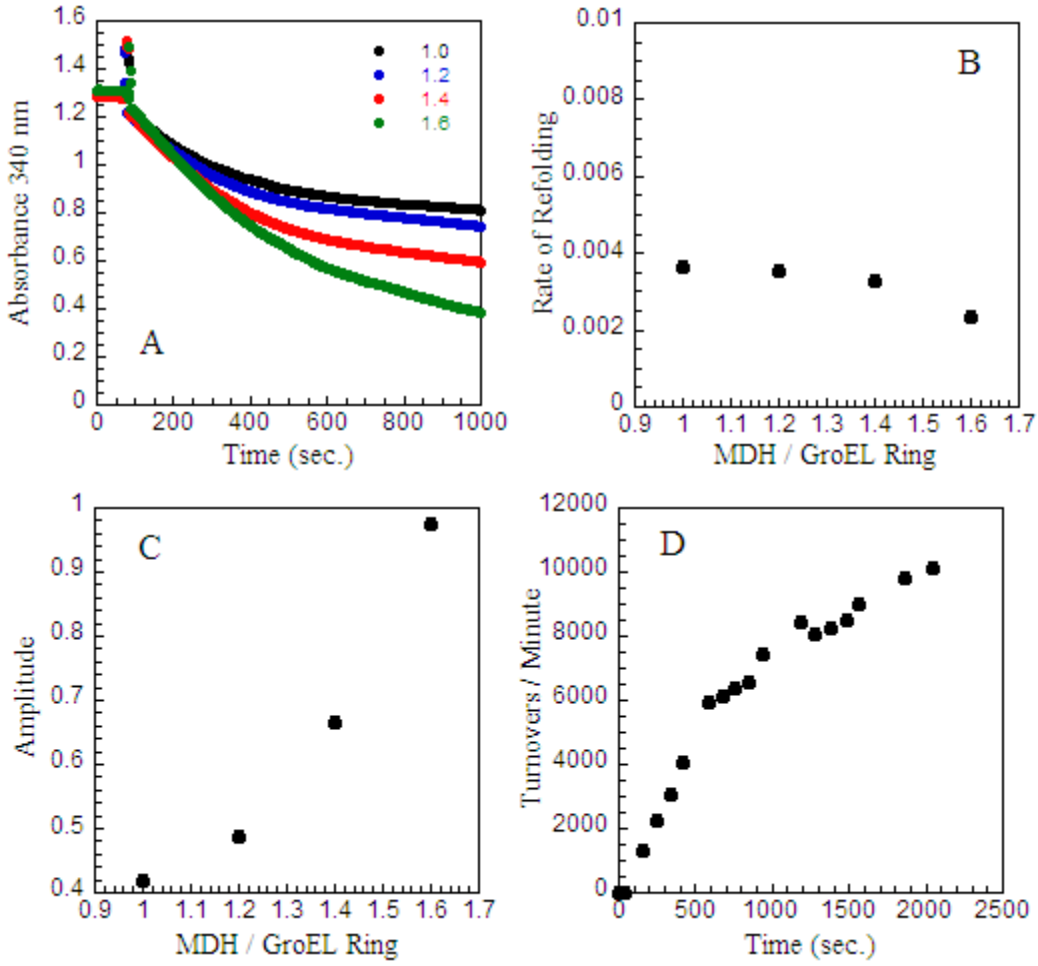

Figure 4-4: Monitoring the Re-folding of MDH by GroEL$_{WT}$/GroES. Various amounts of acid-denatured MDH were added to a cuvet containing 50 mM Tris pH 7.5, 100 mM KAc, 10 mM MgAc, 0.2 mM PEP, 0.2 mM NADH, 1 mM ATP, 4 u LDH, 5 u PK, 2 μM GroEL$_{WT}$, and 2 μM GroES at 30°C. The reaction was monitored in real-time at 340 nm. **A**) Real-time data showing decrease in absorbance. MDH was added after 100 seconds of monitoring GroEL and GroES alone. The figure legend denotes the number of MDHs per GroEL ring. The outlying data at the point of SP addition are the interference of the UV beam by the mixer. **B**,**C**) The data from **A** following MDH addition (the mixing points and data prior to MDH addition were masked) were fit to single exponentials. Rates (**B**) and amplitudes (**C**) are plotted against the MDH amount. **D**) The recovery of MDH activity during re-folding by GroEL/GroES was monitored using the assay described in section 4.2.1. Prior to measuring MDH recovery, the GroEL ATPase "burst" response was confirmed by monitoring the GroEL ATPase activity upon MDH addition. Acid-denatured MDH was fully inactive as confirmed by assaying it before adding it to GroEL/GroES. The activity of folded MDH was measured prior to the experiment to confirm that MDH was being fully refolded by GroEL/GroES.

25% was chosen because this is approximately the point at which all rings contain at least one cross-link, according to the binomial distributions and the rules of probability. ($GroEL_{IRX}$ was not used since it does not respond to SP.) A higher extent is undesirable since rings would begin to lose activity once they contained too many tethers (see Chapter 3). The effect of GroES was also tested. $GroEL_{IAX}$ was cross-linked with oPDM, which allowed the use of DTT in the subsequent assay in order to ensure that the SPs were completely unfolded. The relative effects are shown in Figure 4-5. SP stimulates the activity of reduced $GroEL_{IAX}$ about 3-fold to between 16 and 19 turnovers/minute. SP has very little effect on cross-linked material, whose activity is already approximately 18 turnovers/minute. GroES slows reduced $GroEL_{IAX}$'s ATPase activity by about one half and has less of an effect on cross-linked $GroEL_{IAX}$, as would be expected since most rings will not be able to bind GroES. The relative effect of SP on GroEL is greater in the presence of GroES, for reasons that are not clear, but this was consistently seen throughout these studies. It is possible that the *trans* ring of a bullet has a higher affinity for SP than the rings do in GroEL alone.

4.3.5 Adding Unfolded SP to $GroEL_{IAX}$ Provides a Direct Measurement of $V_{max}T$

When formulating the theoretical models that predict the response of ATPase activity to tethering, it is necessary to estimate several parameters, one of which is $V_{max}T$ (see Chapter 3). An estimate of $V_{max}T$ is obtained empirically by determining the value of $V_{max}T$ which produces a model that best fits the data. $V_{max}T$ cannot be measured directly by locking rings in the T state with tethers, since this also causes a loss in activity. However, if unfolded SP is mimicking a cross-link and holding a ring in the T state, then the rate measured in the presence of SP should be approximately $V_{max}T$,

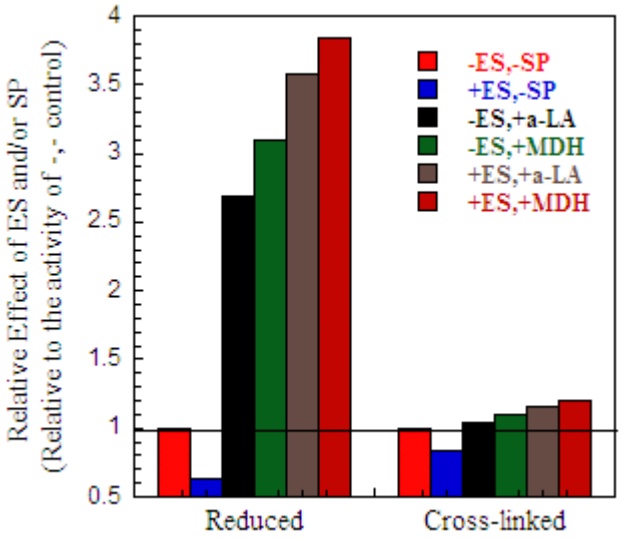

Figure 4-5: Effect of Unfolded SP on Cross-linked GroEL$_{IAX}$. 2 μM GroEL$_{IAX}$ that was 0% or 25% cross-linked was assayed at 37°C with or without 2 μM GroES, 7.4 μM α-LA (25-fold excess over rings), and 0.56 μM MDH (2-fold excess over rings). The rates, relative to the rate measured in the absence of GroES and SP, are shown. The reactions contained 1 mM DTT. Cross-linking was done with oPDM and was confirmed by SDS-PAGE quantitation.

assuming that SP does not cause a loss in activity. This seems a safe assumption, since high concentrations of SP never cause a loss in activity (Figure 4-2). To test whether or not SP provides a measurement for $V_{max}T$, the response of GroEL$_{IAX}$'s ATPase activity to oxidation was tested with and without added α-LA in an experiment similar to those described in Chapter 3. The results are shown in Figure 4-6. In the absence of SP, the data match a theoretical model in which 1 disulfide bond per ring is sufficient to lock the ring in the T state, and 6 tethers per ring cause a loss of all activity ($V_{max}Res=0$). $V_{max}R$ was estimated to be the rate of fully reduced GroEL$_{IAX}$ and $V_{max}T$ was estimated to be 18, as this produced the model which best fit the data. In the presence of SP, the activity of reduced GroEL$_{IAX}$ was 16-17. SP has no effect on the ATPase activity when the

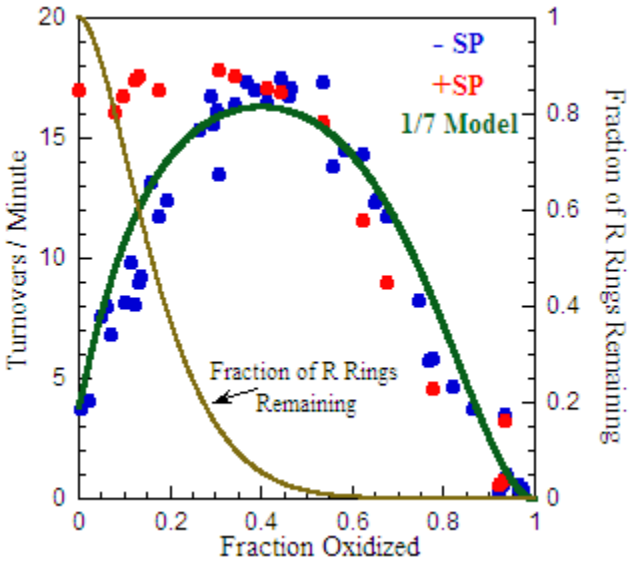

Figure 4-6: Response of GroEL$_{IAX}$ to Oxidation, ± Unfolded SP. Various amounts of diamide were added to 40 μM GroEL$_{IAX}$, and the reaction was allowed to proceed for at least 30 minutes at 37°C at pH 8. After removing a small portion of the oxidized GroEL and adding it to NEM to block the free cysteines, the remainder was added to a reaction mixture containing 50 mM Tris pH 7.5, 100 mM KAc, 10 mM MgAc, 0.2 mM PEP, 0.2 mM NADH, 1 mM ATP, 4 u LDH, 5 u PK, with a final GroEL concentration of 2 μM. The change in absorbance at 340 nm was monitored at 37°C. Halfway through the measurement, acid-denatured α-LA was added to a final concentration of 15 μM, a 50-fold excess over rings. The fraction of subunits oxidized was quantitated using the NEM-blocked samples by SDS-PAGE. The theoretical model shown was plotted using these parameters: $V_{max}R$=3.8, $V_{max}T$=18, $V_{max}Res$=0, and 6 strikes (see section 3.3.2). The thin, brown line represents the fraction of rings remaining in the R state.

population of rings in the R state reaches zero. Thus, the $V_{max}T$ measured in the presence of SP and the $V_{max}T$ predicted by the model are almost identical. At higher levels of oxidation, SP has a slight inhibitory effect on ATPase activity, for reasons not entirely clear.

4.3.6 SP is not a Perfect Mimic of a Cross-link As a final demonstration that SP mimics a cross-link by holding a ring in the T state, the ATPase activity of GroEL$_{IAX}$ was measured in the presence of SP as a function of ATP concentration. If SP is a perfect mimic of a cross-link that locks a ring in the T state, the cooperativity of ATP binding

should be reduced and the Hill coefficient should approach 1. The ATPase activity of both fully reduced $GroEL_{IAX}$ and that which was 50% oxidized was measured as a function of [ATP], with and without 15 μM α-LA (a 50-fold excess over rings). SP once again stimulates the activity of $GroEL_{IAX}$, but only at high ATP concentrations, reaching $V_{max}T$ at approximately 800 μM ATP (Figure 4-7a). With $GroEL_{IAX}$ that is 50% oxidized, SP *inhibits* activity at all [ATP] below 800 μM (Figure 4-7c). The Hill coefficients obtained from the data in Figure 4-7c are 1.2 and 1.5, essentially identical, with and without SP respectively. Rate inhibition was also seen with fully reduced $GroEL_{IAX}$ at very low [ATP] (Figure 4-7b), in which the data appear to be sigmoidal, indicating an increase in the cooperativity of ATP binding.

The observation that SP stimulates reduced $GroEL_{IAX}$ only at high [ATP] is consistent with data from Yifrach and Horovitz, who found that at low [ATP], very high amounts of α-LA (>100-fold excess) were needed to achieve rate stimulation (see (34)). It is possible that the concentration of SP used here was too low to show stimulation at low [ATP], although the absolute [ATP] where this phenomenon is observed in their results and in the results shown here do not quite match. This could be due to differing K^+ concentrations, differing reaction temperatures, or the slightly different way in which the SP was prepared. It is also possible that the difference is due to an unknown property of the mutant.

The increase in cooperativity at low [ATP] is consistent with the idea that SP holds a ring in the T state, but doesn't lock it in the T state. This makes sense, because the SP is not a covalent linkage. The T→R transition is still allowed, but is rendered more difficult by SP. Thus, the transition would be expected to occur at higher [ATP],

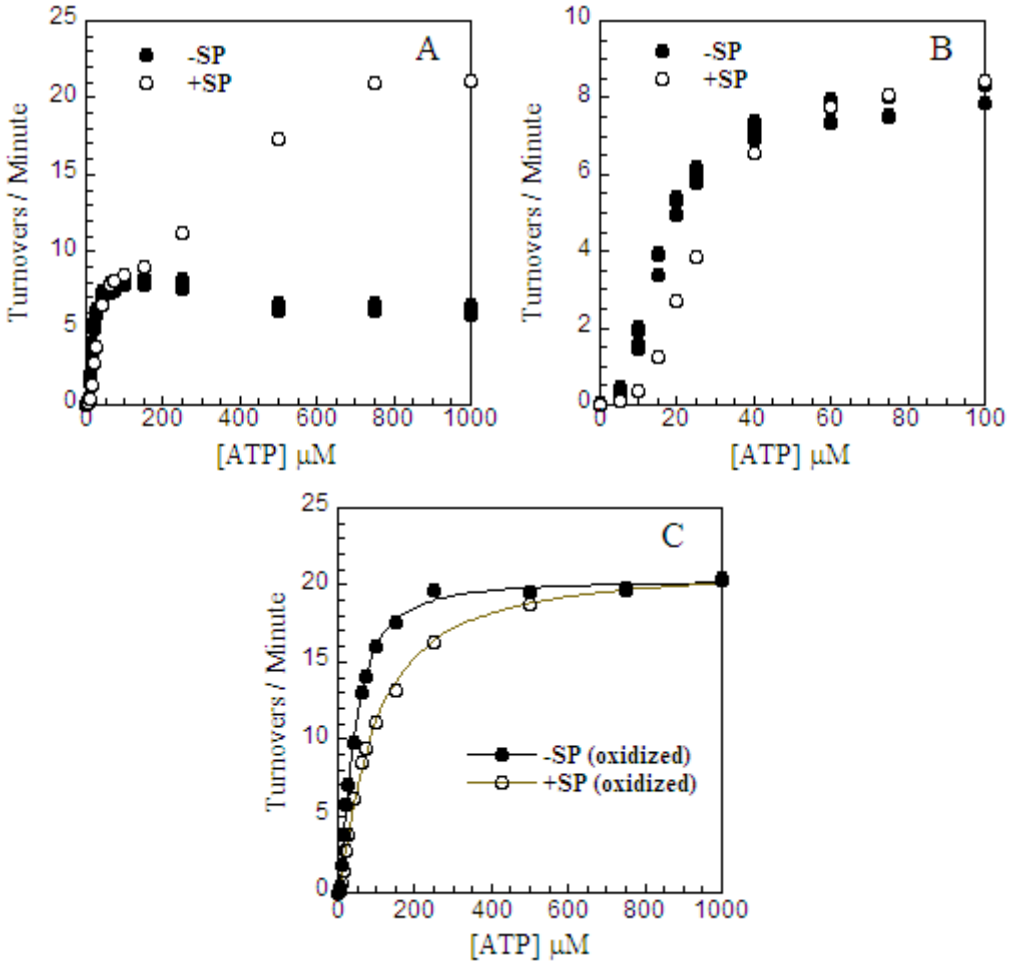

Figure 4-7: Dependence of GroEL$_{IAX}$ ATPase Activity on [ATP] ± SP, ± Cross-linking. The ATPase activity of fully reduced GroEL$_{IAX}$ and that which is 50% oxidized by diamide was determined at various [ATP] with or without 15 μM unfolded α-LA (50-fold excess over rings). Measurements were taken at 37°C with a final GroEL concentration of 2 μM. **A**) Activity of fully reduced GroEL$_{IAX}$ with and without SP. **B**) The data from (**A**) at low [ATP]. **C**) Activity of 50% oxidized GroEL$_{IAX}$ with and without SP. The data were fit to the Hill equation (sec. 3.4.5) and gave the following values: -SP: V_{max}=20 turnovers/minute, K=0.004 μM, n_H=1.5; +SP: V_{max}=21, K=0.004 μM, n_H=1.2.

with increased cooperativity. In the case of a cross-link, the T→R transition is never allowed; therefore, no cooperativity is observed.

However, the observation that SP inhibits activity under some conditions is more difficult to explain. In the case of the fully reduced $GroEL_{IAX}$ at very low [ATP], the reason is almost certainly a decreased affinity for ATP in the SP-bound rings, which is due to the increased cooperativity in ATP binding within a ring. The reason for SP inhibition of rate in the case of oxidized $GroEL_{IAX}$ is more elusive. It is possible that the effect of having both cross-links and SP bound to the same ring is to create an artificial T conformation which has an even more reduced affinity for ATP, but this is only a guess. In conclusion, despite some irregularities in the details, SP in a broad sense seems to closely mimic a cross-link in that it binds to and holds a ring in the T conformation, shifting the T→R equilibrium in favor of the T state.

4.3.7 Short Peptides and a Hydrophobic Amino Acid do not Stimulate ATPase Activity If SP is acting as a tether, holding, but not locking, a ring in the T conformation, then it must be an intersubunit tether that spans two or more SP binding sites. If this is true, then a substrate which can bind to the SP binding sites but which is too short to span two or more sites, should not cause a rate enhancement. To test this prediction, short, synthetic peptides were obtained from Dr. Lila Gierasch. These peptides, which were designed to mimic unfolded SPs with various secondary structural elements, are known through NMR studies to bind to the SP binding sites (75), and are too short to span two adjacent binding sites. Three peptides, DRho2, LDRho2, and Ac-Rho2, were dissolved in 10 mM Tris pH 8. Each peptide contained a single tryptophan, which allowed concentration determination at 280 nm with an extinction coefficient of 5559 M^{-1}. The

peptides were added to an ATPase reaction containing 2 μM $GroEL_{WT}$ at 30°C. At peptide concentrations ranging from 8 μM up to 75 μM, no stimulation of ATPase activity was seen, either in the absence or presence of 2 μM GroES (data not shown). At the end of each measurement, unfolded MDH was added to the reaction to ensure that rate stimulation was possible, and in all cases a 6-7 fold stimulation was seen. It should be noted that the binding of the peptides to $GroEL_{WT}$ was not confirmed, and the binding constants of the peptides were not published, but it is certain that they are able to bind to GroEL (75).

In addition to the short peptides, a hydrophobic amino acid, leucine, was also tested in an ATPase reaction. It has been reported that hydrophobic amino acids such as leucine and isoleucine cause a rate enhancement (76), a result that would invalidate the current hypothesis that an SP must span multiple SP binding sites in order to cause rate stimulation. The effect of added leucine on the ATPase activity of $GroEL_{WT}$ was tested with 2 μM GroEL at 37°C. Leucine concentrations up to 5 mM were tried, and no effect was ever seen on the ATPase activity, either with or without 2 μM GroES (data not shown). It is unknown why rate stimulation was seen in the published report (76). Although the observations with short peptides and with leucine are both admittedly negative results, they do lend further support to the idea that an SP must be able to connect two or more SP binding sites in order to cause rate stimulation.

4.4 Discussion

The stimulation of ATPase activity by unfolded SP has previously been tied to GroEL's allosteric transitions. SP was thought to shift the overall equilibrium from the RR state to the more active TR state (34). The results presented here, in combination

with the observation that the T state has a higher ATPase activity than the R state, modifies the original conclusion. The simplest explanation of the current results is that SP stimulates activity simply by shifting the intra-ring R→T equilibrium in favor of the more active T state. All data presented above support this conclusion on a broad level, from the observation that SP stimulates activity to the V_{max}T predicted by cross-linking experiments, to the observation that SP has no effect on rings already locked in the T state at high [ATP]. In addition, this idea as to how SP affects the allostery of GroEL will be very useful in explaining several observations in the following chapter concerning the release of GroES. With that said, there are some irregularities in the data which imply that this proposed mechanism does not tell the whole story. Perhaps the real reason for rate stimulation is somewhere between the R→T mechanism discussed here and the RR→TR mechanism proposed by others. For the purposes of this discussion, the R→T proposal is a reasonable explanation for most of the observations presented above and cannot be discounted even by the irregularities.

An important result that comes out of these studies, shown in Figure 4-4, is that changes in ATPase activity are coupled to the folding of the substrate protein. Since it is known from studies such as those presented in Chapter 3 that the V_{max} of ATPase activity is, not surprisingly, linked to the allosteric state of the ring, it thus follows that the refolding of the SP is also linked to the allosteric transitions. The coupling of SP binding and refolding to the allosteric transitions of a GroEL ring has major implications for the mechanism of active unfolding. If an SP is actively unfolded, it is unfolded by the motions of the apical domains during the T→R→R' transition upon binding ATP (5). In other words, active unfolding must be coupled to allosteric transitions.

The active unfolding mechanism is further supported by the conclusion that SP mimics a cross-link when binding to the GroEL ring. SP holds, but does not lock, the ring in the T state. Rate stimulation is only seen when the substrate is able to span two or more subunits. In effect, the substrate must be able to act as an intersubunit tether. Since the SP is able to hold a ring in the T state, it must be exerting a force on the subunits to which it is bound, making it more difficult for the ring to undergo its concerted T→R transition. Consider the diagrams in Figure 4-8. These describe hypothetical energy cycles depicting the allosteric transitions of two adjacent subunits and the binding of substrate. In 4-8a, the substrate is a short, synthetic peptide. In 4-8b, the substrate is an unfolded protein bound to two adjacent subunits. When the substrate is a short peptide, the T→R transition can freely occur upon ATP binding, and the substrate binding sites are displaced from each other. However, when the substrate is a protein, the movement of the subunits is resisted by the bound substrate acting as a tether. In order for the apical domains to move during the T→R→R' transition, this resistance must be overcome. If the substrate remains bound, then *work* must be done by GroEL to stretch the SP as the SP binding sites are displaced during the transitions. The SP would continue to stretch during the domain motions until the affinity of the SP for the increasingly buried SP binding sites was so reduced that release of the now-unfolded SP into the central cavity would occur (5). The stretching force imparted by the twisting apical domains has been estimated at 20 pN (5), a force deemed sufficient to partially unfold single domain proteins (77), but one which is much less than the measured forces of interaction between GroEL and two representative unfolded SPs (340 pN and 770 pN for β-lactamase and citrate synthase, respectively, as measured by atomic force microscopy [AFM]) (5, 78).

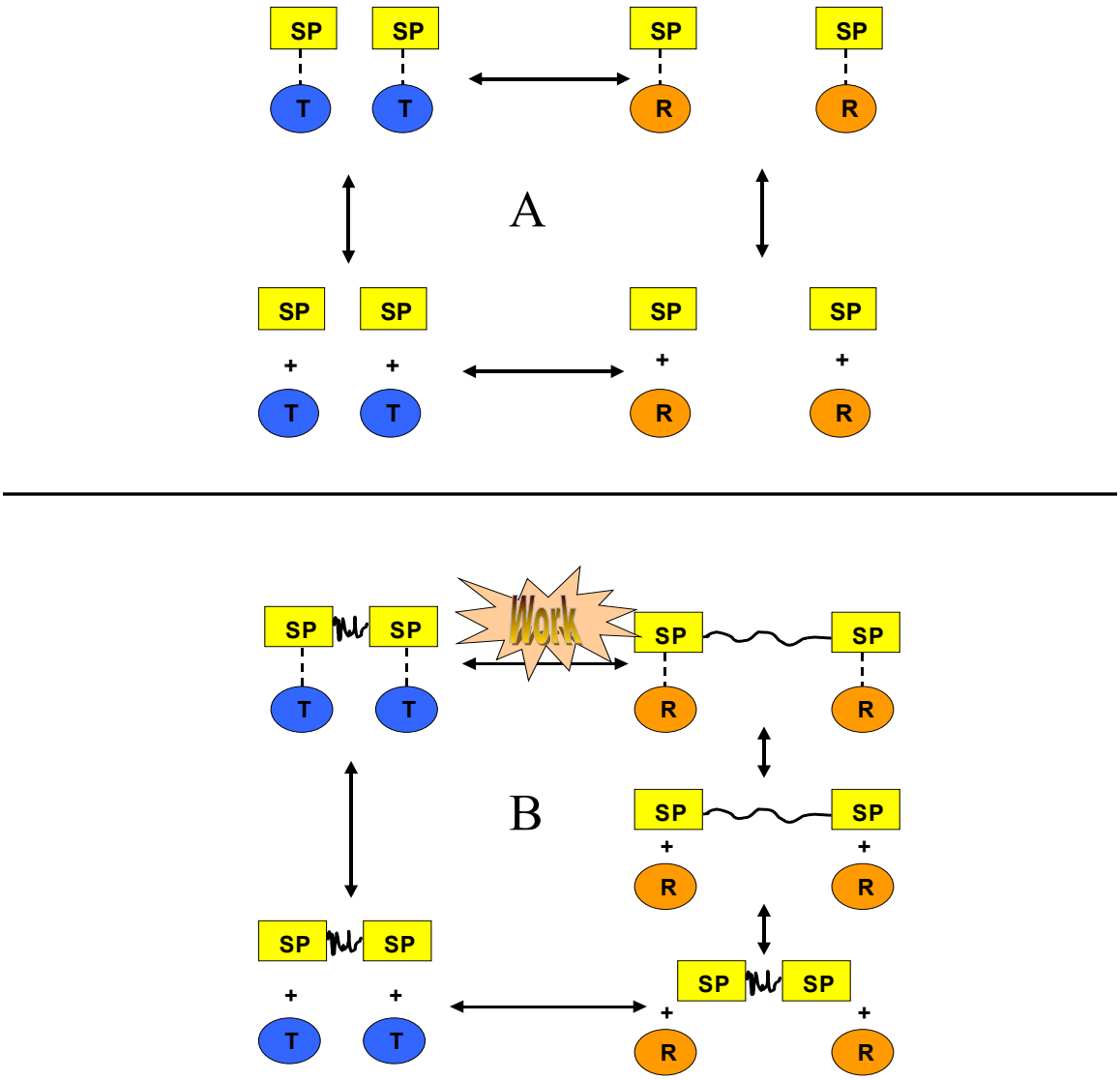

Figure 4-8: Free Energy Cycles: Allosteric Transitions With Different Substrates. Described in the text, these hypothetical energy cycles depict the binding of a substrate (SP) to two adjacent subunits and the allosteric transitions that follow. The displacement of the SP binding sites is depicted by showing the subunits further away from each other in the R state. In (**A**), the substrate is a short peptide incapable of spanning the 23 Å distance between two adjacent binding sites. In (**B**), the substrate is an unfolded protein that can span the distance. It should be noted that, in reality, the two binding sites do not necessarily have to be adjacent. It is important to remember that a T subunit has a higher k_{cat} of ATPase activity than an R subunit, and therefore SP binding to and forcing a subunit to maintain the T conformation will enhance the observed ATPase rate.

One could argue that, even if GroEL does exert force on the SP, unfolding does not occur. Rather, GroEL simply exerts force on the SP until the SP releases from its binding sites. This would require the intermolecular interactions within the misfolded SP to resist the 20 pN stretching force, and would require the stretching force to overcome the force of GroEL/SP interaction. This may be the case for some SPs. Indeed, the ability of GroEL to actively unfold SPs is, to a large extent, dependent on the SP. However, as has been previously implied (5), at least for the two SPs mentioned above, the 20 pN stretching force exerted by the twisting apical domains would not be sufficient to overcome the interaction forces and pull the SP binding sites away from the SP. Therefore, it is more likely that these SPs would remain bound to the apical domains during the T→R→R' twisting motions, allowing the SPs to be stretched until the SP binding sites become at least partially buried. At this point, the GroEL/SP interaction forces would likely be reduced to the point where they can no longer overcome the stretching force, and the SP would be released into the central cavity. Many additional AFM experiments, measuring the interaction of a wide range of SPs with GroEL, will be necessary to gain some understanding of the number of SPs capable of binding tightly enough to GroEL to allow them to be forcefully unfolded (5).

In summary, while the experiments presented in this chapter do not address the magnitude of the forces involved in SP unfolding, they do strongly suggest that active unfolding does indeed occur. As stated in the introduction to this chapter, if an SP restrains the movement of the subunits during the allosteric transitions, then in overcoming that restraint the subunits must exert an opposite force on the SP. These experiments demonstrate that SPs exert a force on GroEL, in that they restrain the T→R

transition by mimicking a covalent tether. This strongly suggests, therefore, that the reciprocal is also true: GroEL exerts a force on SPs. Thus, in discovering the likely cause of ATPase rate stimulation by unfolded SPs, these experiments have indirectly demonstrated a critical requirement of the iterative annealing mechanism (5), that GroEL performs work on SPs.

Chapter 5

Examining the Allosteric Basis for the Release of GroES from the GroEL/GroES Complex

5.1 Introduction

The discharge of GroES from the *cis* ring of a $GroEL_{14}/GroES_7$ complex is initiated by the binding of ATP to the opposite *trans* ring, following the hydrolysis of ATP in the *cis* ring (37). This allows any substrate protein encapsulated beneath GroES to be released into the surrounding environment, whether the SP is properly folded or not (20, 79). This is a critical step in the GroE reaction cycle. It allows for the coordinated breakdown of a folding chamber on one ring of GroEL and the formation of a new one on the other ring. Since one chamber is falling apart as the other is forming, the efficiency of the GroEL machine is optimized (17, 29). The amount of time that GroES spends bound to GroEL is also important, for this is the time period in which an SP can refold in the protective isolation of the *cis* chamber. In the passive unfolding mechanism, in which it is proposed that GroEL promotes protein refolding simply by isolating misfolded SPs in a favorable folding environment (7), the amount of time an SP is allowed to fold in the central cavity is a critical factor. Any reduction in the amount of time the SP spends encapsulated in the central cavity would reduce the chances of its being properly folded when it is released. In contrast, encapsulation time is not the important parameter in the active unfolding, or iterative annealing, mechanism. Under this mechanism, the number of times in which the SP can be forcefully unfolded and given another chance to fold, either inside or outside the cavity, is most important. In this mechanism, the number of times the system turns over is the critical factor, the more the better (19, 46).

GroES release has been implicated as the rate-limiting step in the GroE reaction cycle, occurring at a rate of 0.04 sec^{-1} in the absence of SP (17, 80). However, Rye *et al*. have found that, in the presence of SP, the rate of release is accelerated to 1-2 sec^{-1} (17).

The reason given for the acceleration in these studies was that SP somehow increased the rate of an additional structural transition that occurred in the *cis* ring following *cis*-ATP hydrolysis but prior to ATP binding to the *trans* ring (17). The nature of this structural transition remains unclear, and indeed, the structural basis for any of the events that accompany GroES release are unknown. The structural signal that is communicated between the rings following *trans*-ATP binding is not understood.

The goal of the studies in this chapter was to take a closer look at the events that accompany GroES release. Specifically, an allosteric basis for these events was sought. It was realized that the same mechanism by which SP accelerates the hydrolysis of ATP, ie. the shifting of the T→R equilibrium towards the T state (see Chapter 4), might be responsible for the acceleration of GroES release seen in the previous study. Thus, it was asked whether or not the allosteric state of the *trans* ring (T or R) had any effect on the rate of GroES release. As has been discussed, there are several allosteric effectors of the T→R structural transition, such as SP, nucleotide, and K^+ ions. The effect of these various components on GroES release was therefore tested in an attempt to elucidate the effect of allostery on the release mechanism.

In order to study GroES release, the experimental system devised by Rye *et al*. was used in which single cysteine GroEL and GroES mutants were labeled with fluorescent probes (17, 52). These two probes constitute a fluorescence resonance energy transfer (FRET) pair, in which, upon excitation of the donor probe, energy from the excited state of the donor probe is transferred to the acceptor probe, causing an increase in the emission from the acceptor and a decrease in the emission from the donor. The efficiency of this energy transfer is related to the distance between the two probes (81).

When GroEL is bound to GroES, energy transfer can occur and there is strong emission from the acceptor probe; whereas when GroES is released from GroEL, the distance between them is essentially infinite, no transfer can occur, and emission from the acceptor probe is significantly decreased. GroES release can therefore be measured in a stopped-flow device in which the emission from the acceptor probe is monitored upon excitation of the donor probe as GroES release is initiated.

The results presented in this chapter provide new insights into the events that accompany GroES release. The data obtained here by systematically varying the conditions of the experiments in much greater detail than in the previous studies by Rye *et al*. (17, 37), have allowed for the formulation of a detailed reaction mechanism, which will be described in the subsequent sections. This refined mechanism specifically implicates one event, the release of ADP from the *trans* ring, as being the rate-limiting step in GroES release. The basis for SP stimulation of the rate of GroES release is also discussed. The implications of these findings on the active unfolding vs. passive unfolding debate are discussed in Chapter 6. Some of the data presented in this chapter differ significantly from the data published previously by Rye *et al*. (17), and the possible reasons for this are discussed below, along with the limitations of these studies in determining all of the steps in this unexpectedly complex reaction.

5.2 Methods Specific to Chapter 5

5.2.1 Mutagenesis and Purification The two mutants used for the FRET studies in these experiments were GroEL E315C and GroES 98C (Figure 5-1). GroEL E315C was constructed in pGEL1 using the Stratagene Quick-Change kit using the protocol in the kit documentation. The mutagenic primers were E315C-S:

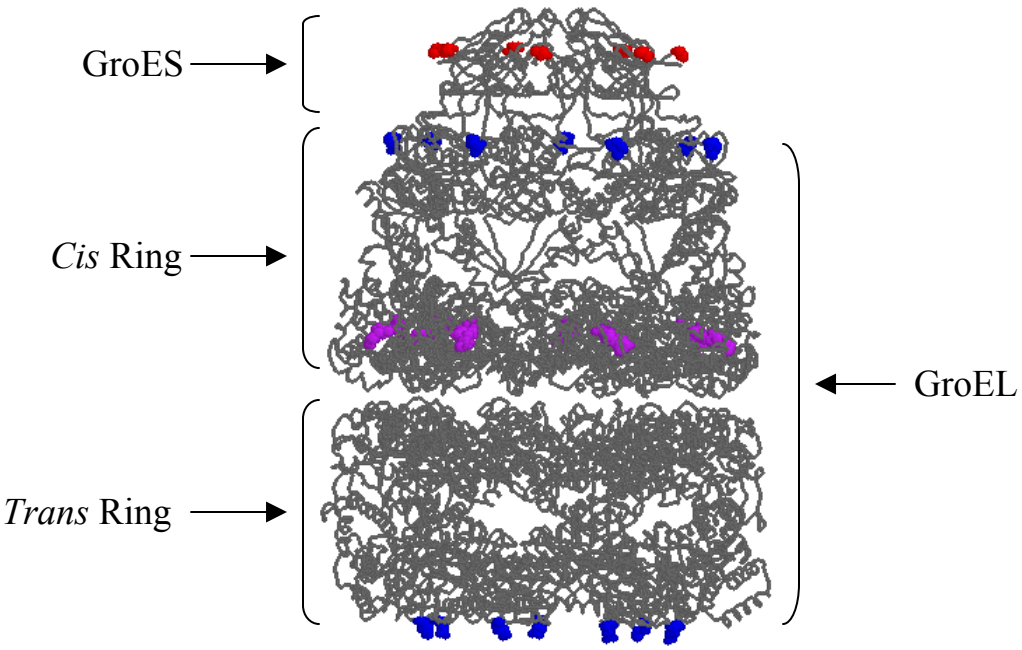

Figure 5-1: GroEL/GroES/ADP Complex with the FRET Residues Highlighted. GroEL E315 was mutated to cysteine and a cysteine was added to the C-terminus of GroES (residue 97 is highlighted). These were labeled with the probes IAEDANS and F5M respectively. These residues are approximately 36 Å apart (Cα→Cα). The *cis* ring ADP is constrained in the nucleotide binding sites, whereas *trans* ring ADP can freely diffuse. This structure was made using PDB file 1aon (14).

GCTGGAAAAAGCAACCCT GTGCGACCTAGGTCAGGCTAAACG and E315C-NS: CGTTTAGCCTGACCTAGG TCGCACAGGGTTGCTTTTTCCAGC. A new Bln I restriction site was also introduced by these primers for purposes of detection. GroEL E315C was purified as described in section 2.4. GroES 98C was created by inserting a cysteine residue at the C terminus of GroES. The mutant was constructed in pGES1 with the Quick-Change kit using primers ES98C-S: GGCAATTGTTGAAGCGTBCTAACCTTGGCTGTTTTGG and ES98C-NS: CCAAAACAGCCAAGGTTAGCACGCTTCAACAATTGCC. These plasmids also eliminated a unique Hind III site from the plasmid sequence. GroES 98C was purified

essentially according to the protocol in section 2.7 but required a slight modification to the SP Sepharose column conditions. The column was run at pH 4.8, and GroES 98C was eluted with a 150 ml gradient from 0 to 300 mM NaCl.

5.2.2 Labeling GroEL E315C and GroES 98C with Fluorescent Probes The donor chromophore, IAEDANS and the acceptor chromophore, fluorescein-5-maleimide (F5M), were purchased from Molecular Probes. For purposes of FRET, the R_0 value for this pair of probes is about 40 Å (82). The distance between the α-carbons of GroEL E315C and GroES 98C is 36Å, close to the R_0 value. Solutions of these probes were made in anhydrous DMF at a final concentration of 20 mM. Prior to labeling, both mutants were freshly reduced with 5 mM DTT. DTT was removed by running the protein on a PD-10 column equilibrated with 10 mM Tris pH 7.5, 10 mM MgAc that had been treated with Chelex resin. GroEL E315C was labeled at several different concentrations with varying amounts of IAEDANS. In one case, 320 μM GroEL was labeled with a 25-fold excess of IAEDANS over $GroEL_{14}$, 575 μM. The estimated extent of labeling with these conditions was 90%. In another, 200 μM GroEL was labeled with 200 μM IAEDANS in phosphate buffer at pH 7.5, leading to a labeling extent of 40%. The experimental results were not dependent on the extent of labeling, as will be discussed in the next section. The labeling reaction was carried out at 25°C for 1 hour in the dark. Unreacted cysteines were blocked with a molar equivalent of NEM, followed by a quench with 10 mM DTT. GroES 98C was also labeled under various conditions. In one case, 470 μM GroES was labeled with a 3-fold excess of F5M over $GroES_7$, 200 μM F5M for 1 hour. Labeling was estimated at 90% under these conditions, but some aggregation was seen. Labeling was also done with 115 μM GroES and 48 μM F5M for

10 minutes. Under these conditions, no aggregation was seen. The experimental results were also not dependent on the extent of GroES labeling. The labeling reaction was quenched with 10 mM DTT. For both proteins, excess label was removed by running the protein on a PD-10 column equilibrated with 10 mM Tris pH 7.5, 10 mM MgAc. The labeled protein was then concentrated and stored at -80°C. The concentration of labeled GroEL ($GroEL_D$) was checked both by checking its absorbance at 280 nm, and by comparing it to GroEL of a known concentration on an SDS-PAGE gel. The concentration of the labeled GroES ($GroES_A$) was measured using a Bradford assay and also quantitative SDS-PAGE since F5M interferes strongly with the absorbance signal at 280 nm. The IAEDANS concentration was measured at 336 nm using an extinction coefficient of 5400 M^{-1} (17). The concentration of F5M was measured at 491 nm using an extinction coefficient of 74500 M^{-1} (17).

5.2.3 Stopped-Flow Fluorescence Measurements Figure 5-2 shows the experimental design schematically. All fluorescence measurements were carried out on an Applied Photophysics SX18MV-R stopped-flow apparatus. The instrument was configured with a 20 μl flow cell with a pathlength of 2 mm and a 530 nm emission cut-off filter. The monochrometer slits were set to position 2, corresponding to a slit width of approximately 9 mm. The syringes and flow cell were thermostatted at 30°C with a circulating water bath (VWR). The total volume of solution pushed into the flow cell per shot was approximately 170 μl, or 85 μl from each syringe. The dead time of the instrument averages about 1 ms according to the instrument documentation and was not explicitly determined during these studies. As per Rye *et al*. (17), the excitation wavelength used for all measurements was 336 nm. The instrument is capable of an

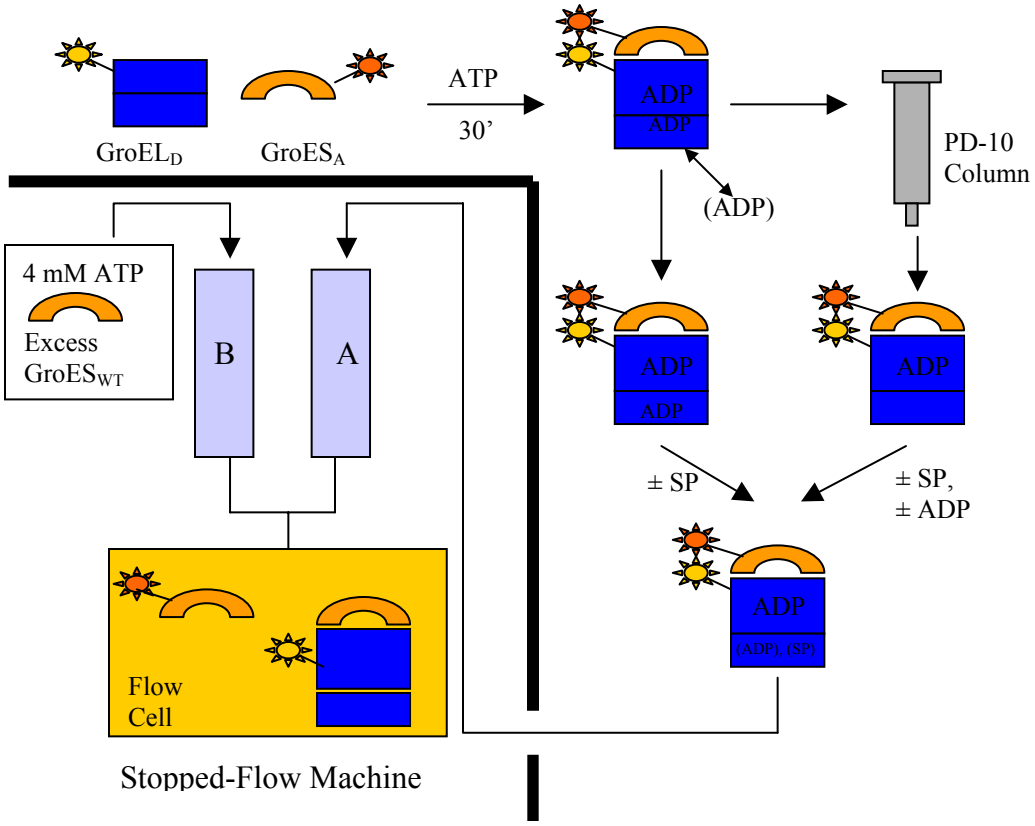

Figure 5-2: Experimental Design for Measuring GroES Release. (17) GroEL$_D$ (40 μM) and GroES$_A$ (20 μM) are mixed with 300 μM ATP (in 20 mM Tris pH 7.5, 100 mM KAc, 10 mM MgAc, 2 mM DTT) to initiate complex formation. The ATP is allowed to completely hydrolyze to 300 μM ADP. ADP is trapped in the *cis* ring under GroES$_A$ and the remaining ADP can diffuse in and out of the *trans* ring. The protein was then either diluted directly to 4 μM GroEL$_D$, 2 μM GroES$_A$, 30 μM ADP, or was loaded on a PD-10 de-salting column to remove the ADP not trapped in the *cis* ring and then diluted to 4 μM GroEL$_D$, 2 μM GroES$_A$, 0 μM ADP. At this point, ADP or unfolded α-LA could be added to the protein solution when required. The GroEL/GroES/±ADP/±α-LA solution was then loaded into syringe A of the stopped-flow device. A solution containing typically 4 mM ATP/20 μM GroES$_{WT}$ in the same buffer was loaded into syringe B, although the ATP was varied where noted. The solutions were rapidly mixed at a 1:1 ratio by the stopped-flow, producing final concentrations of 2 μM GroEL$_D$, 1 μM GroES$_A$, 10 μM GroES$_{WT}$, and (usually) 2 mM ATP. The decrease in the FRET signal was monitored by exciting the solution at 336 nm and recording the total fluorescence emission at all wavelengths above 530 nm. All experiments were carried out at 30°C.

oversampling function in which it collects data points approximately every 40 μs, averages several consecutive data points together, and records the average. This has the effect of removing much of the noise from the final trace, and this function was used for all measurements. The machine had two basic limitations in these studies. Because it is not capable of measuring fluorescence emission at specific wavelengths, but only at all wavelengths above the wavelength of the cut-off filter, it was not capable of monitoring the change in the fluorescence emission of the donor. A second problem occurs because the drive piston that pushes the syringes is pneumatically driven. The pressure on the syringes is released about 30 ms following the shot. This causes some interference in the trace around this time. This can be avoided by forcing the instrument to hold pressure on the syringes until the conclusion on the measurement, but this can only be done on measurements of 5 seconds or less. As will be seen, many of the measurements presented in this chapter show two events, one prior to 200 ms, and one lasting as long as 200 seconds. This required many of the measurements to be performed twice. In one measurement, the events prior to 200 ms were monitored with the pressure held, and in the second measurement events out to 200 sec. were measured with the pressure not held.

Unless otherwise noted, the experimental conditions used for the experiments are as follows. The $GroEL_D$, $GroES_A$ complex was formed at 20 mM Tris pH 7.5, 100 mM KAc, 10 mM MgAc, and 2 mM DTT. The $GroEL_D$ concentration was 40 μM, and the total GroES concentration was 20 μM. The amount of $GroES_A$ used was adjusted depending on the extent of F5M labeling so that the concentration of F5M was always 5 μM. $GroES_{WT}$ was used to bring the total GroES concentration up to 20 μM, and hereafter all GroES in this solution will be called $GroES_A$, since GroES subunits from

different GroES rings will mix rapidly (personal observation). Complex formation was initiated by adding ATP to a final concentration of 300 μM and allowing the reaction to proceed for at least 30 minutes to ensure that all ATP was converted to ADP. At this point the solution was either diluted directly to 4 μM GroEL with 20 mM Tris pH 7.5, 100 mM KAc, 10 mM MgAc, and 2 mM DTT, or was loaded onto a PD-10 column equilibrated in the same buffer to remove the ADP not trapped in the *cis* ring. Buffer was then added to the column to bring the total volume loaded up to 2.5 ml, and the protein was eluted with 2.5 ml of buffer. The eluent was then diluted to 4 μM GroEL with buffer. In either case, the solution was then filtered on a 0.2 μm filter to degas it, and was then loaded into syringe A of the stopped-flow machine. Syringe B, unless otherwise noted, contained 20 mM Tris pH 7.5, 100 mM KAc, 10 MgAc, 2 mM DTT, 20 μM $GroES_{WT}$ (a 10-fold excess over $GroES_A$), and 4 mM ATP. The solutions were mixed 1:1 by the machine, to obtain final concentrations of 2 μM $GroEL_D$, 1 μM $GroES_A$, 10 μM $GroES_{WT}$, and 2 mM ATP (in addition to 15 μM ADP leftover from the formation of the complex if de-salting was not performed) (Figure 5-2). All measurements were done at 30°C. This amount of protein provided an adequate signal, with an acceptable amount of noise.

In each experiment, several traces were averaged together to obtain the final trace shown in the plots. For traces out to 200 seconds, as little as three traces averaged out to a final trace that was practically noise free. For traces done over short time periods, 8-10 traces were averaged to obtain the final trace. Where appropriate, in order to make traces easier to compare, the raw data were adjusted (by addition or subtraction) so that all traces ended at an intensity of zero. In some cases, it was necessary to combine data

obtained at <200 ms with data obtained up to 200 sec. This was done by first adjusting the 200 sec trace so that it ends at zero, and then adjusting the intensity of the short trace so that it matches the point at 200 ms of the long trace. This allowed for a qualitative comparison of one trace to another.

5.2.4 Measuring the Kinetics of GroES Release Using GroES$_{His}$ The kinetics of GroES release were independently confirmed by measuring the exchange of GroES$_{His}$ for GroES$_{WT}$ following ATP addition, using a protocol similar to the one discussed in section 3.2.7. This experiment was designed to mimic the conditions of the stopped-flow experiments as closely as possible. The bullet complex was formed with 40 μM GroEL$_{WT}$, 20 μM GroES$_{His}$, and 300 μM ATP in 20 mM Tris pH 7.5, 100 mM KAc, 10 mM MgAc. This was allowed to react for at least 30 minutes. This was then diluted 10-fold to 4 μM in the same buffer. This solution was then diluted 1:1 with 2 mM ATP and 20 μM GroES$_{WT}$ to initiate GroES$_{His}$ release. In a separate reaction, no ATP was added as a control. As in the stopped-flow experiments, the final concentrations during the release are 2 μM GroEL, 1 μM GroES$_{His}$, and 10 μM GroES$_{WT}$. All solutions were incubated at 30°C. The release reaction was quenched at various time points by adding glucose to a final concentration of 5 mM and 7.5 units of hexokinase. The quenched reactions (120 μl) was then added to 20 μl of Ni-NTA resin on a small spin column (Bio-Rad) which had been equilibrated with 20 mM Tris pH 7.5, 100 mM KAc, 10 mM MgAc. Following sample addition, the column was spun at 2000x g to elute the flow through (the GroEL which has released GroES$_{His}$). 40 μl of buffer was then added to the column, the column was spun at 2000 x g, and the eluent was collected and included in the flow-through. The column was then washed with 120 μl and then 40 μl of 250 mM

imidazole to elute $GroES_{His}$ and GroEL which had not yet released $GroES_{His}$. The 160 µl flow-through and imidazole fractions from each column were then mixed with 32 µl of 6X SDS loading blue, and 30 µl of each sample were loaded on a 12% SDS-PAGE gel poured with 1 mm spacers. The GroEL bands were quantitated by densitometry. The intensities of the flow-through bands were adjusted by subtracting out the intensity of the flow-through band from the control reaction in which no ATP was added to initiate GroES release. The intensities of the imidazole bands were adjusted by subtracting out the intensity of the imidazole band from the release reaction quenched at 200 sec. The fraction of GroES released was then calculated by dividing the corrected intensity of the imidazole band by the total corrected intensities of the flow-through and imidazole bands.

5.3 Results

For a clearer picture of the GroE reaction cycle events that are being measured in these experiments, consider the scheme in Figure 5-3. The events that occur in both rings are depicted as a series of staggered boxes to emphasize that the reaction cycles of each ring, or hemicycles, are offset. The events listed within a box occur in an unknown order, or at the same time. The rate measured by these experiments is the rate of step 5, GroES release. However, step 5 in ring Y, for example, can only occur if step 2 in ring X, ATP binding, has occurred. And, ATP can only bind to ring X if ADP release, step 1, has taken place. Therefore, even though only GroES release is actually observed by the fluorescence measurements, the trace which is obtained may actually reflect ADP release, ATP binding, and any allosteric changes which may accompany these events, in addition to GroES release.

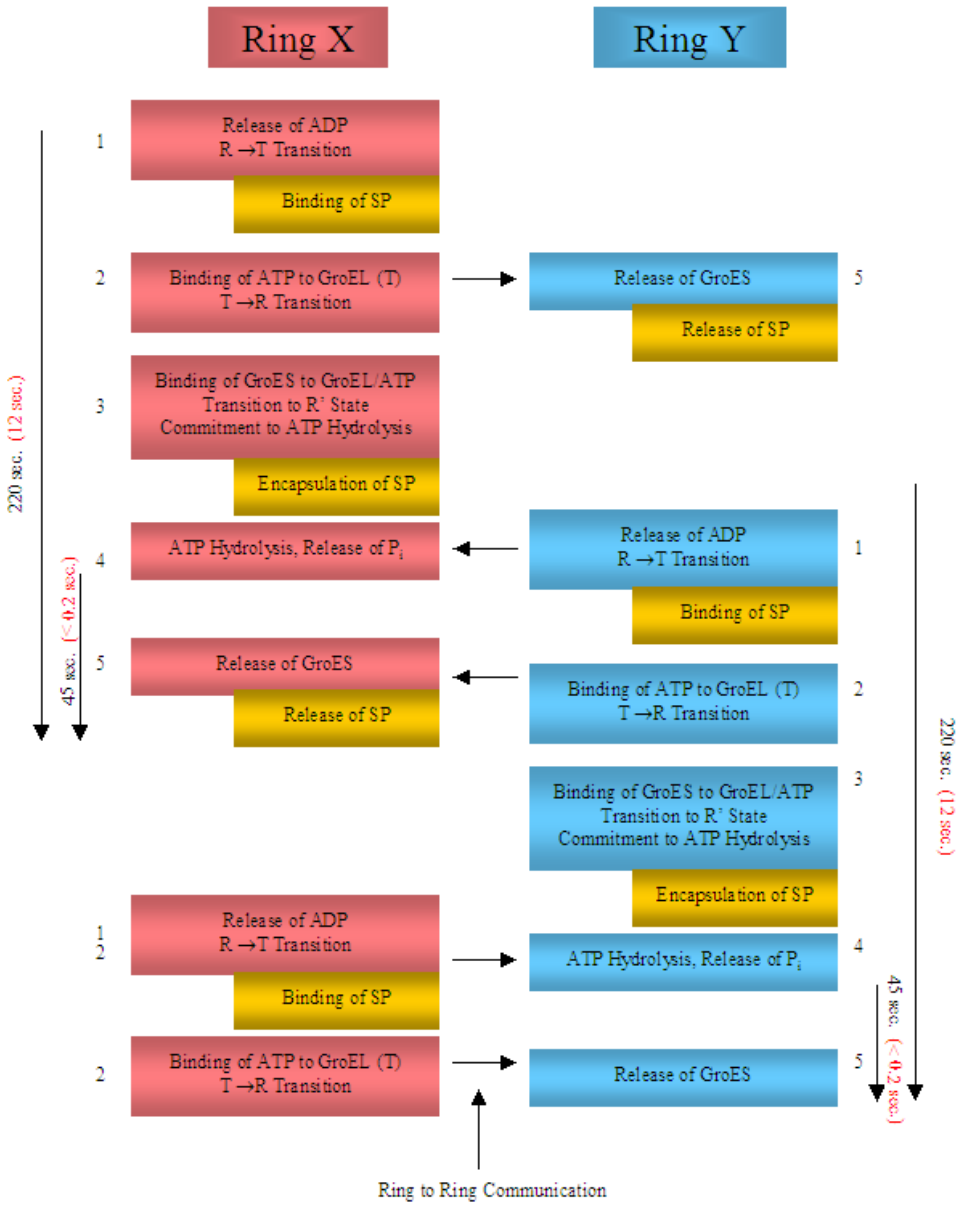

Figure 5-3: Diagramming the Events and Rates of the GroEL Reaction Cycle. The major events of the GroEL reaction cycle are shown for both rings. Blocks 1 through 5 constitute one hemicycle. The events listed within a block occur in an unknown order or occur at the same time. The events of the two rings are offset relative to each other to emphasize that the hemicycles of the two rings occur in an alternating fashion. Events which are specific to SP being present in the system are noted in yellow. The arrows between the rings indicate when inter-ring communication is thought to occur. For example, ATP binding to ring X causes GroES release in ring Y. The total length of the hemicycle is indicated by the long arrow and the hemicycle occurs in the indicated time span (see section 5.3.7). The total length of the GroES release events (ADP release, ATP binding, and the release of GroES, along with any allosteric transitions), as measured by the stopped-flow experiments, is indicated by the short arrow and the events occur within the indicated time span. The time indicated in red is the time measured in the presence of unfolded SP. The implications of these numbers are discussed in Chapter 6.

5.3.1 Confirming the Presence of FRET in the Experimental System As stated above, GroES release was measured by labeling single cysteine mutants of GroEL and GroES with fluorescent probes that constitute a FRET pair (52). The residues that were mutated to cys residues, GroEL E315C and GroES 98C, are shown in Figure 5-1. These residues are approximately 36 Å apart when GroES is bound to GroEL. The R_0 value (the distance at which the energy transfer efficiency is 50%) of the IAEDANS/fluorescein-5-maleimide pair is approximately 40 Å, making this set of probes ideal for monitoring GroEL/GroES dissociation. The release of GroES should result in a decrease in the fluorescence emission of the acceptor probe, F5M, which has an emission maximum at 519 nm. To confirm the presence of FRET in this system, $GroEL_D$ and $GroES_A$ were examined by steady state fluorescence (Figure 5-4). Adding ATP to a solution of $GroEL_D$ and $GroES_A$ causes a noticeable change in the relative peak heights of the donor and acceptor emission. A decrease in the emission of the donor at 473 nm is apparent along with a smaller increase in the acceptor emission at 519 nm. This is what would be expected if ATP were initiating complex formation between GroEL and GroES.

All FRET measurements of GroES release were done using a stopped-flow fluorometer. To confirm that the signal obtained using the stopped-flow device was actually a FRET signal, a series of control experiments were performed. In these experiments, complexes of GroEL and GroES were made in which one or both probes were eliminated from the system. To initiate dissociation, these complexes were rapidly mixed with a large excess of ATP and excess unlabeled GroES or GroEL where appropriate. This experiment is able to test whether or not any spectral changes that occur

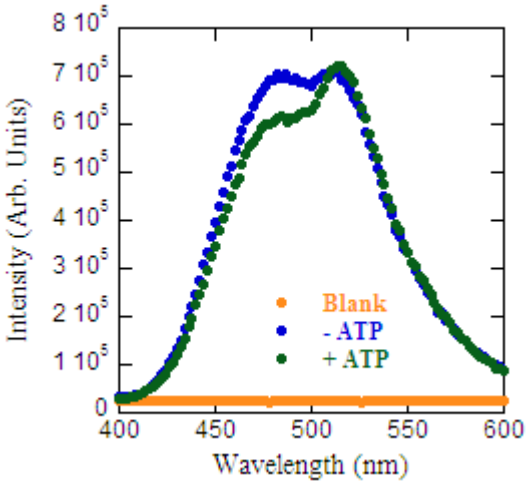

Figure 5-4: Steady-state Fluorescence Measurements Demonstrating FRET. A 4 μM $GroEL_D$, 2 μM $GroES_A$ solution with and without 30 μM ATP was measured in a steady-state fluorescence spectrophotometer. The solution was excited at 336 nm and the emission was scanned from 400 to 600 nm. Donor emission occurs at 473 nm and the acceptor emits at 519 nm.

which are not due to FRET, such as changes in the quantum yields of the donor or acceptor, affect the signal that is obtained (52). The excitation wavelength used in all experiments was 336 nm, which is approximately the absorbtion maximum of IAEDANS. Emission was monitored at all wavelengths above the 530 nm cut-off filter. This filter was used to ensure that the measured signal was not being affected by the donor emission. As shown in Figure 5-5, only in the experiment in which both labeled GroEL and labeled GroES were used was any significant signal change obtained, confirming that the signal change obtained is due to FRET. Because the signal changes obtained in the controls using either of the fluorescent probes by themselves were so small, it was decided that a correction of the FRET signal using these control traces, as was done by Rye *et al*. (17), was unnecessary.

5.3.2 Measuring GroES Release Using FRET The basic experimental design was as follows, and is based on Rye *et al* (17). $GroEL_D$, $GroES_A$, and a 7-fold excess of

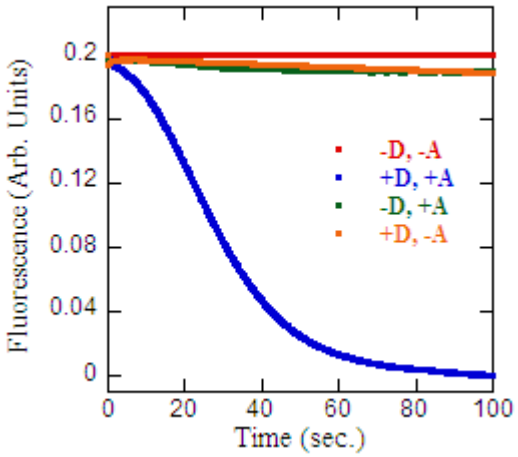

Figure 5-5: Decrease in Signal Requires Both Donor and Acceptor, Confirming FRET. The GroEL/GroES complex was formed using GroEL E315C and GroES 98C with and without their respective labels (Donor, Acceptor) according to the experimental protocol, using 10 mM instead of 100 mM KAc. In the (-D,-A), (-D,+A), and the (+D,+A) experiments, 4 mM ATP and 10 μM $GroES_{WT}$ were loaded in syringe B. In the (+D,-A) experiment, 4 mM ATP and 10 μM $GroEL_{WT}$ was loaded in syringe B.

ATP were mixed a relatively concentrated protein concentrations (40 μM GroEL, 20 μM GroES, 300 μM ATP) since complex formation is more efficient at higher protein concentrations. This was allowed to incubate for at least 30 minutes at room temperature to allow the ATP to fully exhaust. The complex was then diluted to 4 μM and loaded into syringe A of the stopped-flow device. $GroES_{WT}$ at 20 μM and a high concentration of ATP (4 mM) were loaded into syringe B. Upon the solutions being rapidly mixed 1:1, ATP (now at 2 mM) binds to the *trans* ring and dissociates $GroES_A$ from the *cis* ring, and the large excess of $GroES_{WT}$ (10-fold excess) prevents $GroES_A$ from rebinding and reestablishing the FRET signal.

To confirm that only ATP, and not ADP, causes GroES release, each nucleotide was separately used to trigger complex dissociation. As shown in Figure 5-6, only ATP causes a significant change in the FRET signal. The signal decreases with a half time of

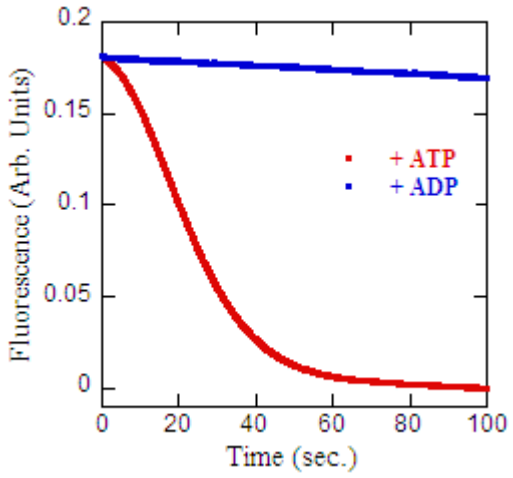

Figure 5-6: Decrease in FRET Signal is Specific to ATP. $GroES_A$ dissociation was initiated using 4 mM ATP or 4 mM ADP in syringe B along with 10 μM $GroES_{WT}$. The rest of the experiment was done according to the standard protocol, using 10 mM instead of 100 mM KAc. The slow decrease seen in the ADP trace, and at the end of most traces shown in this chapter, is probably due to the bleaching of the fluorophores.

about 20 seconds and only does so when ATP is used, beginning with a small lag phase. Only a slight, constant, relatively linear decrease in signal is seen with ADP. This decrease has been attributed to a bleaching of the fluorophores and was seen in all traces, under all conditions, in these stopped-flow studies.

To confirm the necessity of including excess $GroES_{WT}$ in the dissociation experiment, the procedure was attempted without it. As shown in Figure 5-7, when $GroES_{WT}$ is eliminated from syringe B, no change in signal is seen, besides the bleach. Apparently, $GroES_A$ rebinds to $GroEL_D$ almost immediately, allowing for no decrease in signal. Thus, a large excess of $GroES_{WT}$ was included in all subsequent experiments.

5.3.3 GroES Dissociation Results Differ from Those Previously Published The results of the GroES dissociation experiments in Figures 5-5 and 5-6 show traces which have multiple phases. There is a clear lag phase early in the trace, followed by a slow,

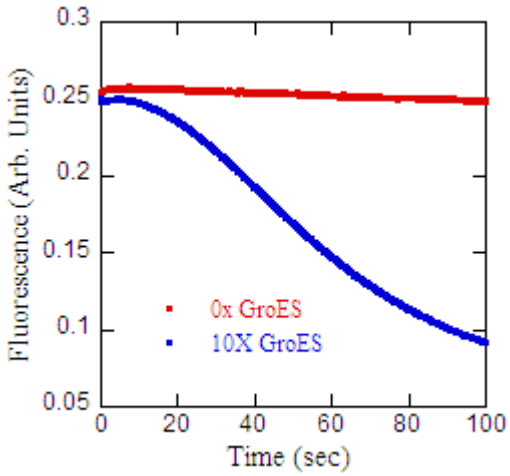

Figure 5-7: Decrease in FRET Signal Requires Addition of Excess Unlabeled GroES with ATP. The experiment was carried out according to the standard protocol with and without 20 μM $GroES_{WT}$ in syringe B.

exponential decay with a half time of 20 seconds. This differs significantly from the traces obtained by Rye *et al*., who saw a faster decrease at a lower temperature (25°C), with no sign of a lag phase (17). This was a cause for concern. There are a few differences between the published protocol and that which is used here. One difference was the extent of labeling of the GroEL and GroES. In the published paper, both proteins were only labeled to an extent of about 30%. In the original preparation of labeled protein used in the present experiments, a labeling extent of 90% was obtained. It was possible that the high extent of labeling with bulky, hydrophobic fluorophores was causing distorted release kinetics. To check this, the proteins were re-labeled with a smaller amount of both probes, and the experiment was repeated. As seen in Figure 5-8, both the heavily labeled and relatively lightly labeled preparations of protein showed identical release kinetics. (The preparations that were lightly labeled showed a smaller overall amplitude change, as would be expected). This eliminated the labeling extent as a possible source of the differences.

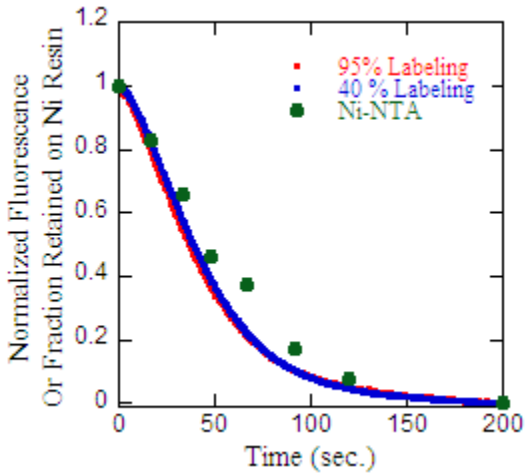

Figure 5-8: FRET Signal is Independent of the Extent of Labeling; Release Kinetics are Independently Confirmed. $GroES_A$ release was measured using different preparations of $GroEL_D$, one of which was 40% labeled with IAEDANS and the other 95% labeled. The amplitudes of the traces were normalized for easier comparison. Also, the kinetics of $GroES_{His}$ release from $GroEL_{WT}$ were measured using the protocol in section 5.2.4. The fraction of $GroES_{His}$ retained following ATP addition was normalized as described in the text.

It remained a small possibility that the FRET signal witnessed in the current experiments was not actually monitoring GroES release, but some other slower event. To check this, a control experiment was performed to monitor GroES release kinetics using a completely independent protocol, described in section 2.2.4. Briefly, the release of $GroES_{His}$ from $GroEL_{WT}$, as triggered by the addition of ATP and $GroES_{WT}$ under the same experimental conditions used in the stopped-flow experiments, was monitored by stopping the release reaction at certain time points using a glucose/hexokinase quench. GroEL that was still bound to $GroES_{His}$ was separated from released GroEL (now bound to $GroES_{WT}$) using a small Ni-NTA column, and the column eluents were quantitated by SDS-PAGE. As shown in Figure 5-8, the GroES release kinetics monitored using this protocol are nearly identical to those obtained using the stopped-flow protocol. Thus, the FRET signal in the stopped-flow experiments is almost certainly measuring GroES

dissociation. It was thus felt that the traces seen using the current protocol were valid, and that some other factor was causing the difference in the traces. Possible reasons will be discussed in section 5.4.

5.3.4 Effect of K^+ Ion on GroES Release The ATPase activity of GroEL is dependent on the concentration of K^+ ion (31). It has been proposed that K^+ affects activity by influencing the T→R equilibrium in favor of the R state (72). This was proposed because at low K^+ concentrations, ATPase activity tends to be higher than at high [K^+]. It was inferred that K^+ was favoring the transition to the less-active R state. Thus, K^+ was used in the GroES release experiments to find out whether or not the allosteric state of the *trans* ring affected the rate of release. At low K^+, the *trans* ring should be in the T state, and at high [K^+], the R state. The results in Figure 5-9, with 3

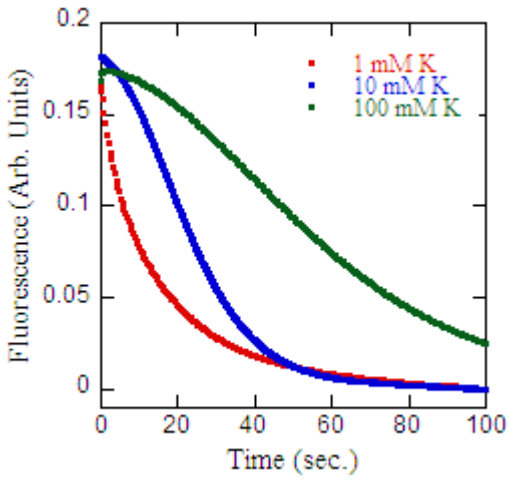

Figure 5-9: Effect of K^+ Concentration on GroES Release. $GroES_A$ release was measured at three different K^+ concentrations. In these experiments, the $GroEL_D/GroES_A$ complex formation step and the release measurement were both done at the stated [K^+]. ADP was not removed prior to measuring the release.

different K^+ concentrations, show that there is a clear decrease in the rate of release with increasing [K^+]. This was not a result of simply increasing the ionic strength, since a control experiment using increasing tetramethyl ammonium chloride, which increases ionic strength and cannot bind to GroEL, showed no effect on the rate of release (data not shown). It was concluded from the experiment with K^+ that the *trans* ring being in the R state was somehow slowing release, and that release was favored by a T state *trans* ring. The remainder of the experiments discussed in this chapter use a K^+ concentration of 100 mM, since this results in the slowest, and easiest to measure, rate of release.

5.3.5 Effect of ADP on GroES Release In the original design of this experiment, 300 μM ATP was used to cause complex formation between 40 μM $GroEL_D$ and 20 μM $GroES_A$. After loading this solution into the stopped-flow after diluting it to 4 μM GroEL and then mixing 1:1 with the ATP/$GroES_{WT}$ solution, the final concentration of the ADP from the complex formation is 15 μM. This is miniscule compared to the 2 mM ATP used to initiate bullet dissociation, and that is why it came as a surprise that removing this small amount of ADP (by running the GroEL/GroES/ADP solution on a PD-10 de-salting column) caused the dissociation kinetics to dramatically change (Figure 5-10a). The PD-10 column removes the ADP not trapped in the *cis* ring, meaning that only 1 μM ADP remains after de-salting, unable to exchange with buffer. Without the residual, exchangeable 14 μM ADP, release occurs very quickly, in less than 50 ms. The effect of ADP on the release kinetics was therefore examined by removing the residual ADP following complex formation, and then systematically adding back varying amounts of ADP (Figure 5-10 b, c, d). As little as 1 μM ADP is enough to affect release. In fact,

two distinct phases can be distinguished. A fast release phase occurs at less than 100 ms (Figure 5-10c). The traces at 0 and 1 μM ADP fit well to double exponential equations, both ADP concentrations giving approximately the same two rate constants with random residuals (not shown). The two phases in each fit had apparent rate constants of 138 and 16 sec^{-1}, and were approximately equal in amplitude. A slow release phase occurs following the usual lag phase between 5 and 125 seconds (Figure 5-10b). This slow phase could not be properly fit to any simple equation due to the presence of the lag phase, but qualitatively, all decays seem to have approximately the same rate. It should be noted that the "overshoot" seen in the slow phase at 0 μM ADP was attributed to the rapid rebinding of $GroES_A$ following rapid release. This effect could be reduced by

Figure 5-10: Effect of ADP on GroES Release. The release kinetics of GroES are strongly affected by the presence of ADP in the $GroEL_D/GroES_A$ solution in syringe A. **A**) $GroES_A$ release is accelerated when the ADP left over from the $GroEL_D/GroES_A$ complex synthesis is removed on a PD-10 de-salting column, as described in the text. The overshoot seen in the trace is dependent on the amount of excess $GroES_{WT}$ added with the ATP during the rapid mix, and is most likely due to $GroES_A$ rebinding under fast release conditions. **B**) $GroES_A$ release was measured in the presence of various [ADP]. The residual ADP left from the complex formation was removed on the PD-10 column, and the stated amounts of ADP were added back. The [ADP] concentrations given are the final concentrations after the mixing in the stopped-flow had occurred. Data fitting was not attempted due to the complexity of the traces. **C**) The events occurring prior to 200 ms were monitored in detail during the same experiment in which the traces in B were obtained by doing separate shots during this short time span. At least 8-10 shots were averaged to obtain each trace, and the mixing pressure was held on the syringes (see 5.2.3). The colors correspond to the ADP concentrations listed in panel **B**. The 0 μM and 1 μM ADP traces could be fit to double exponential equations, both giving rate constants of 138 sec^{-1} for one phase and 16 sec^{-1} for the other. The residuals of the fits were random. The amplitudes of the two phases in each trace were approximately the same. The two phases were never successfully assigned to any specific events. The amplitude changes in the other traces were too small to allow fitting of the data. **D**) The traces in **B** and **C** were combined by matching the first point of the plot **B** trace with the average of the last 10 points of the plot **C** trace, and plotted on a log scale in order to better visualize the varying amplitudes of the fast and slow phases. **E**) The amplitudes of the slow phase measured at each [ADP] were estimated from the traces in **B** and plotted against [ADP].

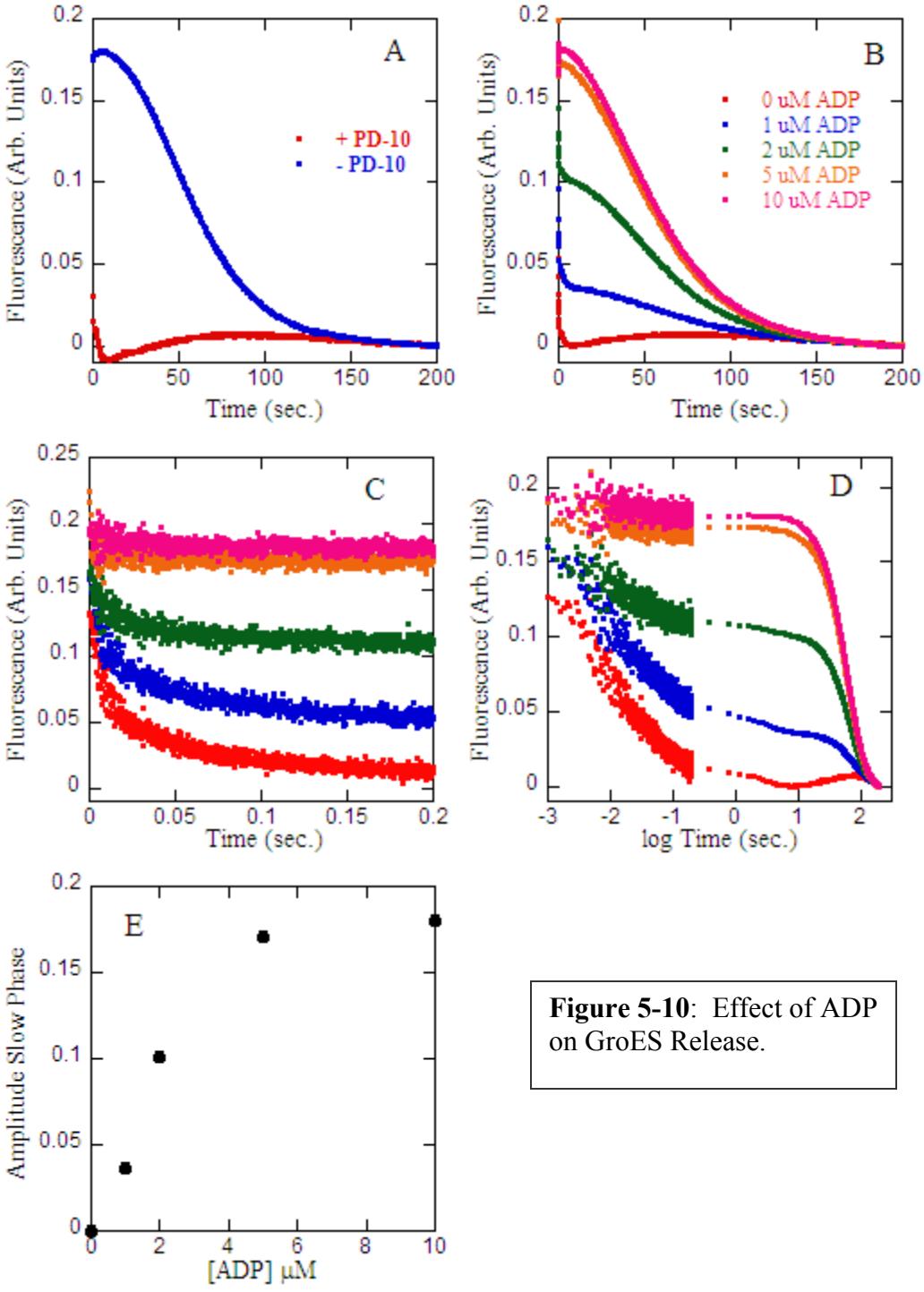

Figure 5-10: Effect of ADP on GroES Release.

increasing the amount of excess $GroES_{WT}$ added with the ATP (not shown). These results indicate that the ADP concentration only affects the relative amplitudes, and not the rates, of the fast and the slow phases, as is seen most clearly when plotting the data on a log scale (Figure 5-10d). The amplitude of the slow phase was estimated and plotted against [ADP] in Figure 5-10e. An [ADP] of 5 μM is nearly enough to eliminate the fast phase entirely.

5.3.6 Effect of Unfolded SP on GroES Release Unfolded substrate protein increases the ATPase activity of GroEL. It has also been found that unfolded MDH increases the rate of GroES release (17). The increase in ATPase activity was attributed in Chapter 4 to SP binding to and holding a GroEL ring in the more active T state. It is therefore tempting to conclude that SP enhances the rate of GroES release by binding to and holding the *trans* ring in the T state, which somehow favors GroES release. The effect of unfolded SP was examined in detail by adding various amounts of the weak-binding, unfolded α–lactalbumin to the $GroEL_D/GroES_A$ complex, both in the presence and in the absence of 15 μM ADP, loading this solution in syringe A, and measuring the rate of $GroES_A$ release. The effect of a wide range of α-LA concentrations in the presence of ADP is shown in Figure 5-11,a and b. α-LA affects both the rate and the amplitude of the release. High amounts of α-LA substantially increase the rate of GroES release. In fact, only a 0.5 molar equivalent of α-LA to 14-mer is enough to speed the release, albeit slightly. Once again, these traces could not be fit to a simple equation due to the lag phase and also to the appearance of a fast phase at higher concentrations of α-LA. However, the half-times of these traces could be estimated, and were plotted against the SP concentration (Figure 5-11c). This is useful because the half-time of the trace can

be thought of as the average amount of time that an intact folding chamber exists on GroEL. It is the mean "residence" time, the average amount of time that an SP can spend folding in the protective environment of the hydrophilic, *cis* ring central cavity. Only 10 α-LA per 14-mer are enough to reduce the residence time to practically zero.

At relatively high amounts of α-LA, a single exponential-like fast phase becomes apparent (Figure 5-11d). This fast phase increases in amplitude and rate with increasing α-LA, to a maximum of about 25 sec^{-1} with a 50-fold excess of α-LA over 14-mer. When the traces are plotted on a log scale (Figure 5-11e), it can be seen that α-LA affects the relative amplitudes of the fast and slow phases. At high [α-LA], all GroES release occurs

Figure 5-11: Effect of Unfolded SP on GroES Release. Freshly reduced unfolded α-LA was added to the $GroEL_D/GroES_A$/±ADP solution prior to loading it in syringe A. The α-LA amount given in each plot is the excess of α-LA over GroEL 14-mers. Since only the *trans* ring is available to bind SP when GroES is bound to the *cis* ring, this number also represents the excess of α-LA over binding sites. α-LA does not refold under the conditions used in these experiments. **A** and **B**) The effect on $GroES_A$ release of several different amounts of α-LA is shown. ADP was not removed prior to the experiment; thus, the final [ADP] after mixing was 15 μM. The data is split amongst two plots for clarity. Again, data fitting was not done due to the complexity of the traces. **C**) The half-time of the traces in **A** and **B** was estimated and plotted against the amount of α-LA used in the experiment. The half-time represents the average amount of time that an SP spends encapsulated in the central cavity under GroES and can be called a "mean residence time." **D**) The fast phase was examined in detail with different amounts of α-LA. 8-10 shots were averaged to obtain each trace, and the mixing pressure was held on the syringes. The 25x and 50x traces were fit to single exponential equations giving an average rate constant of about 25 sec^{-1}. **E**) In the same experiments used to obtain the traces in **D**, the slow phases out to 200 seconds were also measured. The fast and slow traces were combined as in Figure 5-10d, and plotted on a log scale to better illustrate the changing amplitudes of the fast and slow phases. The trace colors correspond to the α-LA amounts in **D**. **F**) The effect of unfolded α-LA on the release of $GroES_A$ in the absence of ADP in the syringe A solution was also measured. All release occurred in the fast phase (<200 ms). 8-10 shots were averaged to obtain these traces, and the mixing pressure was held. The traces fit reasonably well to double exponentials. The two phases had rate constants which increased slightly with increasing α-LA. The rate constant of the faster phase ranged from 135-175 sec^{-1} and the slower phase rate constant ranged from 5-28 sec^{-1}. The amplitudes of the two phases did not change much with increasing α-LA, and both phases had approximately equal amplitudes at all [α-LA]. Again, these two phases could not be assigned to any specific events.

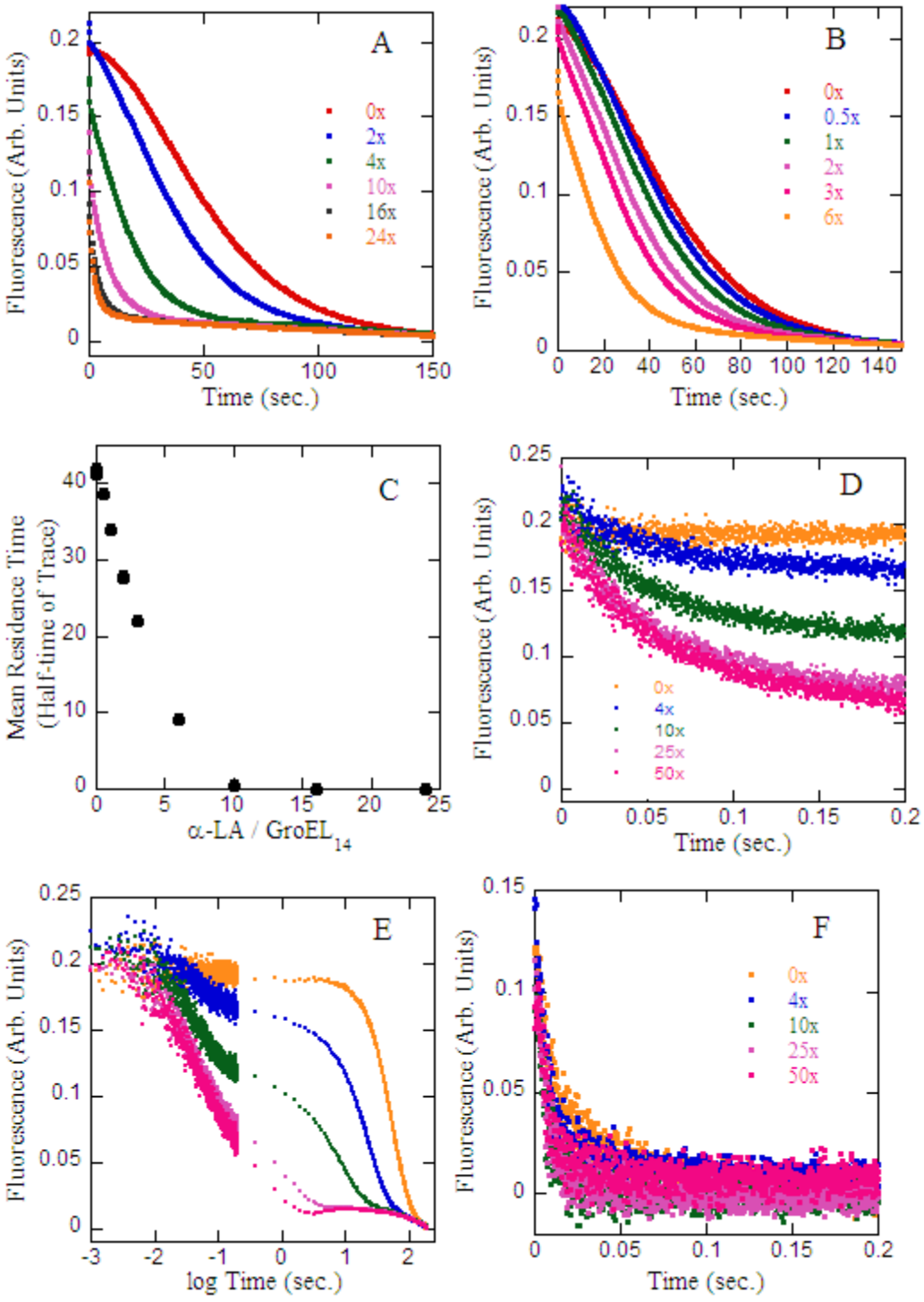

Figure 5-11: Effect of Unfolded SP on GroES Release

within 2 seconds. At mid-range [SP], for example 10x α-LA (Figure 5-11e, green), release seems to be partitioned between the two release phases. This is similar to the effect seen with varying ADP concentrations, although in the case of α-LA the rates, as well as the amplitudes, of the two phases seem to vary with [α-LA], whereas only the amplitudes varied with [ADP].

Finally, the effect of unfolded α-LA on the rate of GroES release in the absence of ADP was examined. ADP was once again removed on a PD-10 column following complex formation. As is shown in Figure 5-11f, all GroES release in the absence of ADP occurs prior to 100 ms. As was the case with the traces in Figure 5-10c, these data fit best to a double exponential model. SP has a small effect on the rates obtained from this analysis. The faster phase rate constant increases from 135 sec^{-1} in the absence of SP to 175 sec^{-1} in the presence of 50x SP, a 30% change. The slower phase increases from 5 to 28 sec^{-1}. This latter phase may correspond to the fast release event seen in the presence of ADP, which had a similar rate (Figure 5-11d).

5.3.7 Relating ATPase Activity to GroES Release As mentioned above, the half-time of GroES release represents the average residence time of an SP in the central cavity. However, the amount of time a ring spends with SP captured in the central cavity below the GroES cap is only part of the reaction cycle of a single GroEL ring. This cycle must also include ATP binding, allosteric transitions, and GroES binding. It would be useful to relate the total reaction cycle time of one ring, or hemicycle time, to the mean residence time. The hemicycle time can be calculated from the ATPase rate. The ATPase rate of GroEL E315C at 30°C in the presence of GroES and increasing amounts of unfolded α-LA was measured (Figure 5-12a), and is very similar to that obtained with

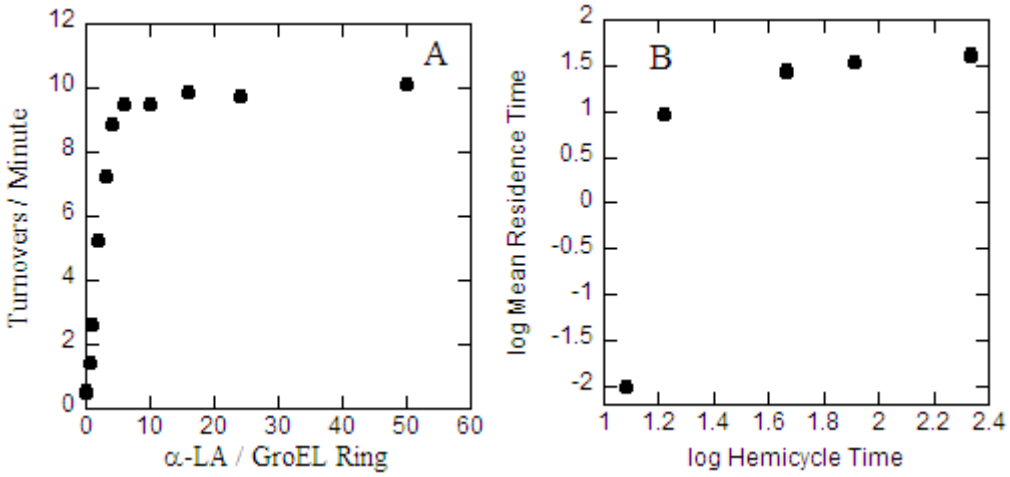

Figure 5-12: Relating the Rate of GroES Release to the ATPase Rate. **A**) The ATPase activity of unlabeled GroEL E315C in response to added α-LA was measured using the coupled enzyme assay at 30°C, 100 mM K^+ with 2 μM GroEL(E315C), and 2 μM $GroES_{WT}$. **B**) The ATPase rate was converted into the hemicycle time, or the total amount of time it takes one ring to proceed through an entire reaction cycle, as described in the text. The hemicycle time was then plotted against the mean residence time recorded with the same amount of added α-LA, both axes on log scales. This allows one to relate the amount of time a GroEL spends releasing GroES to the total time of the reaction.

$GroEL_{WT}$ and GroES (not shown). The hemicycle time can then be calculated using the following logic. For example, if the ATPase rate is 1 turnover/subunit/min., then each ring must turnover 0.5 times per minute. The total cycle time of the ring is the inverse of 0.5 $min.^{-1}$, multiplied by 60 to put the final value in seconds. Thus, a ring with a turnover rate of 0.5 $min.^{-1}$ has a hemicycle time of 120 seconds. The hemicycle time was calculated for the rates measured in Figure 5-12a, and plotted against the mean residence times measured in the stopped-flow experiments when the data was obtained with the same concentration of α-LA (Figure 5-12b). It is important to note that the relationship is not linear. The hemicycle time is always longer than the mean residence time (it has to be), but when the hemicycle time is relatively low (< 15 sec.), the residence time

becomes very short (about 10 msec.). This indicates that in the presence of a high concentration of SP, a ring spends very little of its total cycle time releasing GroES.

5.3.8 Effect of Unfolded SP on GroES Release When SP is Added Under Non Steady-state Conditions In all stopped-flow experiments with SP discussed thus far, the SP was added to pre-formed $GroEL_D/GroES_A$ complex, and the system was allowed to come to equilibrium before release was initiated. The experiment was also done in which the SP was added to the complex/15 μM ADP at the same time as the ATP/$GroES_{WT}$ (the α-LA was added to the syringe B solution). The effect of α-LA on GroES release under these non steady-state conditions is significantly different than the effect seen in Figure 5-11 under steady-state conditions. Increasing [α-LA] only affects the rate of the slow release phase, and not the amplitude (Figure 5-13a). A fast phase prior to 200 ms is not seen (Figure 5-13b, and compare with Figure 5-11d). Thus, the appearance of the fast phase is entirely dependent on the establishment of a pre-equilibrium of the GroEL *trans* ring, ADP, and SP.

5.3.9 Effect of SP at Different ADP Concentrations The effect of SP on GroES release shown in Figure 5-11,a-e was measured in the presence of 15 μM ADP. There is already a strong indication that SP and ADP are affecting GroES release in similar, but opposite ways. High [ADP] slows release; it increases the amplitude of the slow phase. High [SP] speeds release; it increases the amplitude of the fast phase, and it increases the rates of both the slow and the fast phase. The relationship between these two allosteric effectors was explored further by measuring the effect of unfolded α-LA on GroES release at several ADP concentrations (Figure 5-14 a,b). The amplitudes of the slow phases were estimated from the traces and plotted against the [α-LA] (Figure 5-14c). The

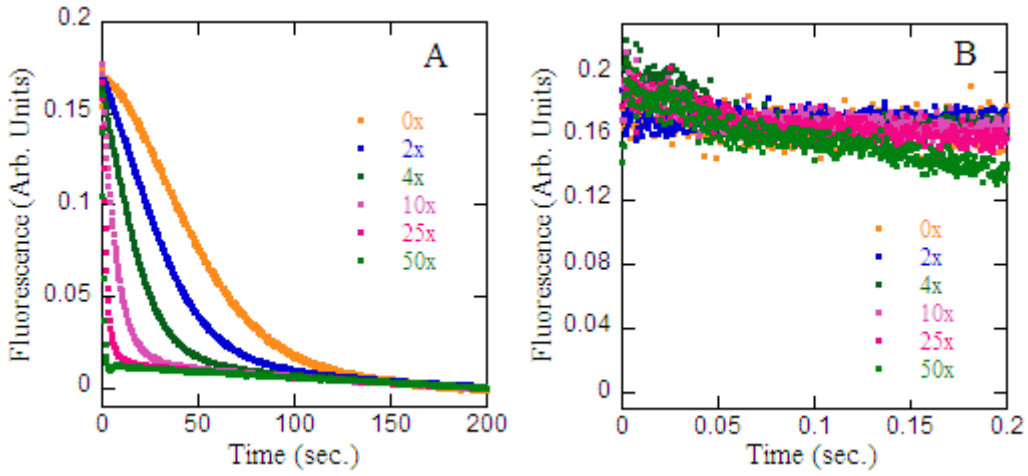

Figure 5-13: Effect of Unfolded SP on the GroES Release Rate When SP is not Included in the Initial GroEL/GroES/ADP Equilibrium. Rather than including α-LA in the $GroEL_D/GroES_A$/ADP solution in syringe A and allowing that solution to reach equilibrium, varying amounts of α-LA were added to the ATP/$GroES_{WT}$ solution in syringe B. $GroES_A$ release was otherwise measured according to the standard protocol, and ADP was not removed ([ADP] upon mixing was 15 μM). The slow phase (**A**) and fast phase (**B**) are shown.

inverse relationship of ADP and SP is apparent from this plot. At high [ADP], a much larger amount of SP is required to decrease the amplitude of the slow phase. Put another way, ADP inhibits the ability of SP to increase the rate of GroES release.

5.3.10 ADP and ATP Compete for the Binding Sites on the* Trans *Ring One way of interpreting the result in which ADP slows GroES release is that ADP bound to the *trans* ring is out competing the incoming ATP for the nucleotide binding sites. If this is true, it demonstrates a remarkable binding affinity of ADP for the *trans* ring, since as little as 1 μM ADP can at least partially out compete 2 mM ATP. It is possible that the lag phase seen in the traces represents the time it takes for ATP to win the competition for the binding sites. It would therefore be predicted that the lag phase could be extended by raising [ADP] and lowering [ATP]. The final ATP concentration after the mix was

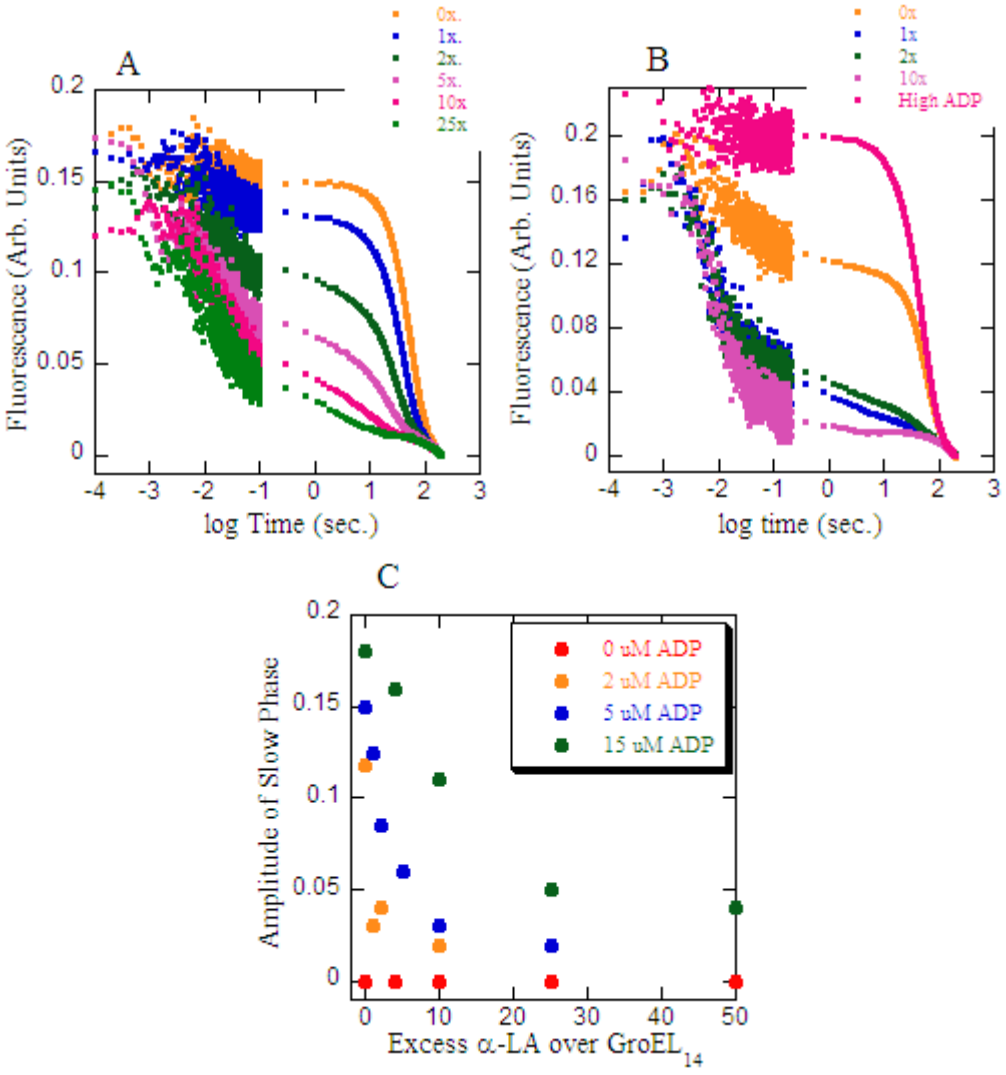

Figure 5-14: ADP Inhibits Unfolded SP's Ability to Stimulate GroES Release. The effect of unfolded α-LA on $GroES_A$ release was measured with several different ADP concentrations in the $GroEL_D/GroES_A$/ α-LA/ADP solution in syringe A. ADP was removed after complex synthesis using a PD-10 de-salting column, and then varying amounts of ADP were added back. The effect of α-LA on GroES release in the presence of 0 μM ADP and 15 μM ADP has already been shown in Figures 5-11e and 5-11f, respectively. The results with 5 μM ADP and 2 μM ADP are shown here in **A** and **B**, respectively, with fast and slow traces matched and plotted on a log scale as before. All ADP concentrations given are the final concentrations following the mixing in the stopped-flow. The "high ADP" trace in **B** is a control using 15 μM ADP and no added SP. **C**) The amplitudes of the slow phases from these 4 plots were estimated and are plotted against the amount of added α-LA at each [ADP].

lowered to 250 μM, and the amount of ADP added back following de-salting on the PD-10 column was varied (Figure 5-15). The rate of release is indeed slowed significantly when a high concentration of ADP is added back, and the lag phase does increase in magnitude. This supports the notion that the lag phase, at least in part, represents the time it takes for ATP to replace ADP on the *trans* ring.

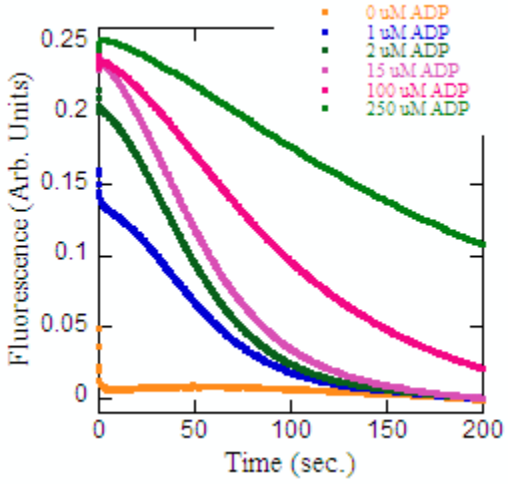

Figure 5-15: Raising [ADP] and Lowering [ATP] Slows Release and Increases the Lag Phase. $GroES_A$ release was measured with varying amounts of ADP in the syringe A solution and only 500 μM ATP in syringe B (250 μM ATP after stopped-flow mixing). The ADP leftover from the $GroEL_D/GroES_A$ complex synthesis was removed by de-salting, and varying amounts of ADP were then added back. The ADP concentrations given are the final concentrations after the mixing in the stopped-flow.

5.3.11 Effect of [ATP] on the Rate of GroES Release The dependence of the GroES release rate on the concentration of ATP used to initiate complex dissociation was tested, both with and without unfolded α-LA, in the absence of competing ADP. The traces, both without and with unfolded α-LA (Figure 5-16 a and b, respectively), fit reasonably well to single exponentials. The fitting was complicated by the appearance of a lag phase a lower [ATP]. In fitting these traces, the lag phase was ignored in an effort to get a general idea of the rate constants. The rates obtained are plotted in Figure 5-16c.

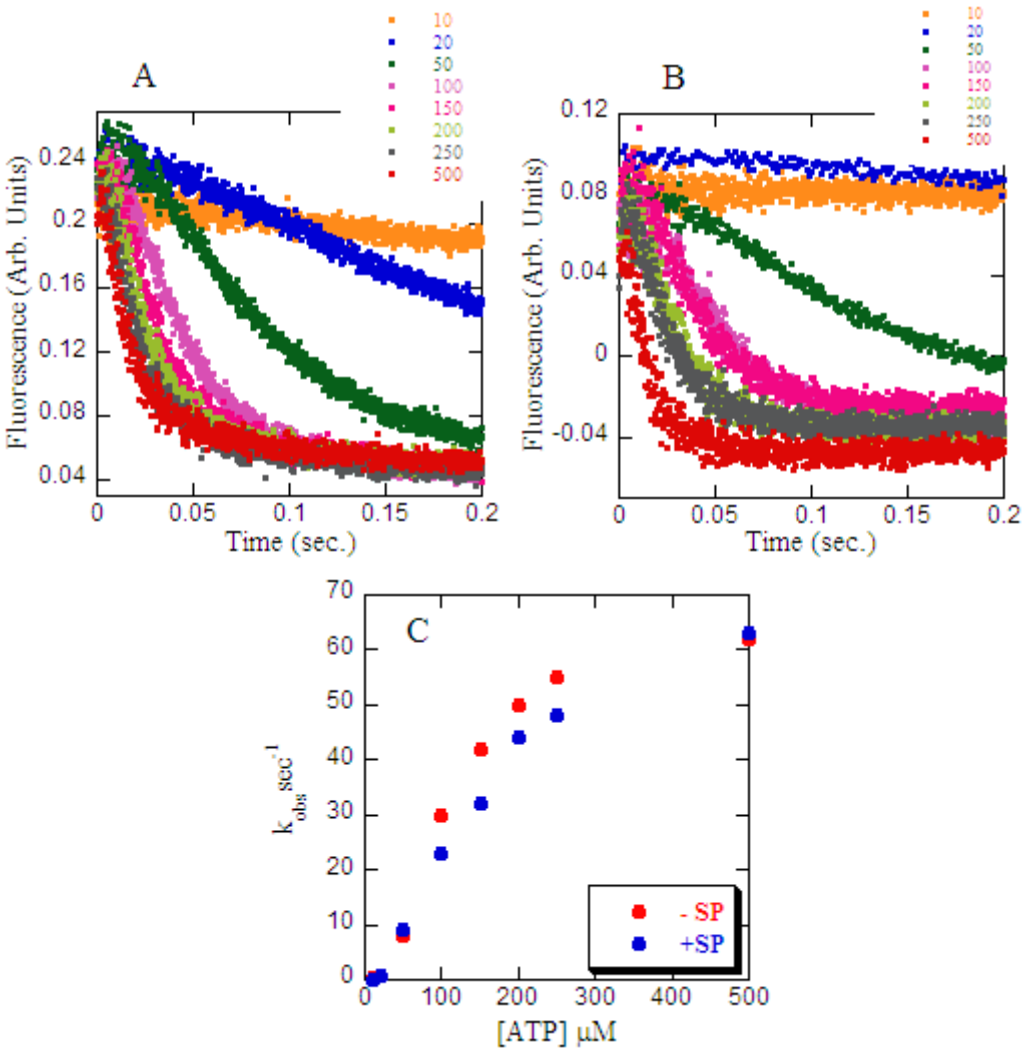

Figure 5-16: Effect of Varying the ATP Concentration Used to Initiate GroEL/GroES Dissociation. The concentration of ATP in the syringe B solution used to initiate $GroES_A$ release was varied, and the effect of this on the release kinetics was measured in the absence of ADP. ADP was removed following complex synthesis by de-salting on a PD-10 column. The ATP concentrations shown in the legends are the final concentrations (in μM) after the stopped-flow mix. This experiment was done both in the absence (**A**) and presence (**B**) of a 50-fold excess (over 14-mers) of α-LA in the $GroEL_D/GroES_A$ solution. 8-10 shots, during which the mixing pressure was held, were averaged to obtain the final traces, and these were fit to single exponential equations. At low [ATP], data was collected for a longer time period to enable data fitting. Also at low [ATP], data fitting was made more complicated by the appearance of a lag phase early in the trace. The data points encompassing the lag phase were ignored during the fitting, and rate constants obtained from these fits are therefore very approximate. **C**) The rate constants obtained from the single exponential fits are plotted against the [ATP]. The dependence of the rate constants on [ATP] is not linear.

Surprisingly, SP appears to inhibit the release rate at lower [ATP], reminiscent of the finding that SP inhibits ATPase activity at low [ATP] (see Chapter 4). It is also apparent that k_{obs} is not linearly related to [ATP], indicating that ATP binding to the *trans* ring is not a simple bimolecular reaction.

5.4 Discussion

5.4.1 Explaining the Difference Between the Published and Current Results

Although the results in this chapter agree with the published results of Rye *et al*. (17) in a general sense (ie. SP causes a stimulation of the GroES release rate), the traces themselves are very different. The published traces were all said to have fit to single or double exponentials, and they contained no lag phase. Also, all of the published rates were faster than those obtained here, even though they were measured at a lower temperature. The published traces were obtained at 10 mM K^+, so they would be expected to show somewhat faster rates than the traces here, which were mostly obtained at 100 mM K^+. However, the published traces still give rates that are significantly faster than the limited number of traces obtained at 10 mM K^+ in the studies for this dissertation. Therefore, the difference in K^+ concentration is not nearly the whole story.

One subtle difference between the two experimental protocols is that Rye *et al*. inserted the E315C mutation into GroEL in which all of the native cysteines had been removed. They did this to prevent any unwanted labeling of the native cys residues, assuming that these were reactive (52). As was discussed in Chapter 3, the native cys residues, in our hands at least, do not appear to be accessible to reaction, and thus the native cys residues were not removed when making the E315C mutant. This choice was made for other reasons as well. GroEL that is cys-free has a significantly lower ATPase

activity (G. Curien, unpublished, and (17)). Also, cys-free GroEL appears to much less stable than $GroEL_{WT}$, and other mutants made in the cys-free background did not survive the acetone treatment (G. Curien and J. Grason, unpublished). Thus, it was felt that the drawbacks of using the cys-free GroEL in these studies far outweighed the benefits of avoiding what would probably have been a miniscule amount of unwanted labeling of the native cys residues. This reasoning seems justified now knowing that the extent of labeling had no effect whatsoever on the GroES release kinetics, and also knowing that labeled GroEL had an ATPase activity identical to $GroEL_{WT}$ (not shown). The fact that Rye *et al*. did choose to use the cys-free background is certainly a difference between the protocols, and is one possible cause of the differing traces.

The most likely cause of the altered traces, however, is the presence of contaminated protein in their GroEL preparations. It is very clear from the data presented above that even a slight amount of unfolded SP has an effect on the rate of release. It is shown in Figure 5-11 that only a 4-fold excess of the weak-binding α-LA increases the rate of GroES release and eliminates the lag phase. Therefore, it does not take much contaminating protein in a GroEL preparation to have a substantial effect on the GroES release kinetics. It is strongly believed that the acetone precipitation used to purify the GroEL used in these studies (see Chapter 2) produces GroEL preparations of the highest purity currently obtainable. The purification protocol used by Rye *et al*. is not made entirely clear, but it certainly did not involve the acetone precipitation. Therefore, it seems highly probable that the faster release kinetics presented in the published paper were due to contaminating protein present in the GroEL preparation. It is thus believed that the data obtained in the current studies is superior in quality to the published data.

5.4.2 Interpreting the Release Kinetics The results presented in this chapter are a first attempt at determining the kinetics of the signaling pathway for GroES release. Several important conclusions can be drawn from the data about the roles of the various allosteric effectors that were used in these experiments. However, this signaling pathway has the potential to be extremely complex, and a robust determination of all the rate constants that might be involved in the pathway cannot be accomplished with the present data. With that said, the results presented here provide us with far more information about this pathway than was known before.

The effect of ADP on the release kinetics seems clear. At low concentrations of ADP, the trace splits into two distinct phases: a fast phase complete within 100 ms, and a slow phase with a half-time of 40-50 seconds (Figure 5-10). When the ADP concentration is zero, only the fast phase is seen, and when the ADP concentration is above 10 μM, only the slow phase is seen. Between 0 and 10 μM, the ADP affects the relative amplitudes of the two phases, but does not seem to affect the rates. One possible interpretation of this data is that in the equilibrium that exists in the GroEL/GroES/ADP solution prior to the ATP addition, there are two populations of GroEL/GroES complexes. The two populations are noted schematically in Figure 5-17, rows A and B. One population has ADP bound to the *trans* ring, and the other does not. Upon ATP addition, the population with free *trans* rings (A) binds ATP immediately, the release signal is sent, and GroES dissociates rapidly, within 100 ms. Referring to Figure 5-3, only step 2 in ring X and step 5 in ring Y are measured. In the other population (B), the incoming ATP is forced to compete with the *trans*-bound ADP. Only after ADP is finally released and ATP is bound can the release signal be sent and GroES dissociate.

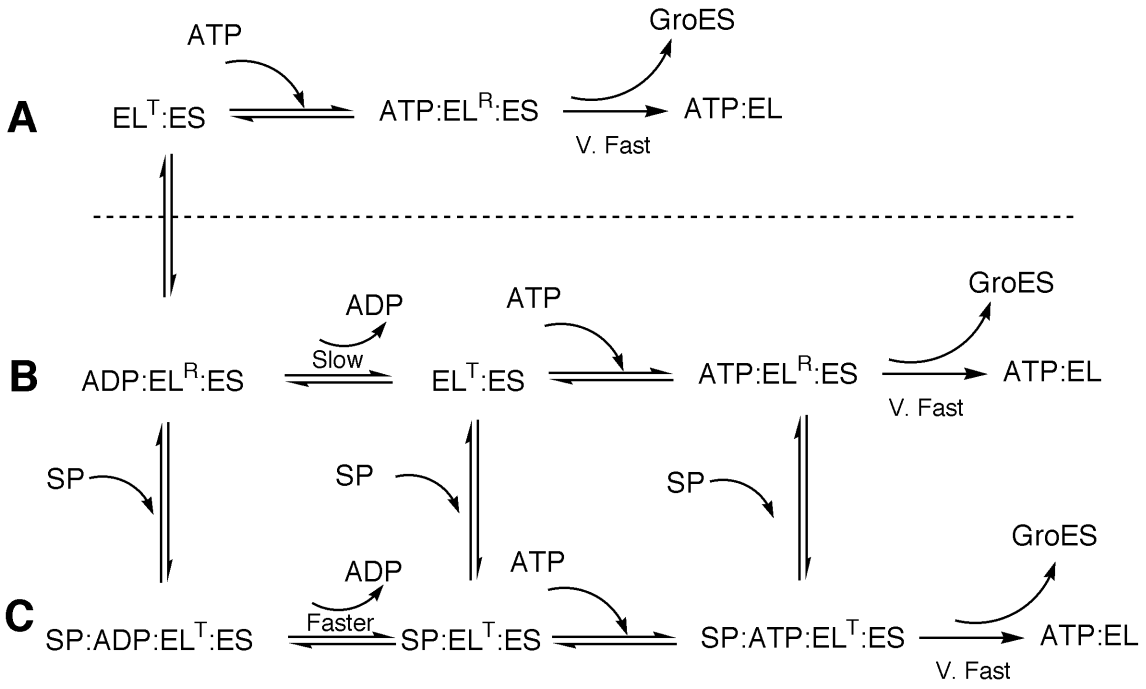

Figure 5-17: A Proposed General Pathway for GroES Release. The data presented in this chapter are consistent with the reaction mechanism shown here. The two release phases that appear at low concentrations of ADP are due to two populations of GroE complexes. One population does not have ADP bound to the *trans* ring and releases GroES by pathway **A**. The other population has ADP bound in the *trans* ring and releases GroES according to the slower pathway in row **B** in which ADP release is rate limiting. The dashed line indicates the two distinct GroE populations present in the GroEL/GroES/ADP equilibrium prior to the initiation of release. The ability of unfolded SP to increase the rate of release and counteract the effect of increased ADP concentrations is best explained by the pathway in row **C** in which the release of ADP is faster in the presence of *trans*-bound SP. The superscripts designate the probable allosteric conformations of the *trans* ring along the proposed pathway, but it is not known if these are the true allosteric states, and nothing is known about how the allosteric states might affect the rate of release. For example, it is not known if the *trans* ring is in the T or R state when the release signal is communicated between the rings, if it actually matters, or if a T→R or R→T transition is required to send the signal. The only allosteric assignment that is probably true is in the first species in row **C** in which SP is favoring a T state *trans* ring. No rate constants are assigned to any individual steps in the pathway due to insufficient information, but assumptions are made about the relative speeds of certain steps. GroES release is assumed to occur rapidly once ATP is bound, and the release of ADP from the *trans* ring is assumed to be faster in the presence of SP than in the absence of SP. This is probably due to the T state having a lower affinity for nucleotide than the *trans* ring.

Again referring to Figure 5-3, steps 1 *and* 2 in ring X and step 5 in ring Y are measured from this population. The presence of the lag phase in the slow phase of the traces indicates a slow, upstream process (or processes, see step 1 in Figure 5-3) that occur(s) prior to the event that is observed in the experiment. ADP release is most likely this slow event, however, the occurrence of other processes, such as allosteric transitions, cannot be excluded. It is safe to assume that in the presence of bound ADP, the *trans* ring spends most of its time in the R state. Perhaps an R→T transition must occur that is coupled to ADP release, since nucleotide is thought to bind less tightly to the T state. Or, the transition may occur once ADP has left, prior to ATP binding. The R→T transition prior to ADP release might also be the slow event, with ADP dissociation occurring relatively fast. There is no way of distinguishing these possibilities from the current data. It should be noted that under physiological conditions, the *trans* ring will always contain bound ADP, and therefore GroES will always be released with the slow kinetics demonstrated here (if no SP is bound). The release of GroES has previously been implicated as the slow step in the GroE reaction cycle (17), and it is demonstrated here that the rate determining step in that process is the release of ADP from the *trans* ring, and possibly the allosteric transitions which accompany that release.

The effect of K^+ on the release kinetics is relatively simple to analyze. Increasing amounts of K^+ slow the release of GroES (Figure 5-9). K^+ is thought to shift the T→R equilibrium towards the R state. Therefore, GroES release is slower when the *trans* ring is in the R state. There could be several reasons for this. The release of ADP from the *trans* ring should be slower when the *trans* ring is in the R state, since R rings have a higher affinity for nucleotide. Thus, the incoming ATP would have a harder time

competing off the ADP from the binding sites. It is also possible that an allosteric transition to the T state needs to occur at some point in the pathway in order for GroES to eventually be released, and this transition would be disfavored by high [K^+]. It will require more experiments under several different conditions to fully determine the effect of K^+ on the release pathway, but it seems reasonable to conclude from the studies with K^+ that, not surprisingly, the allosteric state of the *trans* ring has a large effect on GroES release.

The effect of unfolded SP on GroES release kinetics is more complex. Not only does the addition of SP to the GroEL/GroES solution prior to ATP addition affect the relative amplitudes of the fast and slow phases, but it also appears to affect the rates of the two phases (Figure 5-11e). It has the inverse effect on release to that of ADP. High [SP] speeds release, whereas high [ADP] slows release. In addition, the concentration of ADP affects the magnitude of the release stimulation by SP. At high ADP concentration, higher concentrations of SP are required to stimulate the release rate. However, when ADP is removed from the system and release occurs entirely prior to 100 ms, SP has little additional effect besides a slight possible rate enhancement. The simplest way to explain SP's ability to stimulate GroES release is to consider the conclusions from Chapter 4. It was proposed that SP is able to enhance ATPase activity by forcibly holding a GroEL ring in the T state. When SP binds to the *trans* ring of the GroEL/GroES complex, it should have the same effect. A *trans* ring in the T state will have less of an affinity for bound ADP, thereby favoring its release and the binding of the large excess of ATP once it is added. SP is therefore altering the equilibrium between GroEL/GroES and ADP, creating two populations of GroEL/GroES complexes (Figure 5-17, rows B and C),

similar to the effect of low [ADP]. This explains the appearance of the two phases upon addition of SP to the GroEL/GroES complex, and it explains why SP has little additional effect when ADP is removed.

This does not explain, however, the observation that SP also increases the rates of the fast and slow phases when ADP is present. SP's rate enhancing ability is demonstrated most effectively when it is not included in the initial equilibrium prior to ATP addition but instead is added with the ATP (Figure 5-13). In this case, no fast phase appears, which means that only one GroEL/GroES population exists, one in which all complexes have ADP bound to the *trans* ring. When SP is added in such a way, it still exerts a significant stimulatory effect on the release rate. The exact reason for this is unclear, although it almost certainly has something to do with SP binding to the *trans* ring and holding it in the T state. It may again be an issue of speeding the release of ADP. But, this does not explain why SP stimulates the rate of the fast phase (Figure 5-11d). The fast phase should not be affected by ADP release, since the GroEL/GroES complexes that dissociate during the fast phase do not contain *trans*-ADP. Therefore, the *trans* ring being in the T state must affect some other step in the reaction pathway, possibly one or two of the allosteric transitions depicted in boxes 1 and 2 of Figure 5-3. This step (or steps) is difficult to pinpoint with the data presented here, because the allostery of the pathway is so poorly understood, and the experimental protocol used cannot provide a direct measure of the allosteric transitions. If the pathway contains a slow R→T transition, then SP should speed release. Or, if sending the release signal from the *trans* ring to the *cis* ring requires the *trans* ring to be in the T state, then added SP would again be expected to increase the release rate. There is no way of knowing if

either of those guesses are true without more experimental data, preferably data obtained with another observable.

All experiments discussed thus far used a saturating amount of ATP to dissociate the GroEL/GroES complex. When ADP is removed, and the [ATP] is varied, a non-linear dependence on [ATP] is obtained (Figure 5-16c). This implies that the [ATP]-dependent event that is being monitored in the experiment, probably ATP binding, is at least a two-step process. Obtaining rate constants from this data is not possible, since this typically involves extrapolating the points at low [ATP] to zero. The traces at low [ATP] contain unexplained lag phases and are difficult to fit to single exponential equations. It is therefore not possible to use these data to measure binding affinity or the rate of ATP binding. What is interesting is the result that at low [ATP], SP *inhibits* the rate of GroES release. Since inhibition by SP is only seen at lower [ATP], the rate inhibition is probably a result of decreased ATP affinity for the T state *trans* ring with bound SP. In other words, ATP binding may become rate limiting at lower [ATP]. It is also possible that SP is slowing a downstream T→R transition that is required for GroES release. Again, more study is needed to further elucidate the pathway.

The kinetic data obtained in these experiments allow several important conclusions to be made. First and foremost, ADP release clearly seems to be the rate-limiting step in the GroES release signaling pathway. Second, SP stimulates the rate of GroES release by enhancing the population of *trans* rings in the T state, which not only increases the rate of ADP release, but also might favor an allosteric R→T transition that occurs somewhere in the pathway. However, the limitations of these experiments are also very apparent. The determination of rate constants for all steps in the release

pathway is impossible, since the exact allosteric transitions that must take place along the way are unknown. The reaction cycle in Figure 5-3 notes possible allosteric transitions at several points. If multiple allosteric transitions must occur, the kinetic mechanism will become exceedingly complex (Figure 5-18). Even a partial determination of some of the rate constants involved is difficult because the traces are so complex and difficult to fit. Some rate constants were obtained from double exponential fits of the fast phase (as in Figure 5-10c), but assigning the two rates to individual events is not yet possible. The only conclusion that can be made is that the upper limit on the rate of release is approximately 140-170 sec^{-1}, and the lower limit is around 0.2 sec^{-1}. The fact that the GroES release rate can vary by three orders of magnitude depending on conditions is interesting in itself. This has important biological implications, which will be discussed in the next chapter. A full determination of the kinetic pathway will eventually be possible, but another observable will be needed, preferably one that can monitor the allosteric transitions. The specific allosteric signal sent from the *trans* ring to the *cis* ring that causes GroES release remains a mystery.

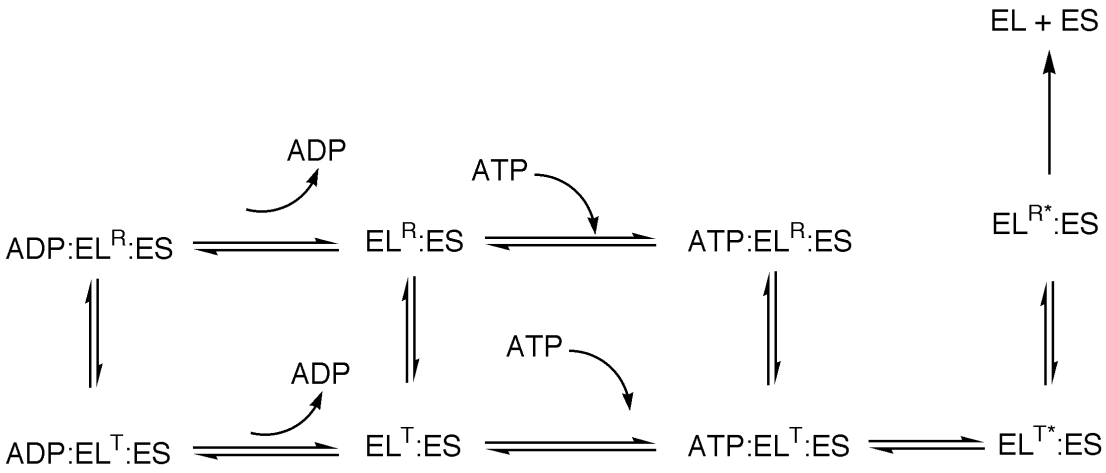

Figure 5-18: A Short Hypothetical Pathway Demonstrates the Potential Complexity of the System. Rate constants were not assigned to any of the steps in the pathway shown in Figure 5-17, and the allosteric states of the *trans* ring at each point were only guessed at. This is because very little is known about the allostery of this pathway, and when one begins to consider the various allosteric states that might be involved in the pathway, things rapidly get complicated. Consider the partial pathway shown above. This is a partial kinetic pathway in the context of these experiments because it does not involve SP. Unlike Figure 5-17, this pathway includes the T→R and R→T transitions that may occur at several points. Nothing is known about the rates of these conversions, and there is currently no good way to measure them. It is not known whether any of the conversions are required for release to occur. Most importantly, the allosteric transitions that might be involved in the final release signal after ATP is bound have not been defined. This example pathway presents a scenario in which release only occurs from an ATP bound-T state *trans* ring. ATP binding may create an "activated" T state (designated by an *) that must then undergo a T→R transition before release can occur, but this is only one of many scenarios. In fact, there is some evidence from experiments with $GroEL_{IAX}$ that the T→R transition is not required for GroES release (G. Curien, unpublished), but there was no kinetic element to these experiments that would provide a hint as to whether release is favored from either a T or R state *trans* ring. Suffice to say, the determination of a complete kinetic mechanism for the potentially complicated GroES release pathway will require many additional experiments.

Chapter 6

Summary and Final Discussion

The issue of whether or not GroEL is able to forcefully unfold SPs remains a controversial issue in the literature, despite 15 years of study by a large number of researchers. If active unfolding does takes place, it does so as a result of the allosteric structural transitions that a GroEL ring undergoes in response to ATP and GroES binding, during which GroEL may perform work on any bound SP. These studies have taken a close look at the concertedness of the transitions, the properties of the T and R states, how the transitions are affected by SP, and how allostery might play a role in one step of the GroEL reaction cycle, the release of GroES in response to ATP binding. In looking at these various aspects of GroEL, compelling evidence has been uncovered which suggests that GroEL does actively unfold substrates, and that GroEL operates most efficiently as an unfoldase, rather than as a passive isolation chamber.

The major conclusions from this dissertation can be summarized as follows. Studies with $GroEL_{IRX}$ (Chapter 3), a mutant into which intersubunit tethers can be introduced in order to lock the rings in the T state, reveal that the T→R→R' transition within a ring is concerted, albeit with the discussed caveats. These studies, in combination with previous studies with another double cysteine mutant, $GroEL_{IAX}$, suggest that all 7 subunits in a ring are forced to undergo domain movements in one concerted motion. This is important, because the upward, twisting motion of the apical domains which occurs during the T→R→R' transition would provide the "power stroke" to any SP unfolding event. Concerted motion within a ring would maximize the potential unfolding force during the power stroke. Additionally, this mutant was revealed to be defective in its inter-ring communication. This was shown by its reduced ability to

release GroES, its reduced negative cooperativity, and this may have something to with the inability of SP to stimulate its ATPase activity.

The stimulation of GroEL's ATPase activity by unfolded SP was examined in Chapter 4. It was suggested that SP is able to enhance ATPase activity because it binds to and enhances the population of GroEL rings in the T state, which has a higher V_{max} of ATPase activity than the R state. SP behaves similarly to a covalent tether in this respect. SP is able to bind to two or more SP binding sites and prevent the T→R transition, acting like an intersubunit tether exerting a mechanical force on GroEL. Therefore, in order for GroEL to undergo its structural transitions, it must be able to exert a countering force on the substrate. Thus, rate stimulation by SP is at least an indirect demonstration that GroEL must perform work on its substrates.

Finally, the release of GroES from GroEL upon the binding of ATP to GroEL's *trans* ring, and the ability of unfolded SP to enhance the rate of this process, was examined in Chapter 5. It was discovered that the rate limiting step in the GroES release pathway was the release of ADP from the *trans* ring prior to ATP binding. It was suggested that one reason SP is able to stimulate GroES release is that it binds to the *trans* ring and shifts the ring's T→R equilibrium towards the T state. The T state has a lower affinity for ADP, and therefore the release of ADP is accelerated. Additionally, it was implied that a T state *trans* ring also enhances the rate of GroES release by another mechanism that remains unknown due to a poor understanding of the allostery and signaling events of the pathway.

The finding that unfolded SP not only has the ability to stimulate ATPase activity, but also to stimulate the rate of GroES release has important implications in a biological

sense. SP can stimulate ATPase activity by as much as 10-fold in the presence of GroES, and it can stimulate GroES release by a remarkable 4 orders of magnitude. In Chapter 5, the relationship between the amount of time an SP can remain encapsulated in the central cavity (mean residence time) and the total cycle time of a single ring (hemicycle time) was explored. The offset hemicycles of the two rings were shown schematically in Figure 5-3. In the absence of SP, the hemicycle time is about 220 seconds, 40-50 of which are spent releasing GroES. With SP, the hemicycle time is reduced to about 12 seconds. Of those 12 seconds, less than 0.1 second is spent releasing GroES. Thus, when unfolded SP is present, not only is the total cycle time reduced, meaning the system cycles more often, but the amount of time the folding chamber remains intact is significantly reduced. Without knowing the rate of GroES association, it cannot be known exactly for how long during the 12 seconds GroES is bound to GroEL, but the important point is that it is far less than it is in the absence of SP. Since the lifetime of the folding chamber is reduced, the amount of time an unfolded SP has to refold in isolation is also reduced in the presence of SP. According to the passive mechanism of GroEL-assisted protein folding, the important function that GroEL serves is to isolate misfolded proteins in a favorable folding environment and protect them from aggregation while they refold (7). But, why would a system, whose key function is to provide a folding chamber, significantly reduce the lifetime of that folding chamber in the presence of the very substrate it is charged with protecting? In other words, the system does not seem to be well designed for the purpose of protecting substrates. Instead, it seems better designed to bind and release substrates as quickly as possible, and the more SP there is, the faster GroEL turns it over. The system appears well designed for the active unfolding

mechanism, in which turnovers are the key (5, 46). Each hemicycle will result in one forced unfolding event, followed by a short refolding period in the central cavity, and then the SP will be released, folded or not. The active unfolding mechanism is most efficient when the system is turning over rapidly; conversely, passive unfolding is least efficient when the system is turning over rapidly. Therefore, without even discussing the mechanism by which SP stimulates activity or GroES release, the simple fact that it does suggests that GroE has evolved to unfold proteins, rather than to act as a passive folding chamber.

The fact that ATPase activity and the rate of GroES release are affected by unfolded SP highlights the importance of using GroEL of the highest purity when making quantitative measurements. Purifying GroEL is not a trivial task; after all, its function is to bind a large variety of other proteins. Even a weak binding SP such as α-LA is able to affect the GroES release rate in only 2-fold excess. However, the problems associated with impure GroEL were made abundantly clear in Chapter 5, where studies with highly pure GroEL provided data that were dramatically different from published data obtained with what was presumably contaminated GroEL. The acetone precipitation procedure (56) used to purify the GroEL for these studies should become the standard protocol in any laboratory seeking to make the kinds of quantitative measurements that were presented in this dissertation. There are too many examples in the literature of GroEL ATPase measurements that give rates which we only observe *after* the deliberate addition of unfolded SP, and which vary dramatically from one laboratory to another. Many of these reports make no specific mention of any procedure that had been used to remove such contaminating SP. There is very little point in attempting the kinds of sophisticated

quantitative analyses being presented in the current GroEL literature if the GroEL preparations used for the analyses are full of contaminating proteins.

This dissertation presents an explanation as to why unfolded SP stimulates ATPase activity and the release of GroES: SP binds to and stabilizes the T conformation of a GroEL ring. This explanation is a reasonable one, because GroEL rings locked in the T state by covalent tethers have a significantly higher ATPase activity than rings in the R state (see results in Chapter 3 with $GroEL_{IRX}$ and $GroEL_{IAX}$), and there are other data in Chapter 4 which also support this explanation. With that said, the real explanation for rate stimulation by SP is almost certainly more complicated. The current explanation does not explain why SP does not stimulate activity in either $GroEL_{IRX}$ or SR1. There is no satisfactory explanation as to why, at relatively low [ATP], SP inhibits the activity of GroEL that is locked in the T state. It is very possible that reducing rate stimulation by SP to a simple effect on the T→R equilibrium is an oversimplification, albeit one which explains most of the data. It is more likely that the allostery of GroEL is more complicated than has been implied by some of the assumptions and conclusions of this dissertation, and that, in fact, there may be additional allosteric states that play a role in the GroEL reaction cycle.

The idea that additional allosteric states exist besides T, R, and R' is not a new one. Their existence was acknowledged during the original synthesis of the nested cooperativity model (33), and it has been shown in cryo-EM studies that the T-state *trans* ring of GroEL/GroES complex is structurally different from a T-state ring of GroEL in the TT state (83). This suggests that the allosteric state of one ring is dependent of the allosteric state of the other ring. This also raises the possibility that there may be

additional allosteric T or R states that exist in the presence of SP, with their own ATP binding affinity and V_{max}. These possibilities significantly complicate any discussion of GroEL's allostery. However, it also provides a potential explanation for why SP does not stimulate the ATPase activity of GroEL mutants in which inter-ring communication is deficient. Consider the following: the binding of SP to a ring may very well hold that ring in the T state, but it may also affect the V_{max} and binding affinity of the other ring. It may be that the unbound ring transits to another allosteric state upon SP binding to the other ring, and that this transition is absolutely required for the SP-bound ring to transit to a more active T state. In fact, this highlights one dangerous assumption present in formulating the theoretical models discussed in Chapter 3, and that is the assumption that the allosteric state of one ring is completely independent of the state of the other. Including an inter-ring dependence and additional allosteric states in the theoretical models would be extremely difficult, and any data fit to these more complicated models would probably not be good enough to be able to distinguish between the various models anyway. This is not to say that the conclusions reached with the current theoretical models are incorrect, however, the fact that the models are almost certainly oversimplifications should be kept in mind. For now, T, R, and R' provide a useful description of allostery as we currently understand it and will suffice until a more robust model of allostery can be developed.

This dissertation has presented a study of GroEL's allosteric properties and how they are related to its role in rescuing misfolded protein substrates. The debate over passive vs. active unfolding will certainly not end here, and it may be difficult to ever fully resolve the question. However, the data documented in these pages make a case

that active unfolding does occur, and that the allosteric structural transitions and catalytic functions that GroEL undergoes are designed to allow it to occur efficiently. Concerted domain movements maximize the unfolding force. Unfolded substrate proteins exert a mechanical force on their binding sites, which obliges GroEL to exert force on the SPs in return. When unfolded SP is present, the GroE system hydrolyzes ATP, releases GroES, and cycles more rapidly, allowing it to perform more unfolding events in a shorter amount of time. In the absence of SP, the system turns over slowly, conserving cellular resources. GroEL does work on its substrates with an efficient power stroke and does so most efficiently when the workload is heaviest. It is the very definition of a machine, and its continued study should provide countless insights into the way Nature has designed other cellular machines. Several of the experiments presented here may be useful in the study of other ringed structures, such the Clp proteases (84), or the PA_{63} heptamer of anthrax toxin (85) . The studies undertaken for this dissertation may provide valuable tools to use in the ongoing study of Nature's skill as an engineer.

APPENDIX

A.1 Equations Used to Find the Number of Moles of Monomers, Dimers, etc. per Moles of 14-mer in a Cross-Linked Sample of $GroEL_{IRX}$.

These equations produce the number of moles of a given species (monomer, dimer, etc.) per moles of 14-mer at any value along the reaction coordinate by multiplying the fraction of 14-mers with a given number of tethers (from the binomial distribution equations) by the probability that those 14-mers contain that particular species, by the number of that species the 14-mer is predicted to contain. For example, using non-real numbers to illustrate, at some point on the reaction coordinate 15% of the 14-mers contain 3 tethers. In these 14-mers, there is a 1/4 probability that two dimers are present. The mole fraction of dimers is then *0.15*(1/4)*2*. The probability numbers were calculated using the scheme in Figure 3-5.

In the following equations, *yx* is the fraction of 14-mers containing *x* tethers. The probability factor has already been multiplied by the number of species contained in the 14-mer for simplicity.

Moles of Monomer = y0*14 + y1*12 + y2*(132/13) + y3*(1320/156) + y4*(11880/1716) + y5*(95040/17160) + y6*(665280/154440) + y7*(3991680/1235520) + y8*(19958400/8648640) + y9*(79833600/51891840) + y10*(239500800/259459200) + y11*(479001600/1037836800) + y12*(479001600/3113510400) + y13*0 + y14*0

Moles of Dimer = y0*0 + y1*1 + y2*(22/13) + y3*(330/156) + y4*(3960/1716) + y5*(39600/17160) + y6*(332640/154440) + y7*(2328480/1235520) + y8*(13305600/8648640) + y9*(59875200/51891840) + y10*(199584000/259459200) + y11*(439084800/1037836800) + y12*(479001600/3113510400) + y13*0 + y14*0

Moles of Trimer = y0*0 + y1*0 + y2*(2/13) + y3*(60/156) + y4*(1080/1716) + y5*(1440/17160) + y6*(151200/154440) + y7*(1270080/1235520) + y8*(8467200/8648640) + y9*(43545600/51891840) + y10*(163296000/259459200) + y11*(399168000/1037836800) + y12*(479001600/3113510400) + y13*0 + y14*0

Moles of Tetramer = y0*0 + y1*0 + y2*0 + y3*(6/156) + y4*(216/1716) + y5*(4320/17160) + y6*(60480/154440) + y7*(635040/1235520) + y8*(5080320/8648640) + y9*(30481920/51891840) + y10*(130636800/259459200) + y11*(359251200/1037836800) + y12*(479001600/3113510400) + y13*0 + y14*0

Moles of Pentamer = y0*0 + y1*0 + y2*0 + y3*0 + y4*(24/1716) + y5*(960/17160) + y6*(20160/154440) + y7*(282240/1235520) + y8*(2822400/8648640) + y9*(20321280/51891840) + y10*(101606400/259459200) + y11*(319334400/1037836800) + y12*(479001600/3113510400) + y13*0 + y14*0

Moles of Hexamer = y0*0 + y1*0 + y2*0 + y3*0 + y4*0 + y5*(120/17160) + y6*(5040/154440) + y7*(105840/1235520) + y8*(1411200/8648640) + y9*(12700800/51891840) + y10*(76204800/259459200) + y11*(279417600/1037836800) + y12*(479001600/3113510400) + y13*0 + y14*0

Moles of Heptamer = y0*0 + y1*0 + y2*0 + y3*0 + y4*0 + y5*0 + y6*(720/154440) + y7*(36000/1235520) + y8*(887040/8648640) + y9*(13789440/51891840) + y10*(145152000/259459200) + y11*(1037836800/1037836800) + y12*(4790016000/3113510400) + y13*(12454041600/6227020800) + y14*(12454041600/6227020800)

REFERENCES

1. Anfinsen, C. B. (1973) Principles that govern the folding of protein chains. *Science* 181, 223-230
2. Sigler, P. B., Xu, Z., Rye, H. S., Burston, S. G., Fenton, W. A., and Horwich, A. L. (1998) Structure and function in GroEL-mediated protein folding. *Annu Rev Biochem* 67, 581-608
3. Matouschek, A., Pfanner, N., and Voos, W. (2000) Protein unfolding by mitochondria. The Hsp70 import motor. *EMBO Reports* 1, 404-410
4. Richter, K., Muschler, P., Hainzl, O., and Buchner, J. (2002) Coordinated ATP hydrolysis by the Hsp90 dimer. *J Biol Chem* 318, 611-620
5. Thirumalai, D., and Lorimer, G. H. (2001) Chaperonin-mediated protein folding. *Annu Rev Biophys Biomol Struct* 30, 245-269
6. Georgopoulos, C. P., and Hohn, B. (1978) Identification of a host protein necessary for bacteriophage morphogenesis (the groE gene product). *Proc Natl Acad Sci USA* 75, 131-135
7. Ellis, R. J., and Hartl, F. U. (1996) Protein folding in the cell: competing models of chaperonin function. *FASEB J* 10, 20-26
8. Shtilerman, M., Lorimer, G. H., and Englander, S. W. (1999) Chaperonin function: folding by forced unfolding. *Science* 284, 822-825
9. Hemmingsen, S. M., Woolford, C., van der Vies, S. M., Tilly, K., Dennis, D. T., Georgopoulos, C. P., Hendrix, R. W., and Ellis, R. J. (1988) Homologous plant and bacterial proteins chaperone oligomeric protein assembly. *Nature* 333, 330-334

10. Braig, K., Otwinowski, Z., Hegde, R., Boisvert, D. C., Joachimiak, A., Horwich, A. L., and Sigler, P. B. (1994) The crystal structure of the bacterial chaperonin GroEL at 2.8 A. *Nature* 371, 578-586

11. Brocchieri, L., and Karlin, S. (2000) Conservation among HSP60 sequences in relation to structure, function, and evolution. *Protein Sci* 9, 476-486

12. Fenton, W. A., Kashi, Y., Furtak, K., and Horwich, A. L. (1994) Residues in chaperonin GroEL required for polypeptide binding and release. *Nature* 371, 614-619

13. Weissman, J. S., Hohl, C. M., Kovalenko, O., Kashi, Y., Chen, S., Braig, K., Saibil, H. R., Fenton, W. A., and Horwich, A. L. (1995) Mechanism of GroEL action: productive release of polypeptide from a sequestered position under GroES. *Cell* 83, 577-587

14. Xu, Z., Horwich, A. L., and Sigler, P. B. (1997) The crystal structure of the asymmetric GroEL-GroES-(ADP)7 chaperonin complex. *Nature* 388, 741-750

15. Hunt, J. F., Weaver, A. J., Landry, S. J., Gierasch, L., and Deisenhofer, J. (1996) The crystal structure of the GroES co-chaperonin at 2.8 A resolution. *Nature* 379, 37-45

16. Azem, A., Kessel, M., and Goloubinoff, P. (1994) Characterization of a functional GroEL14(GroES7)2 chaperonin hetero- oligomer. *Science* 265, 653-656

17. Rye, H. S., Roseman, A. M., Chen, S., Furtak, K., Fenton, W. A., Saibil, H. R., and Horwich, A. L. (1999) GroEL-GroES cycling: ATP and nonnative polypeptide direct alternation of folding-active rings. *Cell* 97, 325-338

18. Chen, S., Roseman, A. M., Hunter, A. S., Wood, S. P., Burston, S. G., Ranson, N. A., Clarke, A. R., and Saibil, H. R. (1994) Location of a folding protein and shape changes in GroEL-GroES complexes imaged by cryo-electron microscopy. *Nature* 371, 261-264

19. Todd, M. J., Lorimer, G. H., and Thirumalai, D. (1996) Chaperonin-facilitated protein folding: optimization of rate and yield by an iterative annealing mechanism. *Proc Natl Acad Sci U S A* 93, 4030-4035

20. Todd, M. J., Viitanen, P. V., and Lorimer, G. H. (1994) Dynamics of the chaperonin ATPase cycle: implications for facilitated protein folding. *Science* 265, 659-666

21. Goloubinoff, P., Gatenby, A. A., and Lorimer, G. H. (1989) GroE heat-shock proteins promote assembly of foreign prokaryotic ribulose bisphosphate carboxylase oligomers in Escherichia coli. *Nature* 337, 44-47

22. Goloubinoff, P., Christeller, J. T., Gatenby, A. A., and Lorimer, G. H. (1989) Reconstitution of active dimeric ribulose bisphosphate carboxylase from an unfoleded state depends on two chaperonin proteins and Mg-ATP. *Nature* 342, 884-889

23. Viitanen, P. V., Gatenby, A. A., and Lorimer, G. H. (1992) Purified chaperonin 60 (groEL) interacts with the nonnative states of a multitude of Escherichia coli proteins. *Protein Sci* 1, 363-369

24. Aoki, K., Motojima, F., Taguchi, H., Yomo, T., and Yoshida, M. (2000) GroEL binds artificial proteins with random sequences. *J Biol Chem* 275, 13755-13758

25. Lin, Z., Schwartz, F. P., and Eisenstein, E. (1995) The hydrophobic nature of GroEL-substrate binding. *J Biol Chem* 270, 1011-1014

26. Buckle, A. M., Zahn, R., and Fersht, A. R. (1997) A structural model for GroEL-polypeptide recognition. *Proc Natl Acad Sci U S A* 94, 3571-3575

27. Privalov, P. L., Tiktopulo, E. I., Venyaminov, S., Griko, Y., Makhatadze, G. I., and Khechinashvili, N. N. (1989) Heat capacity and conformation of proteins in the denatured state. *J Mol Biol* 205, 737-750

28. Murphy, K. P., Privalov, P. L., and Gill, S. J. (1990) Common features of protein unfolding and dissolution of hydrophobic compounds. *Science* 247, 559-561

29. Lorimer, G. (1997) Protein folding. Folding with a two-stroke motor. *Nature* 388, 720-721, 723

30. Viitanen, P. V., Lubben, T. H., Reed, J., Goloubinoff, P., O'Keefe, D. P., and Lorimer, G. H. (1990) Chaperonin-facilitated refolding of ribulosebisphosphate carboxylase and ATP hydrolysis by chaperonin 60 (groEL) are K+ dependent. *Biochemistry* 29, 5665-5671

31. Todd, M. J., Viitanen, P. V., and Lorimer, G. H. (1993) Hydrolysis of adenosine 5'-triphosphate by Escherichia coli GroEL: effects of GroES and potassium ion. *Biochemistry* 32, 8560-8567

32. Gray, T. E., and Fersht, A. R. (1991) Cooperativity in ATP hydrolysis by GroEL is increased by GroES. *FEBS Lett* 292, 254-258

33. Yifrach, O., and Horovitz, A. (1995) Nested cooperativity in the ATPase activity of the oligomeric chaperonin GroEL. *Biochemistry* 34, 5303-5308

34. Yifrach, O., and Horovitz, A. (1996) Allosteric control by ATP of non-folded protein binding to GroEL. *J Mol Biol* 255, 356-361

35. Roseman, A. M., Chen, S., White, H., Braig, K., and Saibil, H. R. (1996) The chaperonin ATPase cycle: mechanism of allosteric switching and movements of substrate-binding domains in GroEL. *Cell* 87, 241-251

36. Ranson, N. A., Farr, G. W., Roseman, A. M., Gowen, B., Fenton, W. A., Horwich, A. L., and Saibil, H. R. (2001) ATP-bound states of GroEL captured by cryo-electron microscopy. *Cell* 107, 869-879

37. Rye, H. S., Burston, S. G., Fenton, W. A., Beechem, J. M., Xu, Z., Sigler, P. B., and Horwich, A. L. (1997) Distinct actions of cis and trans ATP within the double ring of the chaperonin GroEL. *Nature* 388, 792-798

38. Ma, J., Sigler, P. B., Xu, Z., and Karplus, M. (2000) A dynamic model for the allosteric mechanism of GroEL. *J Mol Biol* 302, 303-313

39. Weissman, J. S., Rye, H. S., Fenton, W. A., Beechem, J. M., and Horwich, A. L. (1996) Characterization of the active intermediate of a GroEL-GroES-mediated protein folding reaction. *Cell* 84, 481-490

40. Hartl, F. U., and Hayer-Hartl, M. (2002) Molecular chaperones in the cytosol: from nascent chain to folded protein. *Science* 295, 1852-1858

41. Chen, J., Walter, S., Horwich, A. L., and Smith, D. L. (2001) Folding of malate dehydrogenase inside the GroEL-GroES cavity. *Nat Struct Biol* 8, 721-728

42. Weissman, J. S., Kashi, Y., Fenton, W. A., and Horwich, A. L. (1994) GroEL-mediated protein folding proceeds by multiple rounds of binding and release of nonnative forms. *Cell* 78, 693-702

43. Zahn, R., Perrett, S., and Fersht, A. R. (1996) Conformational states bound by the molecular chaperones GroEL and secB: a hidden unfolding (annealing) activity. *J Mol Biol* 261, 43-61

44. Zahn, R., Perrett, S., Stenberg, G., and Fersht, A. R. (1996) Catalysis of amide proton exchange by the molecular chaperones GroEL and SecB. *Science* 271, 642-645

45. Nieba-Axmann, S. E., Ottiger, M., Wuthrich, K., and Pluckthun, A. (1997) Multiple cycles of global unfolding of GroEL-bound cyclophilin A evidenced by NMR. *J Mol Biol* 271, 803-818

46. Betancourt, M. R., and Thirumalai, D. (1999) Exploring the kinetic requirements for enhancement of protein folding rates in the GroEL cavity. *J Mol Biol* 287, 627-644

47. Farr, G. W., Fenton, W. A., Chaudhuri, T. K., Clare, D. K., Saibil, H. R., and Horwich, A. L. (2003) Folding with and without encapsulation by cis- and trans-only GroEL-GroES complexes.

48. Monod, J., Wyman, J., and Changeux, J.-P. (1965) On the nature of allosteric interactions: a plausible model. *J Mol Biol* 12, 88-118

49. Koshland, D. E., Jr., Nemethy, G., and Filmer, D. (1966) Comparison of experimental binding data and theoretical models in proteins containing subunits. *Biochemistry* 5, 365-385

50. Yifrach, O., and Horovitz, A. (2000) Coupling between protein folding and allostery in the GroE chaperonin system. *Proc Natl Acad Sci U S A* 97, 1521-1524

51. Murai, N., Makino, Y., and Yoshida, M. (1996) GroEL locked in a closed conformation by an interdomain cross-link can bind ATP and polypeptide but cannot process further reaction steps. *J Biol Chem* 271, 28229-28234

52. Rye, H. S. (2001) Application of fluorescence resonance energy transfer to the GroEL-GroES chaperonin reaction. *Methods* 24, 278-288

53. White, Z. W., Fisher, K. E., and Eisenstein, E. (1995) A monomeric variant of GroEL binds nucleotides but is inactive as a molecular chaperone. *J Biol Chem* 270, 20404-9

54. Sambrook, J., Fritsch, E. F., and Maniatis, T. (1989) *Molecular Cloning, A Laboratory Manual, Second Ed.*, Cold Spring Harbor Laboratory Press

55. Laemmli, U. K. (1970) Cleavage of proteins during the assembly of the head of bacteriophage T4. *Nature* 227, 680-685

56. Voziyan, P. A., and Fisher, M. T. (2000) Chaperonin-assisted folding of glutamine synthetase under nonpermissive conditions: off-pathway aggregation propensity does not determine the co-chaperonin requirement. *Protein Sci* 9, 2405-2412

57. Todd, M. J., and Lorimer, G. H. (1998) Criteria for assessing the purity and quality of GroEL. *Methods in Enzymology* 290, 135-141

58. Eisenstein, E., Reddy, P., and Fisher, M. T. (1998) Overexpression, purification, and properties of GroES from Escherichia coli. *Methods in Enzymology* 290, 119-135

59. Kosower, N. S., and Kosower, E. M. (1995) Diamide: An oxidant probe for thiols. *Methods in Enzymology* 251, 123-133

60. Nitao, L. K., and Reisler, E. (1998) Probing the conformational states of the SH1-SH2 helix in myosin: A cross-linking approach. *Biochemistry* 37, 16704-16710

61. Hashimoto, M., Majima, E., Goto, S., Shinohara, Y., and Terada, H. (1999) Fluctuation of the first loop facing the matrix of the mitochondrial ADP/ATP carrier deduced from inermolecular cross-linking of cys56 residues by bifunctional dimaleimides. *Biochemistry* 38, 1050-1056

62. Okazaki, A., Ikura, T., Nikaido, K., and Kuwajima, K. (1994) The chaperonin GroEL does not recognize apo-alpha-lactalbumin in the molten globule state. *Nat Struct Biol* 1, 439-446

63. Peralta, D., Hartman, D. J., Hoogenraad, N. J., and Hoj, P. B. (1994) Generation of a stable folding intermediate which can be rescued by the chaperonins GroEL and GroES. *FEBS Letters* 339, 45-49

64. Ranson, N. A., Dunster, N. J., Burston, S. G., and Clarke, A. R. (1995) Chaperonins can catalyse the reversal of early aggregation steps when a protein misfolds. *J Mol Biol* 250, 581-586

65. Martz, E. (2002) Protein Explorer: Easy yet powerful Macromolecular Visualization. *Trends in Biochemical Sciences* 27, 107-109

66. Nielsen, K. L., McLennan, N., Masters, M., and Cowan, N. J. (1999) A single-ring mitochondrial chaperonin (Hsp60-Hsp10) can substitute for GroEL-GroES in vivo. *Journal of Bacteriology* 181, 5871-5875

67. Brune, M., Hunter, J. L., Corrie, J. E., and Webb, M. R. (1994) Direct, real-time measurement of rapid inorganic phosphate release using a novel fluorescent probe

and its application to actomyosin subfragment 1 ATPase. *Biochemistry* 33, 8262-8271.

68. Brune, M., Hunter, J. L., Howell, S. A., Martin, S. R., Hazlett, T. L., Corrie, J. E., and Webb, M. R. (1998) Mechanism of inorganic phosphate interaction with phosphate binding protein from Escherichia coli. *Biochemistry* 37, 10370-10380.

69. Uebel, M. H. (2001) Recovering intact GroEL complexes formed in vivo. In Department of Chemistry and Biochemistry, University of Maryland College Park, College Park, MD

70. Jai, E. A., and Horowitz, P. M. (1999) Nucleotide and Mg2+ induced conformational changes in GroEL can be detected by sulfhydryl labeling. *J Protein Chem* 18, 387-396

71. McLaughlin, S. H., Smith, H. W., and Jackson, S. E. (2002) Stimulation of the weak ATPase activity of human hsp90 by a client protein. *J Mol Biol* 315, 787-798

72. Widjaja, L. (2002) Allosteric control of GroEL by ATP: Effects of monovalent and divalent cations. In Department of Chemistry and Biochemistry, University of Maryland, College Park, College Park, MD

73. Danziger, O., Rivenzon-Segal, D., Wolf, S. G., and Horovitz, A. (2003) Conversion of the allosteric transition of GroEL from concerted to sequential by the single mutation Asp-155 -> Ala. *Proc Natl Acad Sci U S A* 100, 13797-13802

74. Yifrach, O., and Horovitz, A. (1994) Two lines of allosteric communication in the oligomeric chaperonin GroEL are revealed by the single mutation Arg196-->Ala. *J Mol Biol* 243, 397-401

75. Wang, Z., Feng, H., Landry, S. J., Maxwell, J., and Gierasch, L. M. (1999) Basis of substrate binding by the chaperonin GroEL. *Biochemistry* 38, 12537-12546

76. Richarme, G., and Kohiyama, M. (1994) Amino acid specificity of the Escherichia coli chaperone GroEL (heat shock protein 60). *J Biol Chem* 269, 7095-7098

77. Fisher, T. E., Marszalek, P. E., and Fernandez, J. M. (2000) Stretching single molecules into novel conformations using the atomic force microscope. *Nat Struct Biol* 7, 719-724

78. Vinckier, A., Gervasoni, P., Zaugg, F., Ziegler, U., Lindner, P., Groscurth, P., Pluckthun, A., and Semenza, G. (1998) Atominc force microscopy detects changes in the interaction forces between GroEL and substrate proteins. *Biophys. J.* 74, 3256-3263

79. Burston, S. G., Weissman, J. S., Farr, G. W., Fenton, W. A., and Horwich, A. L. (1996) Release of both native and non-native proteins from a cis-only GroEL ternary complex. *Nature* 383, 96-99

80. Burston, S. G., Ranson, N. A., and Clarke, A. R. (1995) The origins and consequences of asymmetry in the chaperonin reaction cycle. *J Mol Biol* 249, 138-152

81. Lakowicz, J. R. (1999) *Principles of Fluorescence Spectroscopy*

82. Molecular Probes (2003) Handbook of Molecular Probes and Research Products.

83. White, H. E., Chen, S., Roseman, A. M., Yifrach, O., Horovitz, A., and Saibil, H. R. (1997) Structural basis of allosteric changes in the GroEL mutant Arg197-->Ala. *Nat Struct Biol* 4, 690-694

84. Hoskins, J. R., Sharma, S., Sathyanarayana, B. K., and Wickner, S. (2001) Clp ATPases and their role in protein unfolding and degradation. *Advances in protein chemistry* 59, 413-429

85. Mourez, M., Lacy, D. B., Cunningham, K., Legmann, R., Sellman, B. R., Mogridge, J., and Collier, R. J. (2002) 2001: a year of major advances in anthrax toxin research. *Trends in Microbiology* 10, 287-293